โครงการ

การศึกษาการส่งสัญญาณอินเตอร์เฟียรอนในเซลล์มะเร็งตับที่ได้รับการติดเชื้อตับอักเสบชนิดบีด้วยวิธีโปรติโอมิกส์

Proteomic analysis of interferon signaling in HBV-transfected hepatoblastoma cell line

โดย อาจารย์ นายแพทย์ไตรรักษ์ พิสิษฐ์กุล

มิถุนายน 2561

สัญญาเลขที่ RSA5880014

รายงานวิจัยฉบับสมบูรณ์

โครงการ การศึกษาการส่งสัญญาณอินเตอร์เฟียรอนในเซลล์มะเร็งตับที่ได้รับการติดเชื้อตับอักเสบชนิดบีด้วยวิธีโปรติโอมิกส์

Proteomic analysis of interferon signaling in HBV-transfected hepatoblastoma cell line

โดย อาจารย์ นายแพทย์ไตรรักษ์ พิสิษฐ์กุล

คณะแพทยศาสตร์ จุฬาลงกรณ์มหาวิทยาลัย

สนับสนุนโดยสำนักงานกองทุนสนับสนุนการวิจัย และ จุฬาลงกรณ์มหาวิทยาลัย

กิตติกรรมประกาศ

งานวิจัยนี้ได้รับการสนับสนุนจากสำนักงานกองทุนสนับสนุนการวิจัย และ จุฬาลงกรณ์มหาวิทยาลัย

ผู้วิจัยขอขอบคุณศาสตราจารย์ แพทย์หญิง ดร.ณัฏฐิยา หิรัญกาญจน์ หัวหน้าศูนย์เชี่ยวชาญเฉพาะทางด้านภูมิคุ้มกันวิทยาและโรคที่เกี่ยวข้องกับระบบภูมิคุ้มกัน คณะแพทยศาสตร์ จุฬาลงกรณ์มหาวิทยาลัย ที่ให้คำแนะนำที่เป็นประโยชน์เกี่ยวกับเรื่องอินเตอร์เฟียรอนชนิดที่ 3 และ เรื่องการตอบสนองทางภูมิคุ้มกันของไวรัสตับอักเสบบี และผู้วิจัยขอขอบคุณ ดร. ภูริชญา สมภาร และดร. ธรรมกร แซ่ตั้ง นักวิจัยประจำศูนย์เชี่ยวชาญทางชีววิทยาเชิงระบบ คณะแพทยศาสตร์ จุฬาลงกรณ์มหาวิทยาลัย ที่ช่วยสอนเทคนิคต่างๆ ในการทำโปรติโอมิกส์ และการวิเคราะห์ผลโดยใช้ชีวสารสนเทศให้แก่นิสิตของผู้วิจัย

นอกจากนี้ผู้วิจัยขอขอบคุณนายจิราเดช มักเจริญ นิสิตของผู้วิจัย ที่มีส่วนช่วยในการทำการทดลองและวิเคราะห์ผล และทุน 90 ปี จุฬาลงกรณ์มหาวิทยาลัย ที่สนับสนุนการทำวิทยานิพนธ์ของนิสิตของผู้วิจัย โดยวิทยานิพนธ์ดังกล่าวเป็นส่วนหนึ่งของงานวิจัยนี้ สุดท้ายนี้ผู้วิจัยขอขอบคุณทีมวิจัยทุกคนในศูนย์เชี่ยวชาญเฉพาะทางชีววิทยาเชิงระบบ คณะแพทยศาสตร์ จุฬาลงกรณ์มหาวิทยาลัย

บทคัดย่อ

รหัสโครงการ: RSA5880014

ชื่อโครงการ: การศึกษาการส่งสัญญาณอินเตอร์เฟียรอนในเซลล์มะเร็งตับที่ได้รับการติดเชื้อตับอักเสบชนิดบีด้วยวิธีโปรติโอมิกส์

ชื่อนักวิจัย: อาจารย์ นายแพทย์ไตรรักษ์ พิสิษฐ์กุล, คณะแพทยศาสตร์ จุฬาลงกรณ์มหาวิทยาลัย

E-mail Address: trairak@gmail.com

เมื่อไม่นานมานี้ ได้มีการนำอินเตอร์เฟียรอนแลมบ์ดามาศึกษาในการทดลองทางคลินิกในผู้ป่วยไวรัสตับอักเสบบีแบบเรื้อรัง เนื่องจากว่ายาชนิดนี้มีฤทธิ์ในการต้านไวรัสและมีผลข้างเคียงน้อยเมื่อเปรียบเทียบกับอินเตอร์เฟียรอนแอลฟา ทั้งนี้เพราะตัวรับสัญญาณของอินเตอร์เฟียรอนแลมบ์ดานั้นพบเฉพาะในเซลล์เยื้อบุผิวเท่านั้น ในปัจจุบันวิถีสัญญาณต่างๆ ที่ถูกควบคุมด้วยอินเตอร์เฟียรอนแลมบ์ดายังมีการศึกษาไม่มากนัก โดยเฉพาะอย่างยิ่งการศึกษาด้วยวิธีทางโปรติโอมิกส์ โดยในงานวิจัยนี้คณะผู้วิจัยพบว่าอินเตอร์เฟียรอนแลมบ์ดา 3 สามารถยับยั้งการเพิ่มจำนวนของไวรัสตับอักเสบบี โดยยาชนิดนี้ลดการแสดงออกของยีนของไวรัส และลดปริมาณสารพันธุกรรมของไวรัสภายในเซลล์ การศึกษาโปรติโอมิกส์เชิงปริมาณได้ถูกนำมาใช้เพื่อหากลไกที่เกี่ยวข้องกับการลดลงของไวรัสในเซลล์ HepG2.2.15 ที่ถูกกระตุ้นด้วยยาชนิดนี้เป็นเวลา 24 ชั่วโมง อีกทั้งผู้วิจัยยังได้กระตุ้นเซลล์ชนิดนี้ด้วยอินเตอร์เฟียรอนแอลฟาทูเอและพีบีเอส (ตัวควบคุม) เพื่อเปรียบเทียบผลการกระตุ้นของตัวกระตุ้นทั้ง 3 ชนิด โดยใช้เทคนิคการติดฉลากด้วยไอโซโทปที่แตกต่างกันของไดเมทิล ด้วยเทคนิคและวิธีการวิจัยที่ใช้ในการศึกษาครั้งนี้ทำให้ได้ข้อมูลในเชิงลึกที่สามารถสร้างแผนภาพที่ระบุโปรตีนที่มีฤทธิ์ในการต้านไวรัสกับขั้นตอนที่โปรตีนนั้นๆ มีผลต่อวงชีวิตของไวรัสตับอักเสบบี นอกจากนี้คณะผู้วิจัยยังพบว่าโปรตีนที่เกี่ยวข้องกับกระบวนการนำเสนอแอนติเจนให้กับทีเซลล์มีการแสดงออกที่เพิ่มมากขึ้น ชี้ให้เห็นว่าอินเตอร์เฟียลอนแลมบ์ดา 3 มีฤทธิ์ในการกระตุ้นภูมิคุ้มกัน นอกจากนี้อินเตอร์เฟียรอนแลมบ์ดา 3 ยังมีผลทำให้โปรตีน RIG-I มีการแสดงออกเพิ่มมากขึ้น ซึ่งเคยมีรายงานมาว่าการแสดงออกของโปรตีนชนิดนี้จะถูกยับยั้งโดยไวรัสตับอักเสบบี ในงานวิจัยนี้ยังแสดงให้เห็นว่ากระบวนการทางชีวภาพหลายๆ กระบวนการที่ตอบสนองต่อการถูกกระตุ้นด้วยอินเตอร์เฟียรอนแลมบ์ดา 3 และอาจจะเกี่ยวข้องกับการจำกัดการเพิ่มจำนวนของไวรัสตับอักเสบบี ในการศึกษาในอนาคตคณะผู้วิจัยอยากศึกษาต่อยอดฤทธิ์ของอินเตอร์เฟียรอนแลมบ์ดา 3 ที่สามารถกระตุ้นภูมิคุ้มกันได้ในมุมของภูมิคุ้มกันบำบัดโรคมะเร็ง โดยยาชนิดนี้สามารถใช้เป็นยาเสริมร่วมกับการให้นีโอแอนติเจนวัคซีน เพื่อกระตุ้นทีเซลล์ที่มีความจำเพาะกับนีโอแอนติเจนนั้นๆ ทำให้เกิดการกำจัดมะเร็งต่อไป

คำหลัก: โปรติโอมิกส์เชิงปริมาณ, การติดฉลากด้วยไดเมทิล, อินเตอร์เฟียรอนชนิดที่ 3, ไวรัสตับอักเสบบี

ABSTRACT

Project Code: RSA5880014

Project Title: Proteomic analysis of interferon signaling in HBV-transfected hepatoblastoma cell line

Investigator: Trairak Pisitkun, MD., Faculty of Medicine, Chulalongkorn University

E-mail Address: trairak@gmail.com

Project Period: 3 years (1 July 2015 – 30 June 2018)

IFN-λ is a relatively unexplored, yet promising anti-viral agent. IFN-λ has recently been tested in clinical trials of CHB, with the advantage that side effects may be limited compared with IFN-α, as IFN-λ receptors are found only in epithelial cells. To date, IFN-λ's downstream signaling pathway remains largely unelucidated, particularly via proteomics methods. Here, we report that IFN-λ3 inhibits HBV replication in HepG2.2.15 cells, reducing levels of both HBV transcripts and intracellular HBV DNA. Quantitative proteomic analysis of HBV-transfected cells was performed following 24-hour IFN-λ3 treatment, with parallel IFN-α2a and PBS treatments for comparison using a dimethyl labeling method. The depth of the study allowed us to map the induction of anti-viral proteins to multiple points of the viral life cycle, as well as facilitating the identification of anti-viral proteins not previously known to be elicited upon HBV infection. This study also shows up-regulation of many effectors involved in antigen processing/presentation indicating that this cytokine exerted immunomodulatory effects through a number of essential molecules for these processes. Interestingly, immunoproteasome caps were up-regulated while cap components of the constitutive proteasome were down-regulated upon both IFN treatments, suggesting coordinated modulation towards the antigen processing/presentation mode. Furthermore, we reveal that IFN-λ3 restored levels of RIG-I and RIG-G, proteins known to be suppressed by HBV. Enrichment analysis demonstrated that several biological processes including RNA metabolism, translation, and ER-targeting were differentially regulated upon treatment with IFN-λ3 vs. IFN-α2a. Our proteomic data suggests that IFN-λ3 regulates an array of cellular processes to control HBV replication. We would like to further explore the effects of IFN-λ3 on the cancer immunotherapy aspect. IFN-λ3 could be used in adjuction with the neoantigen-based cancer vaccine in order to activate neoantigen specific T cells for anti-tumor effects. In addition, since IFN-λ3 has less side effects compared with type-I IFNs, this treatment could provide a promising strategy to maximize benefits of immunotherapy while reducing their potential harm.

Keywords: Quantitative proteomics, Dimethyl labeling, Type III IFN, Hepatitis B virus

CONTENTS

LIST OF TABLES

LIST OF FIGURES

LIST OF ABBREVIATIONS

2-DE	2-Dimensional gel electrophoresis
Ab	Antibody
ACN	Acetonitrile
ALT	Alanine aminotransferase
BCA	Bicinchoninic acid assay
bp	Base pair
BSA	Bovine serum albumin
cccDNA	Covalently closed circular DNA
cDNA	Complementary DNA
CHB	Chronic hepatitis B
CsA	Cyclosporine A
Ct	Cycle theshold
Ctrl	Control
ddCt	Delta delta cycle threshold
dNTPs	Deoxynucleotide triphosphates
DTT	Dithiothreitol
e^-	HBeAg negative
e^+	HBeAg positive
EC_{50}	Half maximal effective concentration
ELISA	Enzyme-linked immunosorbent assay
FA	Formic acid
FDR	False discovery rate
GO	Gene ontology
GWAS	Genome-wide association studies
HBcAg	Hepatitis B core antigen
HBeAg	Hepatitis B early antigen
HBsAb	Hepatitis B surface antibody
HBsAg	Hepatitis B surface antigen
HBV	Hepatitis B virus

HBx	Hepatitis B x protein
HCC	Hepatocellular carcinoma
HCD	Higher-energy collisional dissociation
HLA	Human leukocyte antigen
IA	Iodoacetamide
ICAT	Isotope-coded affinity tag
IFNR	Interferon receptor
IFN-γ	Interferon-gamma
IFN-α	Interferon-alpha
IFN-β	Interferon-beta
IFN-λ	Interferon-lambda
IL	Interleukin
ISG	Interferon-stimulated gene
iTRAQ	Isobaric peptide tags for relative and absolute quantification
LC	Liquid chromatography
M	Molar
MHC	Major histocompatibility complex
MS/MS	Tandem mass spectrometry
MTT	Thiazolyl blue tetrazolium bromide
NA	Nucleotide analogue
nLC	Nanoliquid chromatography
PegIFN-α	Pegylated IFN-α
pgRNA	Pregenomic RNA
ppm	Parts per million
PTM	Post-translational modification
qPCR	Quantitative polymerase chain reaction
rcDNA	Relaxed circular DNA
RT-PCR	Reverse-transcription polymerase chain reaction
SD	Standard deviation
SDC	Sodium deoxycholate
SDS-PAGE	Sodium dodecyl sulfate-polyacrylamide gel electrophoresis

SEM	Standard error of the mean
sgRNA	Subgenomic RNA
SILAC	Stable isotope labeling by amino acids in cell culture
SVR	Sustained virological response
TEAB	Triethylammonium bicarbonate
TEMED	N,N,N',N'-tetramethylethylenediamine
TFA	Trifluoroacetic acid
TMT	Tandem mass tags
ULN	Upper limits of normal
WB	Western blotting assay

INTRODUCTION

Chronic hepatitis B (CHB) is a major health problem worldwide, affecting 257 million people throughout the world with a prevalence in Africa and South-East Asia (1). Chronic HBV-infected individuals mostly acquire the virus at a young age through vertical transmission or contact with the blood or other body fluids of an infected person. CHB eventually progresses to severe and high-mortality liver diseases including liver cirrhosis and hepatocellular carcinoma (HCC) resulting in 887,000 deaths annually (2, 3).

Current therapeutic agents for CHB are interferon (IFN)-α and nucleos(t)ide analogues (NAs) (4-6). IFN-α is a cytokine that possesses anti-viral and immunomodulatory effects, which promotes control and eradication of viral infection. The advantages of using IFN-α for CHB treatment are the decreased incidence of viral resistance following this treatment and the finite duration of therapy with a higher rate of seroconversion of viral antigens, i.e. HBeAg and HBsAg, compared with NAs. However, the drawbacks of IFN-α treatment are its inconvenient route of administration and its adverse effects such as influenza-like symptoms, nausea, vomiting, cytopenia, and psychiatric disorders. Regarding the latter agent, NAs against CHB, the lack of a 3′-hydroxyl group in these compounds allows competitive incorporation into the viral genome resulting in termination of viral replication (7). Although NAs can directly suppress HBV replication and have fewer unfavorable side effects compared with IFN-α, CHB patients usually require a long-term treatment of these agents, thus increasing the chance of the emergence of viral resistance. In addition, the low rate of HBeAg and HBsAg seroconversion is another limitation of NAs. Therefore, new drugs that overcome restrictions of current anti-HBV treatments are still needed.

Several lines of reasoning suggest that IFN-λ could have a superior combination of efficacy and reduced side-effects. IFN-λ or type III IFN is a cytokine in the class II cytokine family that has recently been used in clinical trials of CHB treatment (8, 9). IFN-λ has 4 subtypes, namely IFN-λ1, -λ2, -λ3, and –λ4. IFN-λ3 was shown to have superior anti-viral potency compared with other IFN-λ subtypes (10). IFN-λ receptor is composed of an IFNLR1 and IL10R2 dimer; hence upon ligand binding, the receptor activates both IFN and IL-10-like signaling pathways. The type I IFN-receptors also form a heterodimer (IFNAR1 and IFNAR2), however, the sequences of all these receptors do diverge, particularly at the C-terminus (11, 12). IFNLR1 is expressed only in epithelial cells including hepatocytes in contrast to IFN-α receptor, which is widely expressed in many cell types throughout the body; thus IFN-λ treatment results in fewer side-effects when compared with IFN-α treatment (9, 13, 14). IFN-λ has been shown to activate the JAK-STAT pathway, inducing formation of the ISGF3

transcription complex, leading to expression of interferon-stimulated genes (ISGs) in similar fashion to type I IFN, but with a different temporal profile compared with those induced by type I IFN (15-17). A limited number of reports regarding IL-10-like signaling pathways have been published, with evidence of STAT3/5 biological activities (18, 19). In fact, no reports have comprehensively investigated the downstream molecular signaling effects of IFN-λ.

To better understand molecular mechanisms underlying direct anti-viral and immunomodulatory effects of IFN-λ3, a comprehensive catalog of protein effectors regulated by IFN-λ3 was compiled using quantitative proteomics analysis in the well-established HBV-transfected hepatocellular carcinoma cell line model viz. HepG2.2.15 cells (20). HepG2.2.15 cells have been widely used as a model of chronic hepatitis B because they support HBV replication and virion secretion (21-27). These new findings could improve the treatment strategy of HBV infection and expand potential applications of IFN-λ3.

LITERATURE REVIEW

Introduction, Epidemiology and route of transmission of HBV infection

Hepatitis B virus (HBV) can cause acute and chronic liver inflammation. Although the safe and effective vaccine which has been available since 1982 has decreased the number of infected people (28), it is estimated that 2 billion people or one-third of the world's population have been affected with this virus worldwide. The prevalence of infection varies greatly across the globe. In highly endemic areas such as Africa and South-East Asia, more than 8% of the population have seropositive to hepatitis B surface antigen (HBsAg) which is used as a marker for HBV infection. The infection mainly occurs in a neonate born from HBV-infected mother at birth during the delivery process or in a child under the age of five through contact with the HBV-infected household. However, the perinatal and early childhood transmission are the minor route of infection in low endemicity where the prevalence is less than 2% such as Northern America and Western Europe. The major sources of transmission in these areas are unprotected sexual promiscuity, received blood or blood products without screening before transfusion, sharing HBV-contaminated needle in drug-abused user or tattooing and occupational exposure of healthcare workers including a doctor, dentist and nurse. Most infected persons are acquired HBV in adolescence or adulthood (29, 30). Approximately 95% of healthy adults affected with HBV can spontaneously and efficiently control viral replication and eliminate virus out of the body and become resolved and self-limiting infection with or without acute hepatitis symptoms including fatigue, low fever, nausea, vomiting, appetite loss, muscle pain, joint aches, pain on the right upper abdomen and jaundice. In contrast, 5% of infected adults and 90% of people exposed to HBV at birth or early childhood fail to clear the virus and establish chronicity (30, 31). It strongly indicates that mature immunity is essential for HBV clearance. World Health Organization (WHO) reported in 2018 that there are 257 million chronically infected people worldwide and 887,000 of these annually die from HBV-related complications such as liver fibrosis, cirrhosis and hepatocellular carcinoma (HCC). Hepatitis B virus infection; therefore, remains one of the seriously major health problems worldwide (28-30).

Characteristic and Molecular virology of HBV

HBV, small DNA virus, is a member of the family hepadnaviridae and genus orthohepadnavirus. In addition to unique genomic organization, HBV differs from other DNA virus because reverse transcription is one of the critical steps in HBV replication (32). Hepatotropism and host-range specificity are also the outstanding characteristics of HBV. This virus is divided into at least 8 genotypes (A-H) based on the difference of its whole sequence genome greater than 8%.

The spread of genotype is distinct geographic spread: for example; genotype A and D are predominant in America and Europe, genotype B and C are most common in high prevalent areas in Africa and South-East Asia (28-33). The structure of HBV enveloped by HBsAg is sphere particle about 42 nm in size and contains icosahedral nucleocapsid composed by hepatitis B core antigen (HBcAg) inside to protect the viral genome from degradation of exogenous nuclease. The partially double-stranded DNA or relaxed circular DNA (rcDNA) and viral polymerase which is covalently linked to the HBV genome are packed within capsid. HBV genome consists of complete minus strand about 3.2 kb in length and incomplete plus strand with variable length ranging 20-80% of the minus-stranded length (34). The two sequences called direct repeat (DR) 1 and DR2 are the regions linking both strands. The full-length minus strand is composed of 4 Open Reading frames (ORFs). The preS/S ORF encoding three surface proteins (HBsAg) including large proteins, middle proteins and small proteins. The PC/C ORF encoding core proteins (HBcAg) and secreted, non-structural proteins (HBeAg). The P ORF encoding viral polymerase including DNA polymerase, reverse transcriptase and RNase H. The X ORF encoding the regulatory HBx protein involving in cell cycle progression, DNA damage repair, signal transduction, apoptosis and up-regulating HBV genes expression by transactivating its promoters or transactivating cellular genes to modify the environment to suit for viral replication. Also, there are several studies reported that HBX associated with hepatic carcinogenesis owing to inhibiting tumor suppressor genes (35, 36).

HBV life cycle

After entry of HBV, virus specifically attaches to the specific receptor, sodium taurocholate cotransporting polypeptide (NTCP), on the hepatocyte surface and penetrate into the cell cytoplasm (37, 38). Many studies reported that the preS1 domain on large surface protein is necessary for receptor binding (39, 40). Following penetration, the nucleocapsid is released from the envelope and then transported to the nuclear membrane by nuclear localization signal from HBcAg on viral capsid. The release of HBV genome into the cell nucleus through nuclear transport receptors Imp-β/Imp-α in importin pathway is taken place at nuclear membrane because of the interaction between viral capsid and nuclear pore complex (40). Inside the nucleoplasm, the viral polymerase is used to repaired to complete the plus strand of rcDNA and then cellular enzymes is utilized to remove RNA-primers used for DNA-plus strand synthesis and viral polymerase including terminal protein on the 5'-end of minus strand. After this step, two complete strands are linked by covalent ligation and this molecule form super-coiled structure (beads-on-a string arrangement) called covalently closed circular DNA (cccDNA) with histone and non-histone protein. The minichromosomal cccDNA served as a template for viral replication and viral RNA synthesis transcribes into 4 RNA species; 3.5 kb

pregenomic RNA (pgRNA) and 2.4 2.1 and 0.7 kb subgenomic RNA (sgRNA) by using host RNA polymerase II (2, 34). All viral transcripts are processed by using cellular transcriptional machinery including capping and polyadenylation at 5'- and 3'-end, respectively before exportation. Translation takes place in the cytoplasm where HBx protein is translated from 0.7 kb RNA and surface proteins are translated from 2.4 and 2.1 kb RNAs. Also that the pgRNA is translated into viral polymerase, HBcAg and HBeAg, it serves as a template for reverse transcription to synthesize negative-stranded DNA. HBV replication is initiated by binding of the terminal protein of viral polymerase to epsilon stem-loop of pgRNA. The RNA-Pol complex is then incorporated into the immature assembling nucleocapsid. This process is triggered by the reverse transcriptase domain in polymerase. Inside the RNA-containing capsid, pgRNA is reverse transcribed into minus-stranded DNA acted as a template for plus-stranded DNA synthesis and followed by degradation of pgRNA by RNaseH. The mature rcDNA-containing capsid is either re-imported into the nucleus to maintain and amplify the cccDNA pool or transported into the endoplasmic reticulum (ER) to envelop and release to the bloodstream. It is estimated that cccDNA about 1-50 copies resided in an infected cell (32). In addition to an infectious particle or Dane particle, envelope proteins themselves can be budded into ER lumen, derived host lipid and secreted as non-infectious particles either filamentous or spherical forms. These particles are produced and exported in a 1,000 to 1,000,000-folds excess over infectious particles. HBV also produces and secretes HBeAg into blood circulation. Although it is not necessary for viral replication, it plays a major role in the contribution of chronic infection due to its immunomodulatory activities (2, 32, 34, 40).

Characteristics and early events in Hepatitis B virus infection

The unique pattern of HBV infection is delayed viral replication after infection and absence of early clinical symptoms that why this infection is different from other viral infections (41, 42). The studies in humans and chimpanzees showed that following infection or inoculation, HBV does not rapidly amplify and spread because HBV-DNA and HBV antigens are undetectable in both serum and liver. Although chimpanzees were inoculated with high doses of HBV, this did not push HBV into a logarithmic phase of replication until 4-7 weeks after inoculation (43). In contrast to the study in acutely hepatitis C virus (HCV)-infected chimpanzees, HCV-RNA was detectable within one week following inoculation and the magnitude of viral titers rapidly increased after the primary manifestation. Several studies in animal models showed that the absence of HBV in the first few weeks of infection did not result from the innate immune response. Because the activation of many cytokines involving in HBV clearance (interferon (IFN)-γ, tumor necrosis factor (TNF)-α and interleukin (IL)-2) and the accumulation of several inflammatory cells in hepatocytes were taken place after HBV started

expansion phase. Furthermore, the results from global gene expression profiling from liver biopsies of HBV-infected chimpanzees demonstrated that no cellular genes were induced during an incubation period of HBV (43). These results confirmed that innate immunity does not influence the early phase of viral replication and spread (42, 44). However, the exact causes of the absence of HBV-DNA and their antigens have not well understood so far. It is possible that the other organs might be the initial site for infection as observed in woodchuck hepatitis virus (WHV) whose bone marrow was the primary site for infection. Nevertheless, WHV is lymphotropic virus thus the missing of human HBV in the early event of HBV infection remains unclear (41). Although many studies showed that IFN-α and -β could efficiently inhibit HBV replication, lack of type I IFN production is one of the outstanding characteristics of early HBV infection. The results from Wieland study confirmed this finding that no type I IFNs and Interferon-stimulating genes (ISGs) were induced in the initial event of HBV infection (43). This virus might develop strategies to evade immune sensors in innate immunity during the lag phase of infection. It has been suggested that 1.) cccDNA, the template for viral RNA synthesis, is located in cellular nucleus 2.) Due to replication inside nucleocapsid, either viral DNA or viral transcripts which are the potent inducers of type I IFN production are not detected by any sensing receptors (41, 42, 44-46).

Immune response in HBV infection

When HBV reach expansion period, most of the hepatocytes are infected and HBV-DNA can be detected in serum and liver as much as 10^9-10^{10} copies/ml (29). During this phase, HBV-infected chimpanzees showed acute hepatitis symptoms and many genes in the liver are induced responding to the infection (43). The large quantities of IFN-γ and TNF-α which might be produced by natural killer (NK) cells and natural killer T (NKT) cells are also observed. There is evidence on humans and animal models showed that these cells were responsible for early inhibition of HBV replication. Despite simulating NKT cells with either α-galactoceramide or HBV antigens in HBV-transgenic mouse model, HBV replication could be inhibited by IFN-γ produced by NKT cells (42, 44). The other study examining in resolved people demonstrated that the vast amount of HBV coincided with a large number of NK cells in the circulation of HBV-infected individuals followed by massive IFN-γ production. About 2-4 weeks later from this, the plenty of HBV-specific $CD4^+$ and $CD8^+$ T cells were recruited into the liver whereas HBV replication had declined (41, 45). The adaptive immune response to HBV is initiated by presenting viral antigen to $CD4^+$ and $CD8^+$ T cells by antigen presenting cells (APCs) including dendritic cells (DCs) and kupffer cells (KCs), macrophages in hepatocytes. In addition to the presentation, APCs can produce IL-12 and TNF-α. Both cytokines are required for development and IFN-γ production of $CD8^+$ T cells while naïve $CD4^+$ T cells need only IL-12 for their

differentiation into T helper (Th)1 cells. After activation, naïve $CD4^+$ T cells will differentiate into Th1 and Th2 based on types of cytokine production while naïve $CD8^+$ T cells become cytotoxic T cells (CTLs). The Th1 cytokines including IFN-γ, TNF-α and IL-2 are essential for the maturation and induction of $CD8^+$ T cells. Conversely, antibody-producing B cells require IL-4 and IL-10 which are produced by Th2 cells for inducing their production of antibody to HBV antigens such as HBsAg, HBcAg and HBeAg. These antibodies play a role in the neutralization of free virus; however, only HBsAb are life-long protective immunity to re-infection. Anti-HBs are synthesized since early infection but they are undetectable due to forming a complex with the excess HBsAg produced during viral replication. CTLs are also responsible for HBV clearance. Depletion of $CD8^+$ T cells in an acute phase of infection, HBV-infected chimpanzees could not control viral replication leading to chronicity. The other study in woodchucks also gives the consistent results. CTLs can control viral replication via cytolytic and noncytolytic mechanisms. The first one, following activation, CTLs can directly destruct the infected cells by stimulation of program cell death through perforin and Fas/Fas-ligand leading to release of the virus. Subsequently, viral particles will be neutralized by antibody from B cells. Another mechanism is the production and secretion of IFN-γ and TNF-α to clear virus via inhibition of pgRNA synthesis, destabilization of viral capsid utilizing the NF-κB pathway, and degradation of viral protein through proteasome-dependent and kinase-dependent pathway and nitric oxide. Although it is found that several HBV components can be a target for CTLs, the core proteins, especially HBc 18-27, are immunodominant epitopes that induce efficient responses. It is widely accepted that CTLs are the principal effector cells for HBV clearance nowadays. However, the coordination of cellular including $CD4^+$ and $CD8^+$ T cells and humoral responses in adaptive immunity is necessary for efficient viral defense (41, 42, 44, 45).

Pathogenesis of hepatitis B

HBV is a non-cytolytic virus. This fact is supported by several clinical studies which indicated that many HBV carriers do not show any symptoms and their livers are minimal injury despite the highly viral replication in their hepatocytes (31). According to studies in chimpanzees and transgenic mice, the histological and biochemical changes in the liver were not observed until the occurrence of specific immunity. Therefore, it is believed that host immune responses to HBV not only result in viral clearance but also lead to liver pathology. The study in transgenic mice shows that liver pathology mainly results from CTLs; however, the non-specific inflammatory cells including neutrophils, NK cells and monocytes together with platelets contribute to severe liver injury (41, 44). In addition to the secretion of antiviral cytokines such as IFN-γ, CTLs can directly destruct infected liver cells through programmed cell death. The high-mobility group box 1 (HMGB1) secreted by apoptotic cells induce

neutrophils into the liver. These cells produce and secrete matrix metalloproteinase (MMP) which degrade the extracellular matrix of the liver resulting in increasing intrahepatic infiltration of inflammatory cells. The chemokines CXCL9 and CXCL10 produced by parenchymal and non-parenchymal in the liver in response to IFN-γ also promote these migrations. Furthermore, platelets secrete some proteins such as P-selectin that interact with CD8+T cells to facilitate these cell into the liver through sinusoids. The more specific and non-specific inflammatory cells influx into the liver, the more severe pathogenesis occur (28, 29, 42, 46).

Chronic hepatitis B

The severity of disease and clinical outcomes of HBV infection are various among people depending on either viral factors or host factors. The efficient and optimal immune response to eradicate virus leading to resolved and self-limiting infection can be observed in people acquired HBV at adolescence or adulthood while the individuals who have over-action of immune response resulting in severe hepatitis and fulminant hepatic failure (3). Conversely, inadequate and improper immunity cause failure of viral clearance and establish of persistence which mostly observed in people exposed to HBV at birth (90%) or early childhood (30%). The chronic hepatitis B (CHB) is defined as the state that HBsAg is still in the serum longer than 6 months because the immune responses are incapable of control and eliminate the virus. The mechanism of HBV chronicity is not well understood, and it might result from either virus or host (31). HBV have evolved strategies to evade immune responses such as mutation of core proteins to escape CTL responses. The plausible factors from virus including HBx protein and HBeAg. The first one HBx protein, multi-functional protein, can alter several cellular pathways and this might influence on immune response and HBV antigen presentation (47). HBx protein can induce the expression of human leukocyte antigen (HLA) class I on hepatocyte surface that facilitate presentation leading to augment of CTLs; however, the increasing number of CD8+ T cells fail to control virus due to lacking effective activities. This phenomenon results in severe liver damage. Another viral factor HBeAg acts as immune tolerogen due to the similarity in structure to HBcAg which are the critical target of immunity. Thus, HBeAg leads to the reduction of response to HBV. In addition to depletion of HBV-specific T cells, HBeAg decreases TLR2 expression on monocytes leading to decrease of TNF-α production. The reduction of this cytokine results in the imbalance of Th1/Th2 responses and this effect causes anti-inflammatory cytokines production such as IL-4 and IL-10. These cytokines subsequently restrain the response of HBV-specific CD4+ and CD8+ T cells. However, the proportion of Th1/Th2 increase after emerging of HBeAb (HBeAg seroconversion) and this lead to effective CTL response as a result of production and secretion of IL-2 and IFN-γ. Besides, the excessive production of non-infectious particle HBsAg might contribute

to the low response of specific-T cells. Other than viral factors, host factors including host genetics and immune status may involve in chronic infection. The studies on the association of HLA-DRB and the ability of HBV clearance in HBV-infected people in Thailand, Gambia, Korea and several western countries give the consistent results that HLA-DRB1*1301-2 are associated with immune response in the protection of CHB (31). In contrast to people with resolved infection, the HBV-specific CD4+ and CD8+ T cells in people with CHB are hypo-responsiveness. The reduction in the number of core-specific CD8+ T cells and their ability to produce IFN-γ are observed especially in HBeAg-positive chronic carriers. HBV-specific CTLs are still detectable in the liver of these carriers but they are incapable of clearing virus due to their low responsiveness and they also cause liver damage. The possible mechanism that can be explained the defect of the immune response in CHB is HBV might inhibit the function of DCs which play a role in T cell priming but this hypothesis is still controversial in the current. The over-expression of programmed cell death (PD)-1 on HBV-specific T cells may be the other mechanisms involving in viral persistence. Generally, PD-1 and its ligands including PD-L1 and PDL-2 are the mechanisms to reduce the inflammation in the liver but the increase in its expression leads to the exhaustion of HBV-specific CTL activity. The activity of CD8+ T cells may be restored by blocking the PD-1 molecule or its ligands. The last probable cause may be the function of regulatory T cells (Treg). These cells express CD4+CD25+ on their surface and they play a crucial role as a negative regulator by inhibition of proinflammatory response. Also, Treg cells can suppress CTL proliferation, inhibit CTL function and diminish the production of IFN-γ and TNF-α. Some studies indicated that the number of Treg cells found in CHB carriers are higher than those of in normal or HBV-resolved individuals. However, depletion of these cells or inhibition of their functions lead to increase in cytokine production of CD8+ T cells (3, 42, 48).

The progression of CHB

In the present, CHB is divided into 4 phases namely immune tolerance, immune clearance (HBeAg-positive chronic hepatitis), low replicative (inactive HBV carrier state) and re-activation phase (HBeAg-negative chronic hepatitis). The HBeAg status and its seroconversion of the first two phases are positive and negative, respectively while low replicative and re-activation phases are negative and positive to HBeAg status and its seroconversion, respectively. The virological, biochemical and histological evidence of each stage are shown in the Table 1.

Table 1. Characteristics of each phase in CHB

Phase	HBeAg	Anti-HBe	HBV DNA (IU/ml)	ALT*	Histological activity
Immune tolerance	Positive	Negative	Very high (>2 x 10^7)	Normal	Normal/ minimal change
Immune clearance	Positive	Negative	High (>2 x 10^4)	Elevated	Hepatic necroinflammation with variable fibrosis level
Low replicative	Negative	Positive	Low (<2 x 10^3)	Normal	Inactive and minimal fibrosis
Re-activation	Negative	Positive	Moderate (> 2 x 10^3)	Elevated	Hepatic necroinflammation with variable fibrosis level

*ALT referred to alanine aminotransferase, the marker for liver injury

The immune tolerance phase is the phase that takes long times more than 10 years especially in a neonate born from chronically infected mother or in people exposed to HBV in early childhood. However, lack or short periods of this phase are observed in the infected people acquired HBV through horizontal transmission. Despite high viral load in the blood circulation, the carriers do not show any clinical appearances of hepatitis because of HBeAg inducing unresponsive HBV core-specific CD4+ and CD8+ T cells. In general, it is not recommended to treat the patients in this phase with anti-viral drugs because the disease progression is not severe and the response to therapy is quite low with 5% of HBeAg seroconversion (anti-HBe) emergence each year. The mechanism of the transition from immune tolerance to immune clearance phase is still unknown. The period of immune clearance phase varies ranging from several months to several years. During this phase, HBV DNA levels are lower than those of in immune tolerance phase as a result of the immune response against HBV. This interaction destroys the infected hepatocytes through apoptosis leading hepatitis. The increase in ALT levels in this period reflects liver inflammation. Approximately 90% of patients achieved HBeAg seroconversion. Of these, 80-90% of patients enter low replication phase while 10-20% was remaining shifts to re-activation phase by skipping the third phase of progression. The yearly rate of HBeAg is 8-12% depending on the age of infection, route of transmission, serum ALT levels, immune status and viral genotype. Many studies reported that good prognosis was observed in the patients who got HBeAg seroconversion before the age of 40 or had a short period of immune clearance with rising ALT levels. In contrast, the patients taking long-time in this phase or getting hepatic flare several times without HBeAg seroconversion increase the risk of cirrhosis and HCC in the future. Low replicative phase takes place following the occurrence of HBeAg seroconversion. In addition to the reduction of HBV DNA and ALT levels, Anti-HBs can be observed in this phase. Although the most of patients have sustained remission, some patients either get HBeAg reversion and then return to the immune clearance phase again or shift to re-activation phase. Although the patients in HBeAg-negative chronic hepatitis phase have seropositive to anti-HBe, HBV DNA levels

are higher than patients in low-replicative phase. Besides, the fluctuated level of ALT reflects that the immune response attempts to control the virus but this reaction is inadequate to inhibit viral replication. The results from the molecular study of HBV from the blood of the patients in this phase show that there are double mutations in basic core promoter (BCP) resulting in the reduction of HBeAg production. This study also demonstrated that mutation in the pre-core gene causing stop codon leads to lack of HBeAg production (3, 31, 42, 46, 48).

Current treatment in CHB

The currently anti-HBV drugs cannot completely eradicate virus due to the persistent form of cccDNA in hepatocytes. Therefore, the short-term purposes of treatment are to suppress viral replication and to achieve HBeAg seroconversion and/or HBsAg seroconversion while the long-term goal of therapy is to delay the development of cirrhosis and hepatocellular carcinoma. Before the beginning of treatment, the indicators should be considered including ALT levels, HBV DNA viral load and histological grade and stage as shown in the following Table 2 (2).

Table 2. Indications of each antiviral treatment

	Interferon (IFN)	**Nucleotide analogues (NAs)**
Age	Less than 60 and healthy	Any
Baseline HBV DNA level	Low	Any
Baseline ALT	Greater than 2-3 X ULN	Any
HBV genotype	A or B	Any
Cirrhosis	No	With or without decompensation

ULN = Upper limits of normal

For example, The American Association for the Study of Liver Diseases (AASLD) recommend that either HBeAg-positive or HBeAg-negative CHB patients with an HBV DNA greater than or equal to 20,000 IU/ml or 2-fold upper limits of normal of ALT level should be treated with anti-viral drugs. In current, there are seven drugs approved for CHB treatment and they are divided into 2 groups namely interferon and nucleos (t) ide analogue based on its actions as shown in the following Table 3 (2).

Table 3. Drugs for CHB therapy

Interferon-based therapy	NA-based therapy	
	Nucleoside analogue-based therapy	Nucleotide analogue-based therapy
IFN-α2a and α2b	Lamivudine	Adefovir
Pegylated IFN-α2a and α2b	Entercavir	Tenofovir
	Telbivudine	

IFN-α is one of the cytokines in immunity that has dual activities including anti-viral and immunomodulatory effects. The former action, IFN-α can inhibit viral replication in several steps of viral life cycle by induction of ISGs possessing anti-viral activities such as 2'-5'-oligoadenylate synthetase (2'-5'-OAS), myxovirus resistance-1 (Mx1), protein kinase R (PKR) and ISG15. This activation affects viral replication through blocking viral transcriptional and translational events and promoting viral RNA degradation (49). The latter action, IFN-α contribute the efficient immune response because it enhances the expression of HLA class I and co-stimulatory molecules on DCs, increase the activity of NK cells and CTLs and promotes the differentiation of naïve T cells to Th1 cells (50). Therefore, IFN-α is used either as anti-tumor drugs such as hairy cell leukemia, malignant melanoma and AIDS-related Kaposi's sarcoma or used as the anti-viral drug in several viral infections such as rhinovirus infection, chronic hepatitis C and chronic hepatitis B. The conventional IFN-α has been approved for treatment of CHB since 1991. The regimen of this drug are subcutaneous administration three times per week for at least 3 months. From the meta-analysis study, it showed that about 33% of HBeAg-positive CHB patients achieved successful responses defined as diminish ALT level, loss of HBeAg and develop HBeAg seroconversion (5). These responses were sustained in the long term despite off-treatment. Several reports indicated that IFN-α might prevent or delayed the development of cirrhosis and HCC. The inconvenience of frequent subcutaneous injection is the disadvantage for this therapy; however, pegIFN-α has been replaced. Pegylated IFN-α is modified interferon by attachment of polyethylene glycol molecule to interferon to improve its immunological, pharmacokinetic and pharmacodynamic properties. The large size of the peg molecule causes IFN-α to increase its half-life due to the reduction of clearance at the kidney. In addition to an increase of biological activity of modified IFN-α, peg moieties may postpone the eradication of recombinant IFN-α by the immune system by reducing the immunogenicity of IFN-α. With these reasons, pegIFN-α allows being administered once weekly. There are 2 forms of pegIFN-α in current namely, pegIFN-α2a (40 kDa of branching peg molecule) and pegIFN-α2b (12 kDa linear peg molecule) (51). The

recommended dose of pegIFN-α2a and pegIFN-α2b for both HBeAg-positive and HBeAg-negative chronic hepatitis patients are 180 μg and 1.5 μg/kg, respectively for 48 weeks. Following completion of pegIFN treatment, HBeAg seroconversion achieves in around 30-40% in patients with HBeAg-positive CHB. More than 80% of these patients have sustained response and loss of HBsAg. The responses including the amount of HBV DNA less than 20000 copies/ml and normalization of ALT level are observed in patients with HBeAg-negative CHB in around 36% after complete treatment. Furthermore, loss of HBsAg is also observed in 3% of these patients and the rate of HBsAg may increase to 10% after 4 years post-treatment (52). Although IFN therapy has benefits including 1) increase of HBeAg and HBsAg seroconversion 2) delay development of progressive disease 3) finite duration of treatment and 4) no drug resistance, the limitations of IFN treatment are following 1) subcutaneous injection 2) moderate HBV DNA suppression and 3) adverse effects such as influenza-like symptoms (fatigue and fever), weight loss, cytopenia, depression, anxiety, abnormal function of thyroid gland and suppression of bone marrow (5). In contrast to indirect action on viral replication of IFN-α, NA directly inhibits viral replication by acting as a competitive inhibitor of the HBV polymerase in several steps of HBV life cycle as shown in the Table 4.

Table 4. Action of NA

Structure	Drug	Polymerase function		
		Priming	Minus strand synthesis	Plus strand synthesis
L-nucleosides	Lamivudine (CA)		x	x
	Telbivudine (TA)			x
Deoxyguanosine analogue	Entercavir (GA)	x	x	x
Acyclic nucleotide phosphate's	Adefovir (AA)		x	x
	Tenofovir (AA)		x	x

CA = Cytidine analogue, TA = Thymidine analogue, GA = Guanosine analogue and AA = Adenosine analogue

These drugs can incorporate into viral genome during viral replication due to the similarity of their structure to natural nucleotide; however, the next nucleotide can't bind to NA because these drugs lack hydroxyl group in their structure. This lead to chain termination and eventual inhibition of viral replication (2). NA can restrain HBV polymerase activity by inhibition of priming in step of reverse transcription, inhibition of RNA dependent DNA polymerase or reverse transcriptase in step of elongation negative strand, and inhibition of DNA dependent DNA polymerase in step of plus strand synthesis. Although NA suppress viral replication resulting in the reduction of HBV DNA in liver and blood circulation, NA do not inhibit cccDNA synthesis in the liver but it is able to reduce the turn-over of virus into the nucleus of hepatocytes resulting in the reduction of cccDNA in the liver. In addition

to inhibition of viral replication, NA can prevent and reduce the development of cirrhosis, liver failure and HCC (5). The 5 approved oral NA drugs for CHB treatment are lamivudine, adefovir, entecavir, telbivudine and tenofovir (2). Treatment with lamivudine results in reduction of HBV DNA, ALT normalization and achievement of HBeAg seroconversion in around 15-20% and 25-30% of patients with HBeAg positive CHB after 1-year and 2-year post-treatment, respectively. However, prolonged therapy with lamivudine cause development of viral resistance 14-24% and up to 76% of case after 1 and 5 years of treatment. This is the reason why lamivudine is limited in current. Due to high rate of viral resistance, lamivudine is not recommended to use as first-line therapy. Although the combination treatment between IFN and lamivudine are able to reduce the emergence of lamivudine-resistant HBV, the responses are not redundant or synergistic effects (4, 7, 53). The second one, adefovir dipivoxil is a guanosine nucleotide analogue. Although the efficiency on suppression of HBV DNA is less than lamivudine, the occurrence of viral resistance is lower than first one with 2% and 29% of case following 1 and 5 years of therapy. Following 1 year of treatment with this drug, the patients with HBeAg-positive CHB achieve HBeAg seroconversion in around 12-18% of case and HBA DNA level in blood circulation is undetectable about 13-21% while HBV DNA level is undetectable approximately 51-63% in case of the patients with HBeAg-negative. Adefovir is suitable for patients with lamivudine-resistant HBV because two drugs are not cross-resistance. Due to the moderate suppression of HBV DNA, this drug is not suggested to treat HBeAg-positive CHB patients who have high HBV DNA level in their blood. Furthermore, it is not recommended to use as first drug for CHB treatment because of its nephrotoxicity. Thus, the use of adefovir is limited and it is mainly used in patients with lamivudine-resistant HBV (5, 7, 53). Entecavir is the first-line therapy for CHB that can efficiently reduce HBV DNA level both in patients with HBeAg-positive (67%) and HBeAg-negative (90%) CHB after 1 year of treatment and this effect still sustain following 5 years of continuous treatment with entecavir. Its potency in suppression of HBV DNA is higher than lamivudine and adefovir because it can inhibit HBV polymerase in 3 steps of HBV life cycle. However, the rate of occurrence in HBeAg seroconversion is not different from lamivudine and adefovir treatment, that is, the loss of HBeAg is achieved about 20% and 30% of patients with HBeAg-positive CHB after 1 and 2 years of entecavir treatment. The emergence of resistance is low with 1.2% after 5 years of treatment; however, the rate may increase up to 51% in patients with lamivudine-resistant HBV following 5 year treatment. The reasons why entecavir is low resistance are the effective viral suppression and the requirement of at least 3 sites of mutation for induction of entecavir resistance (5, 54-56). The reduction of HBV DNA levels by telbivudine treatment are 60% and 88% of patients with HBeAg-positive and HBeAg-negative CHB, respectively after 1 year of treatment. The occurrence of HBeAg seroconversion is 22.5% and 29.6% of case after 1 year and 2 year of treatment. The

emergence of resistance is low with 5% and 25% of case after 1 and 2 years of treatment, respectively. The telbivudine-resistant HBV is cross-resistance to lamivudine and entecavir. The main limitation of this drug is undesired side effect including myalgia and peripheral neuropathy (55, 56). Another drug, tenofovir disoproxil fumarate belongs to extremely HBV reduction and the magnitude of suppression is similar to entecavir and telbivudine. Moreover, tenofovir-resistance is not observed after 4 years of treatment and this drug is used to treat lamivudine-resistant HBV. The HBV DNA level is unquantifiable in around 76% of case and the emergence of HBeAg and HBsAg seroconversion are 21% and 2% of case after 1 year of treatment and 27% and 6% of case after 2 year of treatment in patients with HBeAg-positive CHB. For patients with HBeAg-negative CHB, the reduction of HBV DNA level is about 93% of case. With these reasons, tenofovir is suggested to use as a first-line therapy in naïve both HBeAg-positive and HBeAg-negative CHB patients (5). Although the antiviral treatments for CHB in the present are efficient in the suppression of HBV DNA and achieve HBeAg seroconversion which are the aims of treatment, there are still some limitations which shown in the Table 5. Thus, the novel agents that overcome these restrictions are still required (5, 7, 53-57).

Table 5. Comparison advantages and limitations of each treatment

	Interferon (IFN)	Nucleotide analogues (NAs)
Advantages	No drug resistance	Oral administration
	Increased HBsAg seroconversion	More potent HBV DNA suppression
	More durable off-treatment	Minimal side effects
	Finite therapy duration	
Limitations	Subcutaneous injection	Risk of resistance on prolonged therapy
	Less potent HBV DNA suppression	No increase in HBsAg seroconversion
	Frequent side effects	Less durable off-treatment response
		Long-term therapy

Introduction to Interferon lambda (IFN-λ)

Interferons have been classified into 3 types including type I, II and III based on their structures, receptors and biological functions. Type III IFN or IFN-λ is a novel cytokine of class II cytokine family additionally consisting of IL-10 family (IL-10, IL-19, IL-20, IL-22, IL-24 and IL-26), type I IFN (13 isoforms of IFN-α and 1 isoform of IFN-β, IFN-ε, IFN-κ, IFN-ω and IFN-τ) and type II IFN (IFN-γ). This cytokine discovered in 2003 by two research groups independently contains 3 subtypes including IFN- λ1, IFN- λ2 and IFN- λ3. These cytokines are also known as IL-29, IL-28A

and IL-28B, respectively. In spite of the structural similarity to the IL-10 family, IFN-λs have biological functions like type I IFN. Type III IFNs exert their activities through their receptor complex containing IFN-λR1 (IL-28RA) and IL-10R2 (58, 59).

Gene organization of IFN-λs

The IFN-λ genes are encoded on chromosome 19 at 19q13.3 region. IFN-λ1 gene contains 5 exons while IFN-λ2 and IFN-λ3 consist of 6 exons. In contrast to intron-lacking genes of type I IFN, The exon-intron organization are conserved in IFN-λ genes which are similar to those of IL-10-like cytokines. During duplication, the fragment containing IFN-λ1 and IFN-λ2 genes was copied and subsequently integrated back into the genome in a mirror-inversion or head-to-head orientation with the IFN-λ1 and IFN-λ2 segment. This phenomenon results in the production of IFN-λ3 and non-functional pseudogene IFN-λ4Ψ on the negative strand while IFN-λ1 and IFN-λ2 genes lay on the positive strand. Thus, IFN-λ3 gene is transcribed in the opposite direction of IFN-λ1 and IFN-λ2 genes. The coding region together with the upstream and downstream flanking sequences of IFN-λ3 gene are nearly identical to those of IFN- λ2 gene; therefore, IFN-λ2 and IFN-λ3 are more homologous each other than IFN-λ1. However, the promoter of IFN-λ2 and IFN-λ3 genes are similar to those of the IFN-λ1 gene. The promoter of three IFN-λ genes contains several binding sites for nuclear factor-ΚB (NF-ΚB), interferon regulatory factor (IRF) 3 and 7 which are similar to those of type I IFN. Thus, it is implied that the stimuli activating type I IFN expression may also induce type III expression (60-62).

Induction of type III IFN expression

In response to viral infection, several cell types are capable of IFN-λ production especially plasmacytoid dendritic cells (pDCs); nevertheless, macrophages which are the cells that massively generate IFN-α did not produce IFN-λ. Like type I IFNs, IFN-λs are mainly induced by viral infection. The nucleic acids of virus which are one of the pathogen-associated molecular patterns (PAMPs) are a potent inducer of IFN response. In the cellular cytoplasm, there are several sensing molecules called pattern recognition receptors (PRRs) including retinoic acid-inducible gene 1 (RIG-1) and melanoma differentiation-associated protein 5 (MDA5) to detect the PAMPs while Toll-like receptors (TLRs) -3, -7/8 and -9 detect the PAMPS in the endosome. After recognition, signaling transduction is generated through adaptor molecules and kinases resulting in activation of IRF3, IRF7 and NF-ΚB, which in turn bind the promoter of type I and III IFN leading to IFN production. Both types of IFN are stimulated via these transcription factors; however, IFN-λ2/3 are mainly activated by IRF-7 like

IFN-α while IRF3 primarily induce IFN-β and IFN-λ1. For NF-ΚB pathway, it is the main activators of type III IFN expression because the inhibition of this pathway in DCs results in suppression of IFN-λ production while type I production has a little effect (60, 63).

Signaling pathway of IFN-λ

All 3 subtypes of IFN-λ exert their biological activities by triggering signal to the heterodimeric receptor complex contained IFN-R1 and IL-10R2 which are encoded on chromosome1 (1p36.11 region) and chromosome 21 (21q22.11 region), respectively (58, 59). The former receptor is not only crucial for IFN-λ signaling due to providing the binding energy but also unique for IFN-λ and expresses in specific organs which are epithelial cell origin including pancreas, thyroid, skeletal muscle, heart, prostate testis and liver. While the latter receptor is ubiquitously expressed in many organs and this receptor is also utilized by IL-10 and IL-22. Also, IL-10R2 is required for proper signal transduction (58, 59, 64). After binding of IFN-λ to its receptor complex, the Janus kinase 1 (Jak1) associated with IFN- λR1 and the Tyrosine kinase 2 (Tyk2) associated with IL-10R2 are subsequently activated resulting in cross-phosphorylation each other of two kinases. Following this activation, the two phosphorylated tyrosine (Tyr313 and Tyr517) on intracellular domain of IFN- λR1 are generated docking site for Src homology 2 (SH2) part of signal transducers and activators of transcription (STAT). This result in bringing this protein close to the activated kinases to phosphorylate the tyrosine residues to create a docking site at the C-terminal end of the STAT for the SH2 domain of the other STAT. In this case, the heterodimer of STAT-1 and STAT-2 recruit IRF9 to form the complex called IFN-stimulated gene factor 3 (ISGF3). This transcription factor subsequently translocates into the nucleus where it binds to the promoter of ISGs called IFN-stimulated response elements (ISRE) (60, 61, 63, 64). Consistent with these, Zhang et al. demonstrated that IL28B, IFN-λ3, induced STAT-1 and STAT-2 phosphorylation like IFN-α indicating that IL-28B signals through the JAK-STAT pathway. To confirm this finding, they treated JAK inhibitor 1 which is an inhibitor of Jak1 and Tyk2 into the liver cell line harboring full-length HCV RNA before treatment with IL28B to inhibit JAK-STAT pathway and they found that the expression of known ISG MxA and ISG15 was reduced and IL-28B did not suppress HCV core protein expression (65). From microarray study, it showed that the pattern of genes induced by IFN-λ is nearly similar to those induced by IFN-α with different kinetics. The expression of IFN-α-induced genes was observed since 3 hours of post-treatment and they largely decreased their expression by 24 hours. Conversely, the expression of IFN-λ-induced genes proceeded to increase their expression. Moreover, some genes were induced by IFN-λ but not induced by IFN-α, confirming that IFN-λ might induce these genes through signaling to other pathways (66).

IFN-λ subtypes

All 3 IFN-λ subtypes belong to class II cytokine family. The outstanding characteristics of this family are structural feature and pattern of disulfide bonds. The crystal structure of IFN-λ3 revealed that IFN-λs are an α-helical structure with 6 secondary elements which are similar to other class II cytokines. These cytokines have a unique pattern of disulfide bonds. IFN-λ1 has only 5 cysteines while the remaining have 7 cysteines. The study on the crystal structure of IFN-λ3 also showed that IFN-λ2/3 has 3 disulfide bonds in its structure. However, only 2 disulfide bonds are observed in IFN-λ1. In addition to the disulfide bond, the difference between IFN-λ1 and IFN-λ2/3 is glycosylation. The observation on the production of these proteins in mammalian cells found that both IFN-λ2 and IFN-λ3 were not glycosylated while IFN-λ1 have 1 potential N-linked and 6 potential-linked glycosylation sites. However, these glycosylations seem not to have any effect on its activity. Furthermore, the alignment of amino acid showed that IFN-λ2 were highly identical to IFN-λ3 with 96% sequence identity whereas IFN-λ1 shared 81% sequence identity with IFN-λ2/3. To compare the sequence identity of type III IFN with other class II cytokines, for example, the sequence similarity between IFN-λ3 and IL-19 or IFN-λ3 and IFN-α2 is 21% and 31%, respectively. With consideration of the similarity of amino acid sequence, type III IFNs are closely related to type I IFN more than IL-10-like cytokines (60-62). The potency of all subtypes was tested by regard to the ability of IFN-λ subtypes to protect cell lysis by encephalomyocarditis virus (EMCV). The results determining by EC50 values showed that IFN-λ3 exhibited the highest potency among the others with 2-fold and 16-fold higher than IFN- λ1 and IFN- λ2, respectively. However, the potency of IFN-λ3 is less than that of IFN-α (10-fold) (10). In agreement with these results, Leiliang Zhang et al. demonstrated that all 3 types of IFN-λ suppressed HCV replication and IL-28B seemed to be more potent than the others (IL28B > IL29 > IL28A). However, IFN-α appeared to be stronger to inhibit HCV replication about 15-folds than IL-28B (65). The results from Man-Qing Liu et al. study which determined the antiviral activities of IFN-λs on HIV replication also showed the correlated results (65). The weaker potency of IFN-λ might result from the restricted expression of IFN-λ receptor compared to the broad expression of IFNAR. The activities of IFN-λ2 and IFN-λ3 are different although two cytokines have the high identity and only differ by 6 amino acids. The cause of loss activity are still unclear nowadays; however, there is a hypothesis that the large molecule of Val95 in IFN-λ2 (Gly95 in IFN-λ3) located in helix D domain which is crucial for interaction with IL-10R2 might destabilize this domain resulting in less potency of IFN-λ2 (61).

Biological activities of IFN-λ

The usage of receptors of IFN-λ differs from those of IFN-α; however, signal transduction of both cytokines trigger through the JAK-STAT pathway. Moreover, the patterns of gene expression induced by IFN-λ are nearly identical to that induced by IFN-α. Therefore, IFN-λs possess the antiviral, antiproliferative and immunomodulatory activities like type I IFNs (58, 59, 64, 67). IFN-λs have shown its antiviral effects against several viruses such as encephalomyocarditis virus (EMCV), vesicular stomatitis virus (VSV), influenza A virus (IAV), cytomegalovirus (CMV), human immunodeficiency virus (HIV), hepatitis C virus (HCV) and hepatitis B virus in several experimental models. In addition to the in vitro study, IFN-λ also inhibits vaccinia virus (VV) and herpes simplex virus (HSV) in vivo. In agreement with antiviral function, IFN-λs are able to induce OAS1 and MxA expressions which are known as common features of the antiviral response (68). Besides, like antiviral activity, the antiproliferative effect of IFN-λ is limited in some cell types especially in tissues from the epithelial origin which highly express IFN-λR1 (61, 69). One group studying the antitumor function of this cytokine demonstrated that the tumor size of tumor-introduced mice which were injected with the plasmid harboring murine IFN-λ had smaller than that of untreated mice. They were supposed that this might result from increased NK activity and tumor cells apoptosis which are induced by IFN-λ. Furthermore, IFN-λs contribute the adaptive immune response by up-regulating the expression of major histocompatibility complex (MHC) class I (61, 69).

IFN-λ and viral hepatitis

There are many studies about the effect of IFN-λs on HCV. All of these showed that HCV replication was suppressed in a dose-dependent manner after IFN-λs stimulation by determining the reduction of either HCV RNA or protein expression (65, 68, 70, 71). The combination treatment either between IL-29 and IFN-α or between IL-29 and IFN-γ on hepatocyte cell line containing HCV RNA showed that the reduction of HCV RNA expression after treatment with combinations was higher than that treated with individual cytokines. The co-treatment of IL-29/IFN-α and IL-29/IFN-γ reduced HCV RNA expression by 92 and 98%, respectively (68). Recently, the genome-wide association studies (GWAS) have indicated that a single nucleotide polymorphism (SNP), rs12979860, in the upstream of IL28B was associated with the response to pegIFN-α plus ribavirin (RBV) treatment and spontaneous clearance of HCV. Following standard therapy of pegIFN-α and RBV, the HCV-infected patients with CC genotypes have the rate of sustained virological response (SVR) higher than those with CT or TT genotypes (72-74). However, this SNP is not associated with clearance of HBV DNA, HBsAg and HBeAg (75-77). Although the SNP in the IL28B gene is not linked to the clinical outcomes

of HBV infection, IFN-λs have shown their antiviral activity against this virus. In 2005, Robek et al. determined the antiviral function of IFN-λ2 against HBV replication by using murine liver cell line harboring HBV (HBV-Met) as a model. The experimental result showed that 10 ng/ml of murine IFN-λ2 could inhibit HBV replication greater than 90% at 24 hours after post-stimulation and this result was also observed in HBV-Met cells treated with 200 U/ml of IFN-β at the same time (71). Consistent with this study, the study of Seung-Ho Hong et al. also showed that IFN-λ1 suppressed HBV replication in human hepatocyte containing HBV cell line at 48 hours after post-treatment (78). As described above, the antiviral activity of IFN-λ is weaker than that induced by IFN-α; however, the restricted its receptor expression resulting in less of unfavorable side effects and the prolonged response of IFN- λ may let this cytokine be the novel therapeutic agent. Recently, a clinical trial showed that the SVR of the patients with chronic hepatitis c treated with pegIFN-λ1 together with RBV for 24 weeks were similar to that of patients treated with standard regimen but the rapid reduction of HBV RNA level was observed in patients treated with pegIFN-λ1. Also, the patients treated with pegIFN-λ1 had fewer adverse effects and lesser elevated ALT that those treated with a standard course (79). For treatment with CHB, a clinical study revealed that pegIFN-λ1 reduced the amount of HBV DNA, HBsAg, and HBeAg greater than pegIFN-α in the early phase of on-treatment. At the end-of-treatment, the effects of pegIFN-λ1 on virologic, serologic, biochemical responses were comparable to pegIFN-α. However, no non-inferiority was observed in pegIFN-λ1 at week 24 post-treatment. The fewer adverse events were found in the patients treated with pegIFN-λ1 (9). In addition to reducing HBV DNA and HBsAg levels, another clinical study demonstrated that peg-IFNλ showed immunomodulatory effects by the maintenance of HBV-specific CD8+ T cells and enhancement of natural killer cell polyfunctionality (80).

The tools used to study molecular mechanism

So far, we have known that IFN suppresses HBV replication by preventing the association of viral RNA and immature nucleocapsids which take place in the cytoplasm (81). Although several studies proposed the molecules involving in antiviral properties of IFN including MxA, apolipoprotein B mRNA-editing, enzyme-catalytic, polypeptide-like 3G (APOBEC3G) and myeloid differentiation primary response protein (MyD88), the picture of global effects responding to IFN is not complete (82-84). A microarray is a powerful tool providing the information about the biological process in mRNA level. XIONG Wei et al. used this tool to study about the global effects of IFN-α and IFN-β on HepG2 and HepG2.2.15 (HBV-transfected cell line) showed that the functional categories of IFN-α responsive genes were cell cycle, apoptosis, extracellular matrix, signal transduction, interferon-

inducible and proteasome components. From this result, the researchers were interested in MyD88 which are one of the components in signal transduction responding to IFN-α and they confirmed the role of this gene in antiviral activity by cloning this gene into the plasmid and then co-transfecting with HBV replicative cell line (85). MyD88 could inhibit HBV replication and reduce the synthesis of HBsAg and HBeAg. Although microarray is a large-scale quantitative analysis of mRNA expressions, mRNAs do not reflect the exact functional molecules while proteins do. Protein is vital components of an organism which play a role in physiological processes and complex biological networks are mediated by proteins. Furthermore, due to post-transcriptional processing and post-translational events, the poor correlation between mRNAs and proteins has been demonstrated. Therefore, high-throughput study at the proteome level, proteomics, should be carried out (86, 87). Jianhua Wang et al. studied the global proteins of HBV-transfected cell responding to IFN-α using proteomics utilizing 2-dimensional gel electrophoresis (2-DE) and mass spectrometry (MS). They found that IFN-α-responsive proteins were involved in ATP binding, cell cycle, apoptosis, ATPase activity and electron transport. From this result, they were interested in prohibitin which its function are cell cycle, apoptosis and proliferation. Prohibitin can bind and interact with p53 which possess antiviral and antitumor properties; however, p53 and its downstream apoptosis protein, caspase7, could not be observed in 2-DE. This result might be from the low amount of proteins and low sensitivity of gel staining. Nevertheless, the mRNA expression of prohibitin, p53 and caspase7 were detectable using RT-PCR. To confirm this result, annexin V-FITC/PI assay revealed that IFN-α induced cell apoptosis. The researchers indicated that IFN-α induced prohibitin to bind to the p53 protein and allow infected cells to apoptosis (23). Although 2-DE is commonly used, there is some limitations including poor reproducibility (gel-to-gel variation), low sensitivity in identifying proteins with extreme pH (too low pH or too high pH), low sensitivity in identifying proteins which their molecular weights are too low or too high, labor-intensive technique, time-consuming as well as detection of low abundance or hydrophobic proteins (88-90). To overcome these limitations, gel-free proteomics has been developed. This technique, complex mixture of proteins are digested in solution and subsequently fractionated and analyzed by tandem mass spectrometry (88, 90, 91).

Quantitative proteomics

MS is a powerful tool for protein identification; however, it not provide the quantitative information from peptide intensities. Because of the efficiency of ionization, signals generated from MS are variable from peptide to peptide. Quantitation strategies using stable isotope labeling provide qualitative (protein identification) and quantitative information. Stable isotope labeling allows samples more than 2 different states to be analyzed in a single run (92). The chemical and physical properties

of one isotope-labeled peptides are identical to the other isotope-labeled peptides but the difference in mass introduced by isotope labeling which can be distinguished by MS. The relative intensities of different isotopes generated by MS reflect the relative quantity of the peptides in various states of the samples (93). Each method of isotopic labeling can be introduced into different sample level either in viable cell in cell culture (stable isotope labeling by amino acids in cell culture, SILAC) or in protein level (isotope-coded affinity tag, ICAT) or in peptide level (isobaric peptide tags for relative and absolute quantification (iTRAQ), tandem mass tags (TMT), and dimethyl labeling) via metabolic or chemical labeling (94, 95). Stable isotope labeling by amino acids in cell culture (SILAC) is based on metabolic labeling in cultured cells. The isotopically labeled amino acids such as 13C6-Arg are added to the culture medium; therefore, these isotopes incorporate into the cells during their growth. This labeling will complete when the cells grow and divide into several passages. After that, the differentially labeled cells are combined, digested and analyzed by MS. The quantitative information is obtained by comparing the relative peak intensities generated from these differentially labeled peptides at the MS1 scan (96). Isobaric peptide tags for relative and absolute quantification (iTRAQ) and tandem mass tags (TMT) label the samples at the peptide level by covalent labeling of primary amine both N-termini and side chain of lysine residues with isobaric tags. The isobaric tag contains 3 part namely, a reporter group, a mass balance group, and a peptide-reactive group. At the MS1 scan, all differentially labeled peptide have identical m/z due to the constant total mass of isobaric tags. Therefore, the relative quantification is obtained from the MS2 scan. Stable isotope dimethyl labeling is a simple, reliable and cost-effective quantitative proteomic method based on chemical labeling at the peptide level. The principle of this techniques is reductive amination. The formaldehyde interacts with the Ɛ-amino group of the side chain of a lysine residue or the N-terminus of a peptide (primary amine) to form Schiff base and these intermediates are subsequently reduced by sodium cyanoborohydride to form a secondary amine and convert to dimethyl amines as shown in the following Figure 1.

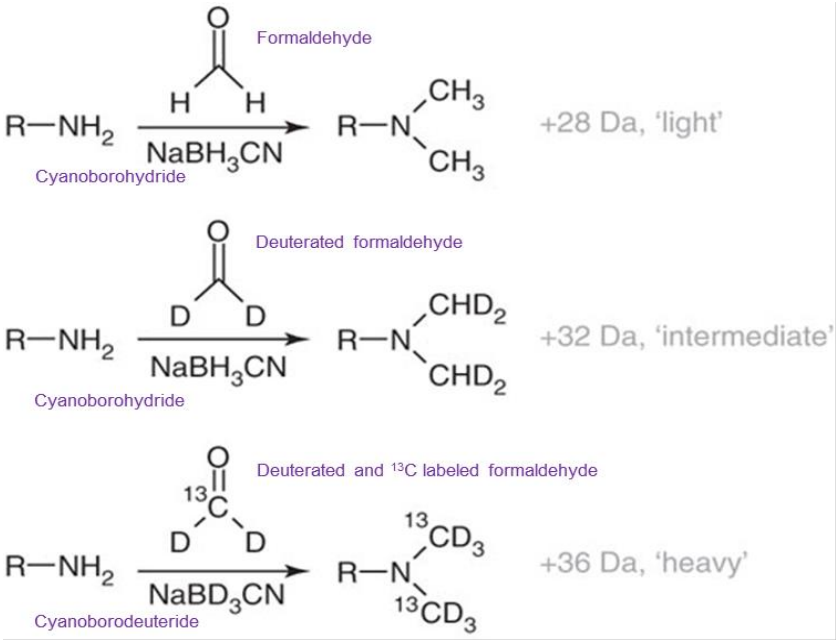

Figure 1. The reaction of dimethyl labeling.

Multiplex at least 3 labeling can be generated by different combinations of isotopomers of formaldehyde and cyanoborohydride: CH2O/NaBH3CN (light), CD2O/NaBH3CN (medium) and 13CD2O/NaBD3CN (heavy). The first combinations generate a mass increase of 28 Da while the medium and heavy labeling generate a mass increase of 32 Da and 36 Da, respectively. The labeled peptide differ in mass by only 4 Da between light and medium labeling and between medium and heavy labeling whereas light and heavy labeling have mass difference 8 Da. Like SILAC, the quantification of this method is based on MS1-scan (97, 98). The advantages and limitations of each labeling was showed in the Table 6.

Table 6. Comparison of strengths and weaknesses of each labeling technique

	Strengths	Limitations
SILAC	Introduction of isotope label at the cell or organism level No limits to amount of sample to be labeled	Not applicable to human samples Expensive to culture and reach full incorporation Labeled arginine might convert to proline
Dimethyl labeling	Cheap reagents Quick reaction Can be automated by performing the reaction online with LC-MS Applicable to any sample (animal/human tissue samples) Capable of labeling of sub-micrograms to milligrams of sample	Introduction of isotope label at peptide level Small isotope effect in LC separation
iTRAQ	Labeling of up to ten different samples No increased complexity at MS level Applicable to any sample (animal/human tissue samples)	Introduction of isotope label at peptide level Reagents are chemically not very stable Expensive reagent Choice of the mass spectrometer is limited to those capable of measuring at low m/z Peptide quantification is based on a single tandem mass spectrum

EXPERIMENTAL PROCEDURES

Experimental design and statistical rationale.

Mixing of dimethyl-labeled samples corresponding to IFN-λ3, IFN-α2a, and control (PBS) treatments were performed at n = 5 vs. the typical n = 3 in order to emphasize depth. Only biological replicates were performed. The normality of all proteomics, western-blotting and qPCR data was evaluated with the Shapiro-Wilk test. In all cases, the unpaired Student's t-test or one-way ANOVA was selected when the distribution of the data was normal; otherwise the Mann–Whitney U test was applied. For proteomic analysis, peak intensity $\log_2$ ratios (L/M, L/H, M/H) were compared against a value of 0 (no change, $\log_2(1)$). Significance was based on the following criterion: p-value < 0.05 or cases where proteins were detected in only one condition making standard statistical analysis inapplicable, with the requirement that these proteins must be identified in at least 4 of 5 experiments. Proteins not fulfilling the above criteria as well as those appearing in fewer than 3 experiments, were excluded from downstream analysis. Regarding western-blotting and qPCR experiments, n=3 was set. One-way ANOVA was performed for these experiments with p-value < 0.05 considered significant. In the case of DAVID enrichment analysis, all proteins identified by mass spectrometry were input as background. When Fisher-based enrichment analysis was performed against an in-house database of proteomic/transcriptomic studies, resulting log(p-values) were conservatively adjusted by subtracting the log value corresponding to the total of all possible study/study combinations in the database.

Chemicals and reagents.

Culture media and all supplements used in this study were purchased from Gibco. Recombinant IFN-λ3 (5259-IL-025) was purchased from R&D Systems as a lyophilized form and dissolved to a concentration of 100 µg/ml in sterile PBS containing 0.1% BSA. Aliquots of reconstituted IFN-λ3 were stored at -80°C until use. Recombinant IFN-α2a (11100-1) was purchased from pbl assay science as a solution. The Lot No. of this product is 6336 which activity and specific activity are 1.68×10^8 units/ml and 7.3×10^8 units/mg, respectively. The concentration of IFN-α2a was adjusted to 100 µg/ml in PBS containing 0.1% BSA and kept at -80°C until use. All reagents used in cDNA synthesis and qPCR were obtained from Applied Biosystems. Formaldehyde-d_2 and cyanoborodeuteride were purchased from Cambridge Isotope Laboratories (CIL). Triethylammonium bicarbonate (TEAB), 50% formic acid (FA), sodium deoxycholate (SDC), formaldehyde, deuterated ^{13}C-labeled formaldehyde, sodium cyanoborohydride, and thiazolyl blue tetrazolium bromide (MTT) powder were purchased from Sigma. All reagents used in SDS-PAGE electrophoresis were

purchased from Bio-Rad Laboratories. Anti-SAMHD1 (#12361), anti-STAT1 (#9175), and anti-GAPDH (#5174) antibodies were purchased from Cell Signaling Technology (CST). Anti-OAS3 (ab64163) was purchased from Abcam. Odyssey Blocking Buffer and IRDye 680RD secondary antibody were obtained from LICOR-Biosciences. Trifluoroacetic acid (TFA) and 25% ammonia solution were purchased from Merck. Dithiothreitol (DTT) and iodoacetamide (IA) were purchased from GE Healthcare. All other reagents not mentioned here or not specified elsewhere were obtained from Thermo.

Cell culture and cell stimulation.

HepG2.2.15 cells are stable HBV-transfected cells derived from a hepatoblastoma HepG2 cell line (20). These cells contain a plasmid which expresses the complete genome of HBV, which integrates into host cellular DNA (20, 99). Because HBV within HepG2.2.15 replicates and secretes HBsAg, HBeAg and HBV DNA into the culture media, HepG2.2.15 has been widely used as a model of chronic hepatitis B (22, 99). The HepG2.2.15 cell line was kindly provided from Professor Antonio Bertoletti (Singapore Institute for Clinical Sciences, A*Star). These cells were maintained in Dulbecco's Modified Eagle's Medium (DMEM) supplemented with 10% Fetal Bovine Serum (FBS), 1% MEM Non-Essential Amino Acids (MEM-NEAA), 1% Penicillin/Streptomycin and Geneticin (G418) at a final concentration of 150 µg/ml. The cultured cells were grown in a humidified incubator at 37^{o}C with 5% CO_2. One million HepG2.2.15 cells were seeded into 6-well plates with 1 ml media and maintained in complete DMEM for 24 hours. For determining the effects of IFN-λ3 on HepG2.2.15, these cells were left untreated or treated with 1, 10, 100 or 1000 ng/ml of IFN-λ3 and incubated for another 24 hours. For proteomics analysis, HepG2.2.15 cells were plated at 5 x 10^6 cells in T-75 flasks and grown in complete DMEM for 24 hours at 37^{o}C. These cells were subsequently cultured in media with 100 ng/ml of IFN-λ3 or 100 ng/ml of IFN-α2a or PBS (control) for another 24 hours. For further qPCR experiments with an optimized concentration of IFN-λ3, HepG2.2.15 cells were stimulated with or without 100 ng/ml of IFN-λ3 for 0, 8, 16, and 24 hours.

RNA isolation, reverse transcription, and qPCR for gene expression.

TRIzol Reagent was used to extract total RNA as specified in the accompanying manual. Briefly, the culture medium was discarded from culturing plates and 1 ml of TRIzol Reagent was directly added into each well followed by mixing the cells several times and incubating for 5 minutes at room temperature to ensure that the cells were completely lysed. Phase separation was generated by adding 100 µl BCP (bromochloropropane, MRC), used instead of chloroform, with vigorous shaking. Following incubation at room temperature for 3 minutes, the mixtures were centrifuged at

12,000 x g for 15 minutes at 4^{o}C. The colorless aqueous phase containing RNA was transferred into a new tube, precipitated by absolute isopropanol with incubation at room temperature for 10 minutes and centrifuged at 12,000 x g for 10 minutes at 4^{o}C. Subsequently, RNA pellet was washed with 75% ethanol followed by centrifugation at 7,500 x g for 5 minutes at 4^{o}C to remove any salts. The dried pellet RNA was re-suspended with RNase-free water and incubated in heat box at 60^{o}C for 10 minutes. The concentrations of RNA were measured by spectrophotometer (Nanodrop, Thermo SCIENTIFIC) and their purities were determined by the ratio of absorbance at wavelength of 260 nm to 280 nm. RNA was stored at -80^{o}C until further use. Complementary DNA (cDNA) synthesis was carried out using the Taqman Reverse transcription kit. Two hundred micrograms of RNA were served as template in the reaction. The master mix was prepared according to manufacturer's recommendation described in appendix. Conditions for reverse transcription were as specified in the manual that was 25^{o}C for 10 minutes, followed by 48^{o}C for 30 minutes and 95^{o}C for 5 minutes. cDNA was kept at -20^{o}C until further use. Relative gene expression was measured with the ABI Prism 7500 sequence detection system (Applied Biosystems). All primers and probes were designed with the "primer express 3" program (Applied Biosystems), and are shown in Supplementary Table S1. The master mix for all target genes composed of RNase-free water, 20 μM of each forward and reverse primers and Power SYBR Green PCR Master Mix. For housekeeping gene 18s rRNA, the components of master mix were similar to those of target genes but probe was utilized to monitor gene amplification instead of SYBR green dye. To monitor gene amplification, the intensity of fluorescence from the 18S housekeeping gene was monitored via *Taq*man probe while all target gene levels were monitored via SYBR green dye. To test the specificity of SYBR green dye, melting curve analysis was conducted for all target genes. The condition of amplification for both target and housekeeping genes was 1 cycle at 95^{o}C for 5 minutes followed by 40 cycles at 95^{o}C for 15 seconds and 60^{o}C for 1 minute. The Melting curve analysis was performed only in the reactions using SYBR Green as a detector to ensure the specificity of primers and target genes. The intensity of fluorescent generated by SYBR Green or probe which was higher than threshold was measured as a Ct value Relative gene expression was calculated with the 2^{-ddCt} method. The Student's *t*-test and one-way ANOVA were used to compare the relative expressions of target genes in cells treated with various doses of IFN-λ3. A p-value less than 0.05 was considered significant.

DNA extraction and absolute qPCR.

After trypsinization and PBS-washing, cellular DNA was extracted using the QIAamp DNA Blood Mini Kit (Qiagen) according to manufacturer's instructions. In brief, cell pellets were re-suspended inh PBS followed by adding QIAGEN proteinase and AL buffer. After vortex-mixing and

incubation at 56°C for 10 minutes, absolute ethanol was added to the mixtures. These mixtures were applied into QIAamp Spin columns and centrifuged at 8000 x rpm for a minute. Buffer AW1 was added into the columns followed by centrifugation at 8,000 x rpm for 1 minute. Before DNA elution, Buffer AW2 was added into the columns and then centrifuged at 14,000 x rpm for 3 minutes. Distilled water was used as an eluent to elute DNA from columns and DNA was kept at -20°C until use. Quantification of HBV viral load was performed by absolute quantitative real-time PCR using the ABI Prism 7500 sequence detection system. For ease of plasmid amplification, we used plasmids containing only the HBV gene *preS1* as a surrogate marker for HBV DNA (preS1 was chosen because it is highly conserved across all HBV genotypes). First, preS1 plasmids were extracted from *E. coli* transformants with the GeneJET Plasmid Miniprep Kit (Fermentas). The concentration of extracted plasmids was measured by spectrophotometer and copy/µl was determined by following formula.

$$\text{Copy/µl} = \frac{6.02 \times 1023\ (\text{copy/mol})\ X\ \text{DNA amount (g/µl)}}{\text{DNA length [Plasmid size + inserted gene](bp) X 600}}$$

The plasmid concentration was adjusted and diluted in a range of 10^7, 10^6, 10^5, 10^4, 10^3 and 10^2 copy/µl. These concentrations were used to construct a standard curve. Both standard and sample *pres1* were amplified at the same time using conditions described above. The fluorescent intensities were specified as C_t values. For standards, C_t values at the above concentrations were used to plot a standard curve. This curve and sample C_t values were used to calculate the amount of HBV DNA in the samples. The Student's *t*-test and one-way ANOVA were used to compare viral loads in cells treated with various levels of IFN-λ3, as well as untreated cells. A p-value less than 0.05 was considered significant.

MTT assay.

HepG2.2.15 cells were seeded in 96-well plates at a density of 1 x 10^4 cells per well and incubated for 24 hours. The culture media was removed and replaced with fresh complete media in the absence or presence of IFN-λ3 (1, 10, 100 and 1000 ng/ml). The cells were further incubated for 24 hours followed by addition of 10 µl 5 mg/ml MTT solution in each well with gentle shaking. Due to photosensitivity of MTT, this step was performed with light protection. After 4h incubation, the resulting purple formazan crystals were dissolved with dimethyl sulfoxide (DMSO, Riedel-deHaën) and subsequently measured with ELISA plate reader (Thermo) at wavelength 570 nm. The absorbance values of cells treated with each concentration of drug were compared to that of control (untreated) cells and % cell viability was calculated. This experiment was performed in biological triplicate.

Protein extraction and in-solution digestion.

After trypsinization, the cells were lysed in 5% SDC in 25 mM TEAB containing 1X protease inhibitor cocktail (Thermo), followed by sonication. All cell debris was removed by centrifugation at 15,000 x g for 10 minutes and supernatant protein concentrations of each sample were measured via BCA Protein Assay (Thermo). Equal amounts of protein from treated and untreated HepG2.2.15 were reduced and alkylated by dithiothreitol (DTT) treatment for 30 minutes at 37^{o}C and iodoacetamide (IA) treatment for 30 minutes at room temperature in the dark, respectively. These samples were further quenched with DTT at least 15 minutes at room temperature before incubating with trypsin (Promega) at a ratio of 1:50 at 37^{o}C overnight. These mixtures were incubated with 0.5% trifluoroacetic acid (TFA) for 30 minutes and then centrifuged to remove SDC precipitate. The amount of tryptic peptides of each sample was determined with the Pierce Quantitative Fluorometric Peptide Assay (Thermo).

Dimethyl labeling.

Equal amount of peptides from untreated, IFN-α2a treated, and IFN-λ3 treated HepG2.2.15 were reconstituted in 100 mM TEAB and labeled with light reagents, medium reagents, and heavy reagents, respectively, as shown in the Table 7 for an hour at room temperature. 1% (vol/vol) of ammonia solution and FA were sequentially used to stop the reaction. These steps were performed on ice. Labeling efficiency was tested before combining these three samples. The mixed labeled-peptides were dried in a SpeedVac centrifuge at room temperature.

Table 7. Dimethyl labeling reagents

	Untreated	**IFN-α2a treated**	**IFN-λ3 treated**
Dimethyl labeling	Light	Medium	Heavy
Formaldehyde isotope	4% CH_2O	4% CD_2O	4% $^{13}CD_2O$
Cyanoborohydride isotope	0.6 M $NaBH_3CN$	0.6 M $NaBH_3CN$	0.6 M $NaBD_3CN$

High-pH reversed phase fractionation.

The pooled peptides were reconstituted in 0.1% TFA and separated into 10 fractions to reduce complexity using the Pierce High pH Reversed-Phase Peptide Fractionation Kit (Thermo) according to the instructions. Briefly, the high-pH step-elution solutions were prepared as following Table 8. The resins in spin column provided in the kit were twice conditioned in acetonitrile followed by centrifugation at 5,000 x g for 2 min. Next, the resins were washed twice in 0.1% TFA followed by

centrifugation at 5,000 x g for 2 min. The dissolved peptides were loaded onto the column and centrifuged at 3,000 x g for 2 min. The column was washed with LC-MS graded water followed by centrifugation at 3,000 x g for 2 min. The elution solution no. 1 was applied onto the column followed by centrifugation at 3,000 x g for 2 min and collection the eluate as fraction no.1. These steps were repeated using the remaining elution solutions. Eluates of each fraction were dried in a vacuum centrifugation before LC-MS/MS analysis.

Table 8. The high-pH step-elution solutions preparation

Fraction no.	% ACN	ACN (µl)	0.1% Trietylamine (µl)
1	2.5%	50	1950
2	4.0%	80	1920
3	5.5%	110	1890
4	7.0%	140	1860
5	8.5%	170	1830
6	10.0%	200	1800
7	12.5%	250	1750
8	17.5%	350	1650
9	25.0%	500	1500
10	50.00%	1000	1000

LC-MS/MS and analysis.

The fractionated samples were resuspended in 0.1% FA to a final volume of 15 µl prior to MS injection. The peptides were then analyzed via an EASY-nLC1000 system (Thermo) coupled to a Q-Exactive Orbitrap Plus mass spectrometer (Thermo) equipped with a nano-electrospray ion source (Thermo). The peptides were eluted in 5-40% acetonitrile in 0.1% FA for 70 min followed by 40-95% acetonitrile in 0.1% FA for 20 min at a flow rate of 300 nl/min. The MS methods included a full MS scan at a resolution of 70,000 followed by 10 data-dependent MS2 scans at a resolution of 17,500. The normalized collision energy of HCD fragmentation was set at 32%. An MS scan range of 350 to 1400 m/z was selected and precursor ions with unassigned charge states, a charge state of +1, or a charge state of greater than +8 were excluded. A dynamic exclusion of 30 s was used. The peaklist-generating software used in this study was Proteome Discoverer™ Software 2.1 (Thermo). The SEQUEST-HT search engine was employed in data processing. MS raw data files were searched against the Human Swiss-Prot Database (20,219 proteins, June 2017) and the Hepatitis B Virus Swiss-Prot Database (225 proteins, June 2017), as well as a list of common protein

contaminants (www.thegpm.org/crap/). The following parameters were set for the search: (1) digestion enzyme: trypsin; (2) maximum allowance for missed cleavages: 2; (3) maximum of modifications: 4; (4) fixed modifications: carbamidomethylation of cysteine (+57.02146 Da), as well as light, medium, and heavy dimethylation of N-termini and lysine (+28.031300, +32.056407 and +36.075670 Da); (5) variable modifications: oxidation of methionine (+15.99491 Da). The mass tolerances for precursor and fragment ions were set to 10 ppm and 0.02 Da, respectively. Known contaminant ions were excluded. The Proteome Discoverer decoy database together with the Percolator algorithm were used to calculate the false positive discovery rate of the identified peptides based on *Q*-values which were set to 1%. The Precursor Ions Quantifier node in Proteome Discoverer™ Software was employed to quantify the relative MS signal intensities of dimethyl labeled-peptides. The control channels were used as denominators to generate abundance ratios of IFN-λ3/control and IFN-α2a/control. Log2 of the normalized ratio was used to calculate the mean and standard deviation of fold change across all five biological replicates. When these ratios were found in less than 3 experiments, the relevant proteins were excluded. Significantly differentially regulated proteins were determined by Mann–Whitney U test and unpaired t-tests with p-value < 0.05 considered significant.

Bioinformatics.

We compiled a list of defense response to virus using a variety of resources as follows. The online resource Database for Annotation, Visualization and Integrated Discovery (DAVID, v6.8, https://david.ncifcrf.gov/) and Reactome (https://reactome.org/) were employed to classify the proteins regulated by IFN-λ3 into functional categories using all proteins identified by MS as background (for DAVID). We used terms such as ‘antiviral’, ‘antigen processing/presentation’ to help extract a custom list of broad antiviral proteins. Additionally, the list contains proteins involved in the HBV life-cycle that were derived from manual literature curation. Further analysis of up-/down-regulated proteins was performed against an in-house database currently under assembly. The goal is simply to expand on DAVID’s method by emphasizing datasets from individual MS and RNA-seq studies. Probabilities presented here are generated using Fisher’s exact test with a background proteome size of 10,000 and are unadjusted. For consistency, lists of proteins with altered expression in our own HBV work are generated by filtering out all cases where differential expression is not accompanied by a p-value < 0.05 (i.e. fold-change is not a factor); the lists are then subjected to Fisher analysis.

Western blotting for MS confirmation.

15 mg of protein from IFN-λ3-treated and untreated HepG2.2.15 was subjected to SDS-PAGE electrophoresis. Both 10% separating and 4% stacking SDS-PAGE were prepared as describe

in appendix. The electrophoresis was performed with a constant voltage 120V for 75 minutes. Proteins were transferred onto nitrocellulose membranes using the Trans-Blot Turbo Transfer System (Bio-Rad). The transferred membranes were stained with Ponceau S dye (AppliChem) to ensure that proteins were completely transferred onto the membranes followed by destaining with MiliQ. The membranes were blocked with Odyssey Blocking Buffer for an hour at room temperature with shaking, washed three times with TBST for 15 min and probed with anti-OAS3, anti-SAMHD1, anti-STAT1, or anti-GAPDH antibodies at 1:2,500 dilution at 4^{o}C overnight. After washing three times with TBST, the probed membranes were incubated with IRDye 680RD secondary antibody at 1:10,000 dilution for 1 hour in the dark followed by three washes with TBST. The membranes were visualized using Odyssey CLx (LICOR-Biosciences).

Data Deposition.

The mass spectrometry proteomics data, including annotated spectra for all modified peptides and proteins identified on the basis of a single peptide, have been deposited to: 1) the ProteomeXchange Consortium via the PRoteomics IDEntifications (PRIDE) partner repository with the dataset identifier PXD007896 and 2) the MS-Viewer (http://msviewer.ucsf.edu/prospector/cgi-bin/msform.cgi?form=msviewer) with the following keys: dhjzinh2g0, tjnx2fzkzu, 3xzzxfanwm, ac4wmxx0tv, and ao9nga6qqm.

RESULTS

Validation of responses to IFN-λ3 treatment in HBV-transfected hepatoblastoma cell line model

HepG2.2.15 is a hepatoblastoma cell line that contains a stable HBV expression plasmid that has been validated as an HBV infection model in previous reports (20, 99). The response to type III IFN treatment in HepG2.2.15 cells has not been reported. To determine whether HepG2.2.15 cells respond to IFN-λ3, we performed qPCR to investigate the expression of the classical ISGs, namely *OAS1*, *Mx1* and *ISG15* in HepG2.2.15 cells treated with various amounts of IFN-λ3 for 24h. Figure 2 shows that IFN-λ3 could significantly increase the expression of these 3 ISGs in a dose-dependent manner. These results indicated that HepG2.2.15 cells responded to IFN-λ3 stimulation.

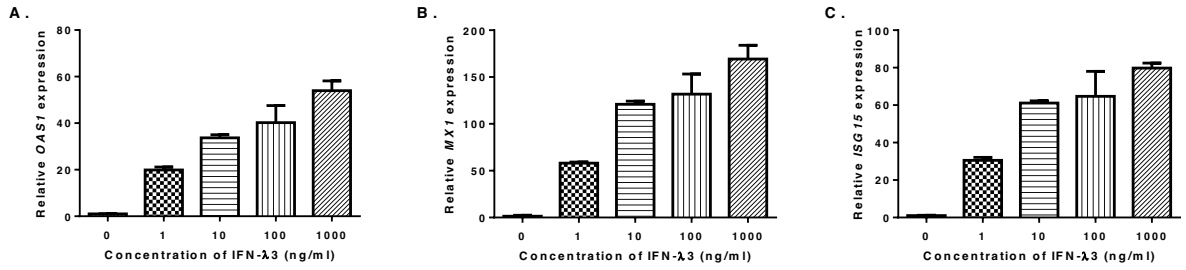

Figure 2. Relative quantification of ISG transcripts in HepG2.2.15 treated with IFN-λ3 for 24 h. The relative expression of *OAS1* (A), *Mx1* (B) and *ISG15* (C) genes in HepG2.2.15 cells 24h post-stimulation with different doses of IFN-λ3 is shown using Mean ± SEM. As with type I IFNs, all 3 ISGs were significantly elevated by IFN-λ3 treatment ($p < 0.001$) at all doses compared with a PBS control. These experiments were performed in triplicate.

For thoroughness, we investigated the anti-HBV effects of IFN-λ3 by determining the differential changes at 3 points in the viral life-cycle including the levels of *preS1* (typically used as a representative gene for HBV transcripts, given its high conservation across all genotypes), replicative intermediate pre-genomic RNA (pgRNA), and intracellular HBV DNA (both rcDNA and cccDNA). qPCR was performed on HepG2.2.15 RNA following treatment with various amounts of IFN-λ3 for 24 hours. As shown in Figure 3A and 3B, IFN-λ3 reduced both *preS1* and pgRNA expression compared with control in a dose-dependent manner. Measurement of intracellular HBV DNA showed that copy numbers of virus in IFNλ3-treated HepG2.2.15 cells were diminished in a dose-dependent manner relative to control (Figure 3C). The reduction reached significant levels when the doses of IFN-λ3 were 100 ng/ml (p-value = 0.04) and 1,000 ng/ml (p-value = 0.0134). Collectively, these results indicated that IFN-λ3 inhibits HBV replication in HepG2.2.15 at the given time point.

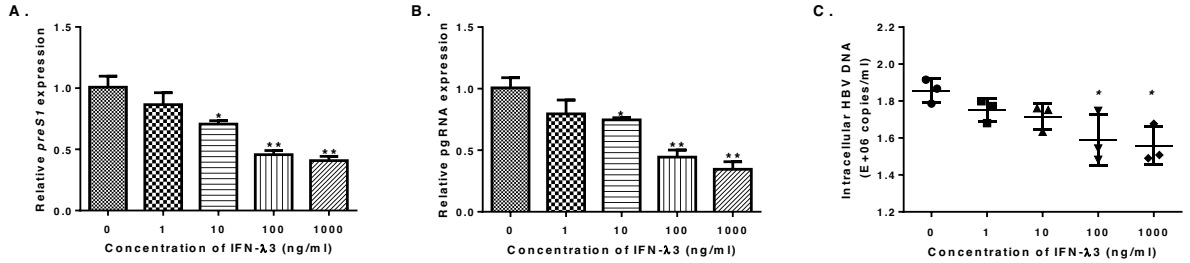

Figure 3. Effects of IFN-λ3 on HBV replication. HepG2.2.15 cells were incubated with IFN-λ3 (1, 10, 100 and 1,000 ng/ml) or treated with PBS for 24 hours. The relative transcript expression and the amount of HBV DNA are shown as Mean ± SEM. IFN-λ3 significantly inhibited *preS1* and pgRNA expression at doses equal to or greater than 10 ng/ml (A and B). IFN-λ3 significantly suppressed viral propagation at doses equal to or greater than 100 ng/ml (C). These experiments were performed in triplicate. (* represents a p-value less than 0.05 and ** represents a p-value less than 0.01).

Before we investigated the cellular response to IFN-λ3, the toxicity of this drug was considered. The MTT cytotoxicity assay was performed to determine HepG2.2.15 viability under distinct concentrations of IFN-λ3. The percentage of viable cells is illustrated in Figure 4. The increasing doses of IFN-λ3 significantly promoted cell death only at the highest two doses in this experiment, where the viable HepG2.2.15 cells reduced to 94% and 84% in 100 ng/ml and 1000 ng/ml conditions, respectively. Thus, we settled on 100 ng/ml of IFN-λ3 for further experiments because this dose showed the ability to significantly inhibit HBV replication with minimal cytotoxicity on HepG2.2.15 cells.

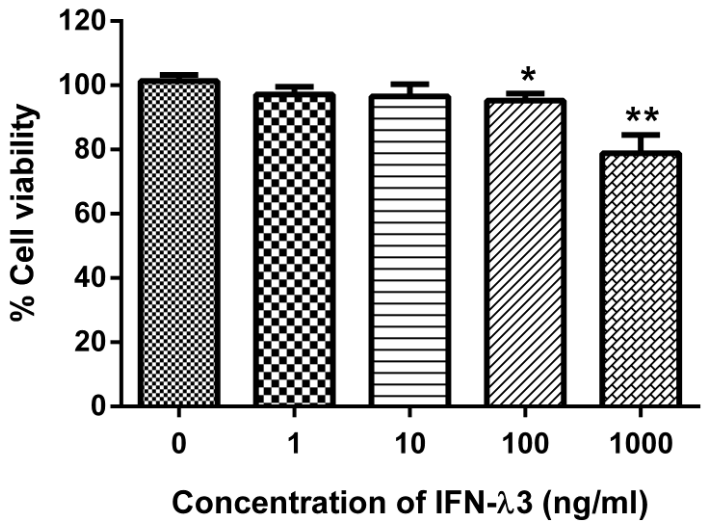

Figure 4. IFN-λ3 cytotoxicity assay. The viability of HepG2.2.15 after IFN-λ3 treatment was determined by MTT assay. The percentage of cell viability is shown as Mean ± SEM. IFN-λ3 showed minimal effect on cell viability when the doses were less than 1,000 ng/ml. These experiments were performed in triplicate. (* represents a p-value less than 0.05 and ** represents a p-value less than 0.01).

Quantitative proteomics analysis of IFN-λ3 responses in HepG2.2.15

Figure 5 shows the schematic workflow of this study. Briefly, untreated, IFN-α2a-treated, and IFN-λ3-treated HepG2.2.15 cells were lysed and digested with trypsin. The tryptic peptides of these groups were labelled with light, medium, and heavy dimethyl reagents. Labeling efficiency was tested before combining these three samples and we found that greater than 99% of peptides were labeled as shown in Table 9. The pooled samples were fractionated for subsequent LC-MS/MS analysis.

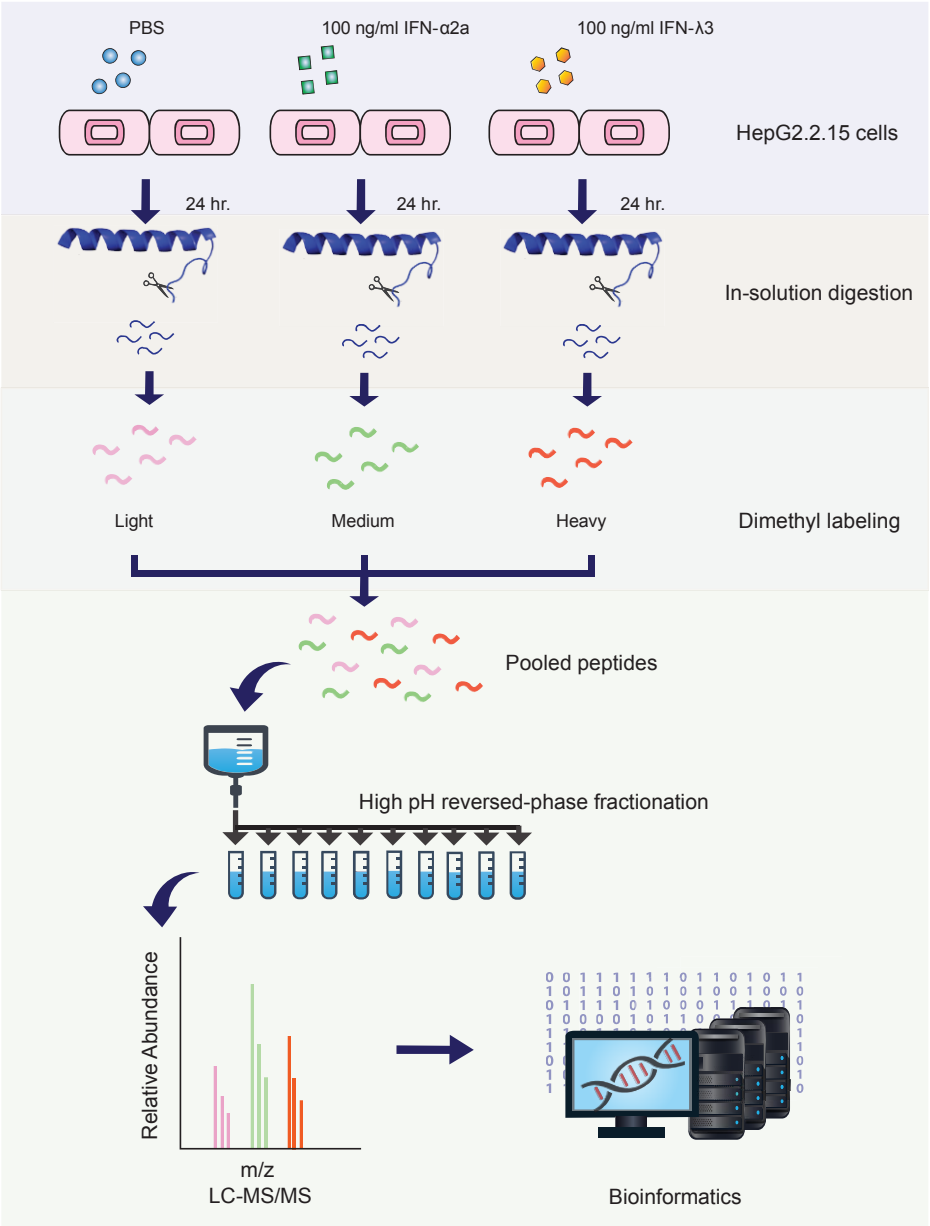

Figure 5. Quantitative proteomic workflow. HepG2.2.15 cells were treated with 100 ng/ml of IFN-λ3 and IFN-α2a and PBS for 24 hours. Cell lysates of each group were digested and then labeled with different dimethyl reagents. After combining the 3 samples, these peptides were fractionated and then analyzed by LC-MS/MS.

Table 9. Dimethyl labeling efficiency

Labelling	Labeled peptides	Total peptides	% Efficiency
Light	**5,775**	**5,786**	**99.81**
Medium	**5,232**	**5,255**	**99.56**
Heavy	**4,849**	**4,865**	**99.67**

In total, 4,670 proteins were identified at a false discovery rate (FDR) of less than 1%, with 1,471 proteins identified on the basis of a single peptide. For the IFN-λ3 treatment condition, 2,904 proteins were identified in at least 3 of 5 replicates allowing evaluation of significance, shown in the corresponding volcano plot (Figure 6). 737 proteins showed significant changes in abundance, with a slight bias towards down-regulated proteins in response to IFN-λ3 stimulation.

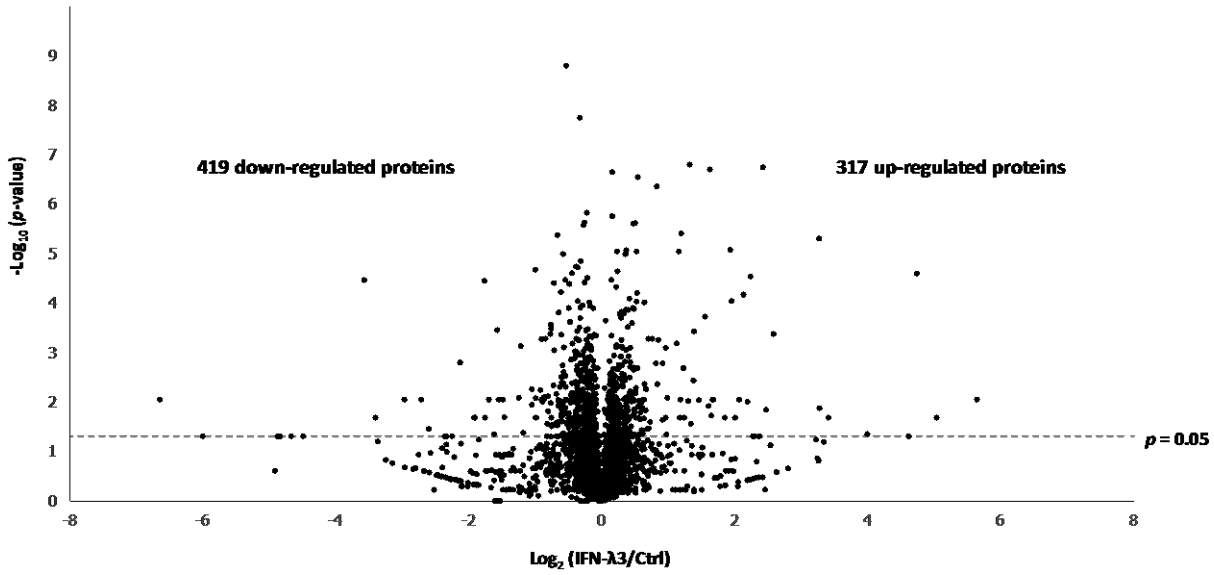

Figure 6. Volcano plot. Volcano plot shows the distribution of identified proteins according to p-value and fold change, indicating significant level with a dashed line (p-value < 0.05).

Table 10 displays a list of significantly regulated proteins with $\log_2$(IFN-λ3/Ctrl) ratios of greater than |1|. We should point out that our primary intention in this work is to explore IFN-λ3

effects on HepG2.2.15 cells; the effects of IFN-α2a would be secondary, for the sake of comparison with IFN-λ3 effects, and will be presented at the last part of the Results section.

Table 10. A list of significantly up-regulated (A) and down-regulated (B) proteins with log_2(IFN-λ3/Control) ratios of greater than |1|.

A.

Accession number	Description	Gene ID	Average Log_2 ratios	Pathway
O14879	Interferon-induced protein with tetratricopeptide repeats 3	IFIT3	4.74	Antiviral defense (Inhibit viral protein synthesis)
Q96AZ6	Interferon-stimulated gene 20 kDa protein	ISG20	3.28	Antiviral defense (Degrade viral RNA)
P05161	Ubiquitin-like protein ISG15	ISG15	3.27	Antiviral defense
Q15646	2'-5'-oligoadenylate synthase-like protein	OASL	2.58	RLR signaling pathway
O95786	Probable ATP-dependent RNA helicase DDX58	DDX58	2.47	RLR signaling pathway
Q9Y6K5	2'-5'-oligoadenylate synthase 3	OAS3	2.42	Antiviral defense (Degrade viral RNA)
Q29960	HLA class I histocompatibility antigen, Cw-16 alpha chain	HLA-C	2.24	Antigen processing and presentation
P09914	interferon-induced protein with tetratricopeptide repeats 1	IFIT1	2.19	Antiviral defense (Inhibit viral protein synthesis)
P42224	Signal transducer and activator of transcription 1-alpha/beta	STAT1	2.13	Type I and III IFN signaling
Q63HN8	Isoform 2 of E3 ubiquitin-protein ligase RNF213	RNF213	1.95	Ubiquitin proteasome pathway
Q01628	Interferon-induced transmembrane protein 3	IFITM3	1.93	Antiviral defense (Inhibit viral entry)
P52630	signal transducer and activator of transcription 2	STAT2	1.65	Type I and III IFN signaling
P29590	Protein PML	PML	1.63	Antiviral defense (Inhibit viral transcription)

Accession number	Description	Gene ID	Average Log_2 ratios	Pathway
P28838	cytosol aminopeptidase	LAP3	1.61	Antigen processing and presentation
Q10589	bone marrow stromal antigen 2	BST2	1.55	Antiviral defense (Inhibit viral egress)
Q6IA86	Isoform 6 of Elongator complex protein 2	ELP2	1.46	Regulation of transcription
Q08380	Galectin-3-binding protein	LGALS3BP	1.39	Cell adhesion
Q9H0P0	Cytosolic 5'-nucleotidase 3A	NT5C3A	1.38	Antiviral defense (Inhibit reverse transcription)
P35527	Keratin, type I cytoskeletal 9	KRT9	1.34	Intermediate filament organization
P41226	ubiquitin-like modifier-activating enzyme 7	UBA7	1.32	Ubiquitin proteasome pathway
Q9Y3Z3	deoxynucleoside triphosphate triphosphohydrolase SAMHD1	SAMHD1	1.19	Antiviral defense (Inhibit reverse transcription)
Q9BQE5	apolipoprotein L2	APOL2	1.22	Movement of lipids in the cytoplasm
P01892	HLA class I histocompatibility antigen, A-2 alpha chain	HLA-A	1.16	Antigen processing and presentation
Q9Y6A9	Signal peptidase complex subunit 1	SPCS1	1.13	Proteolysis

B.

Accession number	Description	Gene ID	Average Log_2 ratios	Pathway
Q9BX93	Group XIIB secretory phospholipase A2-like protein	PLA2G12B	-1.05	Lipid catabolic process
Q15427	Splicing factor 3b subunit 4	SF3B4	-1.05	mRNA processing
Q9NPA8	Transcription and mRNA export factor ENY2	ENY2	-1.18	Regulation of transcription
P62158	Calmodulin	CALM3	-1.22	Regulation of synaptic vesicle exocytosis
O75410	Isoform 2 of Transforming acidic coiled-coil-containing protein 1	TACC1	-1.25	Cell proliferation
O75438	Isoform 2 of NADH dehydrogenase [ubiquinone] 1 beta subcomplex subunit 1	NDUFB1	-1.47	Mitochondrial electron transport, NADH to ubiquinone
Q12929	Epidermal growth factor receptor kinase substrate 8	EPS8	-1.57	Actin polymerization-dependent cell motility
Q9NZD2	glycolipid transfer protein	GLTP	-1.62	Intermembrane lipid transfer
Q13126	Isoform 2 of S-methyl-5'-thioadenosine phosphorylase	MTAP	-1.76	Nucleobase-containing compound metabolic process
Q58FF7	Putative heat shock protein HSP 90-beta-3	HSP90AB3P	-3.58	Protein folding and response to stress

All HBV proteins were identified in this study. However, calculation of significance could not be performed due to absence in multiple MS runs, with the exception of putative X-Core fused protein (which showed no significant change). Based on spectral counts, all of the HBV peptides were apparently expressed at very low levels relative to the entire HepG2.2.15 proteome (below 1 ppm, see in PRIDE partner repository as mentioned in Data Deposition). This finding is in agreement with a previous study that specifically examined intracellular HBV proteins in HepG2.2.15 cells, but found them to be undetectable (100). Note that all HBV proteins, except HBV pol and HBx, are secreted (101-103), likely causing intracellular levels of these proteins to be scarce.

To confirm the results from MS analysis, three proteins known to be differentially regulated in response to HBV infection, namely 2'-5'-oligoadenylate synthase 3 (OAS3) (104), Sterile α motif (SAM) and histidine/aspartate (HD)-containing protein 1 (SAMHD1) (105-107), and signal transducer and activator of transcription 1 (STAT1) (108, 109) were selected for validation by western blot analysis. Consistent with MS results, OAS3, SAMHD1 and STAT1 were up-regulated as a result of IFN-λ3 treatment (Figure 7).

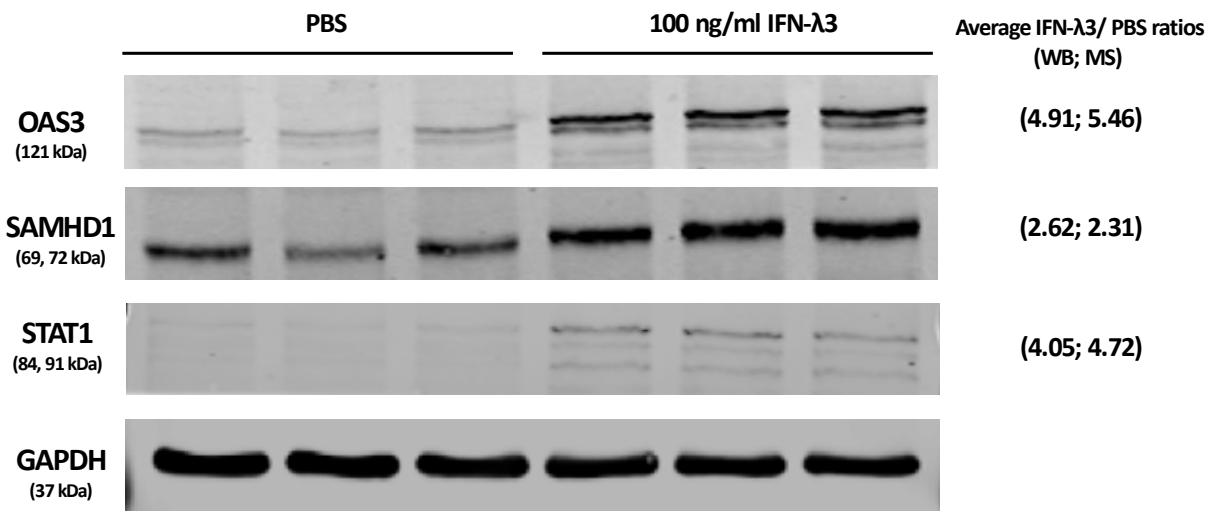

Figure 7. Validation of altered proteins by immunoblotting assay. SDS-PAGE was performed on treated and untreated lysates, followed by membrane transfer and incubation with anti-OAS3, anti-SAMHD1, anti-STAT1, and anti-GAPDH overnight. The proteins of interest were visualized using the LI-COR Odyssey system. Consistent with proteomic results, the expression of OAS3, SAMHD1 and STAT1 increased after IFN-λ3 treatment. These experiments were performed in triplicate.

To further explore the possible roles of transcriptional regulation for significantly altered proteins, we selected a number of proteins involved in antiviral processes for qPCR analysis. Figure 8 show that upregulation was seen at both protein and RNA expression levels without exception. However, no clear pattern emerged when down-regulated proteins were examined for transcript levels.

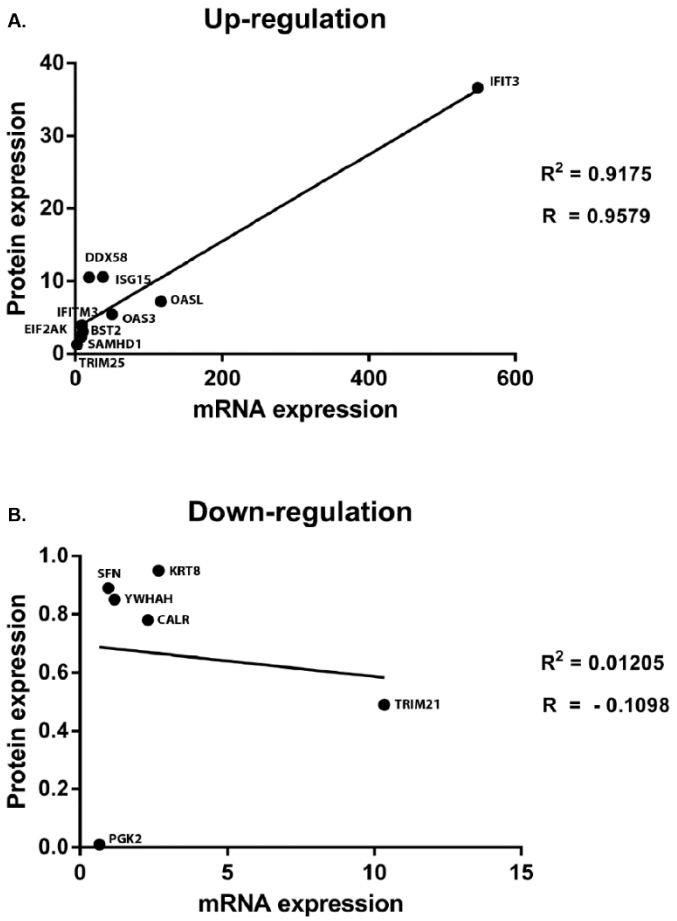

Figure 8. Correlation of mRNA and protein levels of up- and down-regulated proteins. Various up- and down-regulated proteins were selected to investigate their transcript expressions by qPCR. Clear correlations between protein and mRNA expression were seen in up-regulated proteins (A) but not in down-regulated proteins (B).

Bioinformatics analysis and anti-viral/immunomodulatory process mapping

The DAVID bioinformatics tool was used to classify and cluster significant functions of all up- and down-regulated proteins. Upon IFN-λ3 treatment, we found several biological processes expected to be canonically regulated on general IFN stimulation, such as immune response and viral infection defense. Additionally, however, several biological processes not previously emphasized upon interferon stimulation emerged from this work, including metabolism of RNA, major pathway of rRNA processing in the nucleolus and cytosol, selenoamino acid metabolism, peptide chain elongation, translation, prefoldin mediated transfer of substrate to CCT/TriC, transcription-coupled nucleotide excision repair (TC-NER), unfolded protein response (UPR), interleukin-23 signaling, and hypusine synthesis from eIF5A-lysine.

Following enrichment analysis, we conducted a protein-by-protein search for relevance to the viral processes. We manually searched the viral literature, as well as using DAVID's antiviral defense groups and antigen processing/presentation groups, to construct a map of points at which these proteins may partake in viral processes (Figure 9) (as described in Experimental Procedures). We also built a map displaying steps at which IFN-λ3 treatment could promote antigen processing and presentation of viral proteins. Finally, we constructed a map that highlights points at which IFN-λ3 stimulation may heighten expression of proteins in the RIG-I pathway that have been shown to be inhibited via HBV infection. Unless otherwise stated, we found no proteins that contradict the patterns that we report below.

Regarding the HBV life cycle, we identified many proteins which may be involved at numerous points (Figure 9). At the early steps of viral attachment, entry, and cytosolic release from endosomes (Figure 9, step 1 and 2), we detected an increased expression of IFITM3, known to alter intracellular cholesterol homeostasis, preventing viral fusion with endosomes in at least 4 out of 7 of the Baltimore viral groups (110). RAB5C and RAB7A, proteins previously implicated in viral trafficking (Figure 9, step 2), were down-regulated upon IFN-λ3 treatment (111), though RAB7A did not reach statistical significance. Two other trafficking proteins not mentioned in the viral literature, AP2B1 and EEA1, were significantly down-regulated. Regarding cytosolic-to-nuclear transport of the HBV capsid along microtubules (Figure 9, steps 4), we found that several molecules involved in microtubule assembly and function evinced decreased expression after IFN-λ3 treatment, consistent with the literature. These proteins were DCTN1, DCTN2, KIF5B, MAP4, and MACF1 (112, 113). For nuclear import (Figure 9, step 5), all identified proteins known to play roles herein (113, 114) were found to decrease as a result of IFN-λ3 stimulation (IPO5, IPO7, CALR, CALM, RANBP1, and TPR). Within the nucleus (Figure 9, step 7), all identified ISG products shown previously to limit or degrade viral mRNA (49, 115, 116) were observed to be up-regulated: ADAR1, OAS3, ISG20, PML, XRN2, ZC3HAV1, and TRIM25. At the level of RNA export (Figure 9, step 8), ENY2 and CALR were down-regulated. Regarding translation (Figure 9, step 9), antiviral proteins (EIF2AK2, IFIT1, and IFIT2) involved in protein synthesis increased in treated cells, as shown in previous work with type I IFN treatment (49, 116, 117). In addition, almost all identified translation initiation factors (EIF1AY, EIF2S3, EIF2B1, EIF3B, EIF4G1, EIF4B, EIF4G2, and EIF5A) decreased in this study. Encapsidation follows translation of viral proteins (Figure 9, step 10). Interestingly, RIG-I was upregulated and has been shown to interfere with the interaction between pgRNA and HBV polymerase, required for encapsidation (118). Other effects of RIG-I upregulation are discussed below. Reverse transcription, which occurs within the capsid (Figure 9, step 11), has been demonstrated to be inhibited by SAMHD1 (HBV and HIV) (106, 119) and NT5C3A (IAV and CSFV) (120, 121); these proteins were upregulated

in our study upon treatment. Proteins that might interfere with viral assembly (Figure 9, step 12.1) were not identified in this study. Finally at the egress step (Figure 9, step 13), two upregulated proteins thought to play a role in inhibiting HBV export, BST2 and C4A, were detected after IFN-λ3 stimulation.

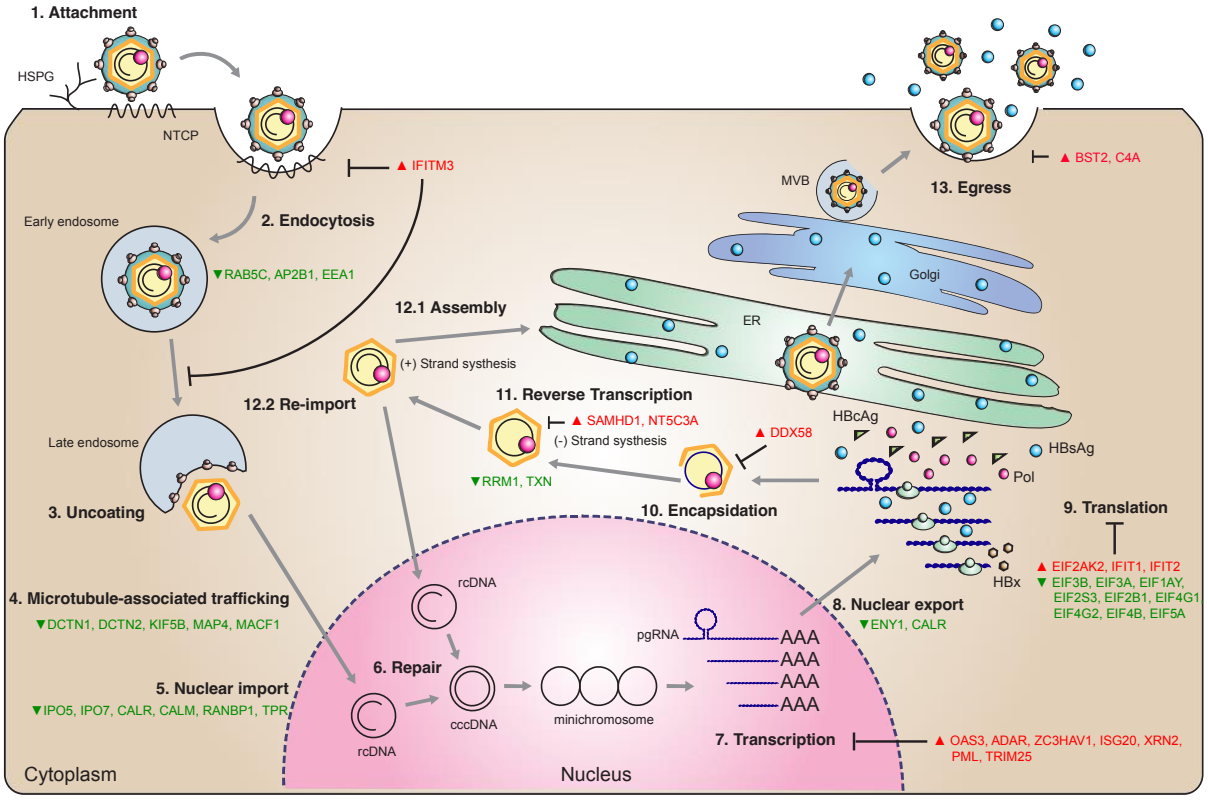

Figure 9. Illustration of HBV life-cycle mapped to anti-viral proteins that were identified in this study. Antiviral proteins and host cellular factors of interest identified in this study were mapped into the HBV-life cycle. These proteins were identified at most steps of HBV replication. Proteins in red and green text represent up- and down-regulated proteins, respectively.

Regarding antigen processing and presentation, we identified 22 proteins that are involved in this process (Figure 10). Among proteins in the degradation-related ubiquitination cascade, we found only upregulation, specifically UBA7 (E1), UBE2L6 (E2), and SYVN1 (E3) after IFN-λ3 stimulation. Two ubiquitination enzymes were downregulated, but have not been reported to instigate degradation. All deubiquitinating enzymes (DUBs) identified in this study, i.e. USP14, UCHL3, UCHL5, and OTUB1, decreased as a result of IFN-λ3 treatment. Downstream of these processes, core proteasome components, PSMA7, PSMB7, and PSMG2, were up-regulated with no exceptions. Importantly, both cap components (PSME1 and PSME2) associated with the immunoproteasome were up-regulated,

while all significantly altered cap components of the constitutive proteasome were down-regulated. Evidence of possible post-proteasome processing was seen in the upregulation of a cytosol aminopeptidase, LAP3. Next, we saw upregulation of proteins involved in transport of peptides from the cytosol to the ER as well as assembly of peptide-HLA class I complexes; these proteins included TAP2, TAPBP, HLA-A, HLA-B, and HLA-C. Other proteins involved in the above step did not reach statistical significance but tended to increase expression following IFN-λ3 treatment; TAP1, PDIA3 (ERP57), and B2M. CALR, a player in this process, was actually down-regulated, the reasons for which will be discussed later.

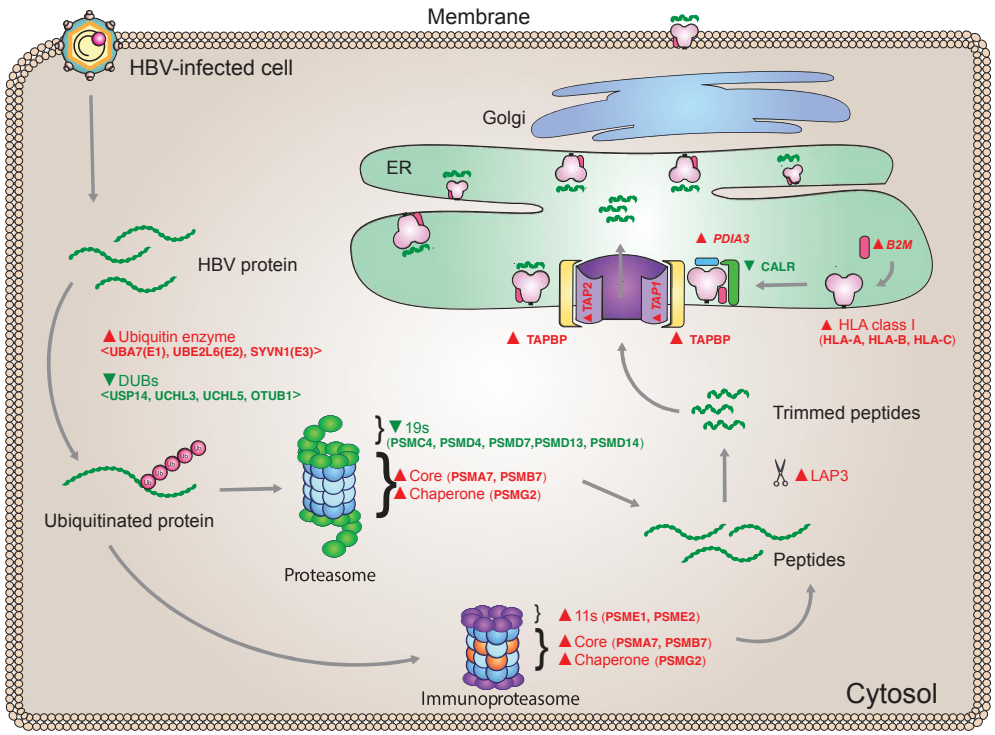

Figure 10. IFN-λ3 enhanced antigen processing/presentation. IFN-λ3 not only upregulated HLA class I expression but it also increased the expression of other effector molecules involved in antigen processing and antigen presentation. Ubiquitinating enzymes that promote protein degradation were found to be upregulated while deubiquitinating enzymes known to remove ubiquitin were found to decrease after IFN-λ3 treatment. Although all identified subunits of the constitutive proteasome cap were down-regulated, the 2 subunits of the immunoproteasome cap as well as some subunits of the proteasome core were elevated in expression. Several effector molecules involved in peptide loading on class I HLA as shown in red text were up-regulated with the exception of CALR, which was down-regulated as shown in green text. The italic red text represents proteins with increased expression levels that failed to reach statistical significance.

One of the important functions of the innate immune response against HBV is the sensing of viral RNA, leading to IFN activation, which includes components such as toll-like receptors, RIG-I, and MDA5. Here, we saw significant upregulation of RIG-I upon treatment, which could counteract the known suppression of RIG-I by HBV. Enhancers of RIG-I activity, such as OASL, TRIM25, and

IFIT3 (RIG-G) were also significantly upregulated. Increased levels of type I and III IFNs, which are activated by RIG-I, would be expected, but were not observed via MS. However, qPCR work confirmed significant upregulation of these IFNs at the transcript level (Figure 11).

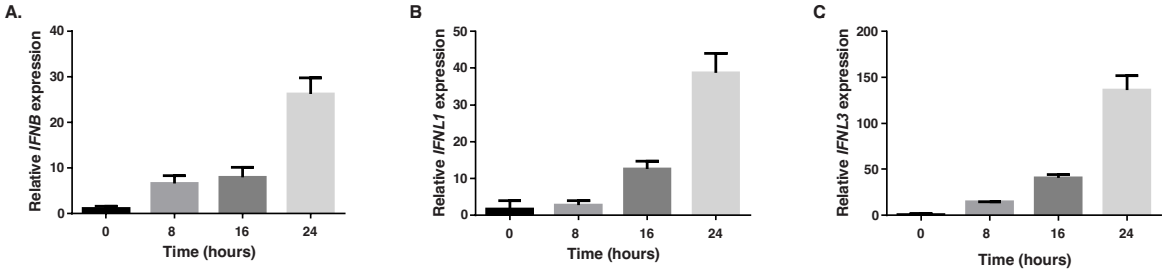

Figure 11. qPCR analysis of *IFN* genes. Total RNA of HepG2.2.15 cells treated with IFN-λ3 for 8, 16, and 24 hours or left untreated was extracted and then converted to cDNA. The expression levels of *IFNB*, *IFNL1*, and *IFNL3* (A, B, and C) were found to be upregulated in a time-dependent manner after IFN-λ3 treatment.

It is likely that the increase in IFN I and III gene expression due to RIG-I upregulation could lead to more production of IFNs at the protein level and in turn activate IFN receptors as positive feedback. All three canonical ISGF3 components (STAT1, STAT2, and IRF9) downstream from IFN receptor activation were upregulated, probably as a result of both initial IFN-λ3 treatment and further generation of type I and III IFNs (Figure 12).

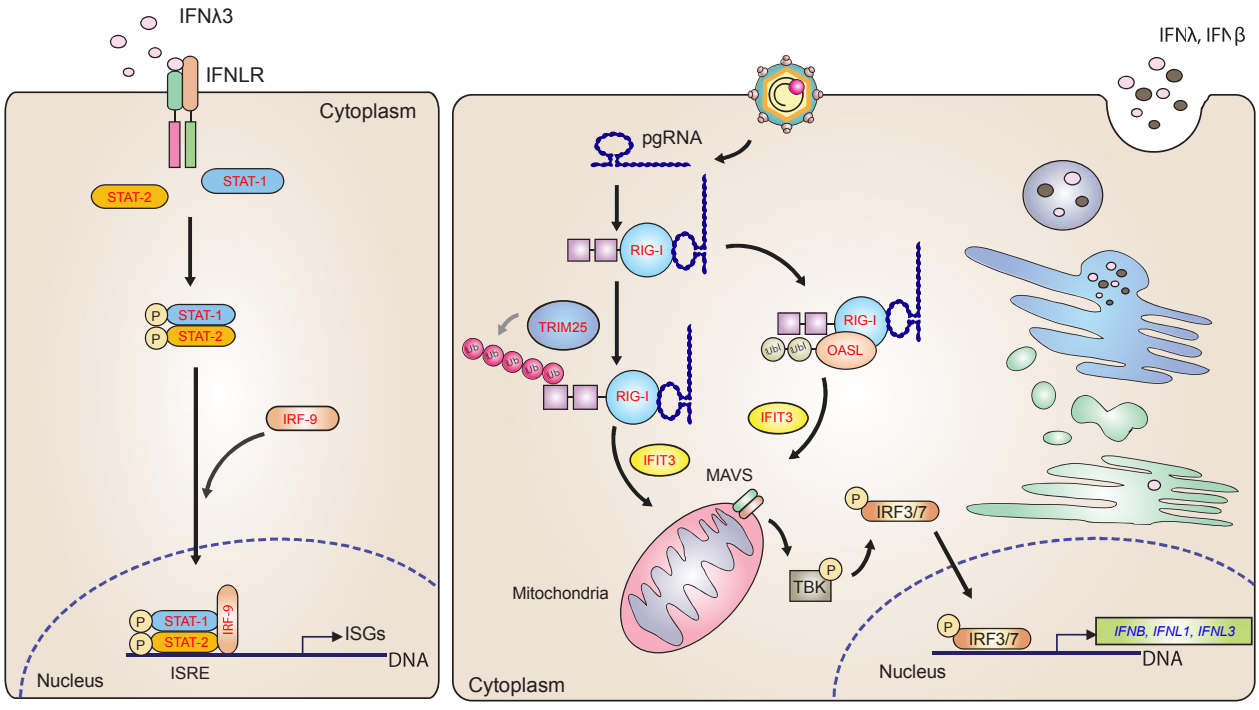

Figure 12. IFN-λ3 rescued the RIG-I signaling pathway. IFN-λ3 upregulated the expression of RIG-I and IFIT3, which have been reported to be suppressed by HBV. IFN-λ3 also elevated the expression of OASL and TRIM25. These proteins promote type I and type III IFN production. These IFNs, in turn, activate the JAK-STAT pathway and induce the expression of ISGs. It is likely, then, that IFN-λ3 provides positive feedback to amplify ISG expression to control HBV replication. Proteins in red text represent upregulated proteins, while the blue text represents the up-regulated transcripts.

We found a number of likely antiviral proteins that do not conveniently fit into the above viral processes. Firstly, three 14-3-3 proteins (YWHAZ, YWHAH, and SFN) were found to be down-regulated following IFN-λ3 treatment. Another down-regulated protein of interest was cyclophilin D (PPIF). Finally, CHID1 was actually the single most upregulated protein in our study on IFN-λ3 treatment. Though not prominent in the viral literature, CHID1 is known to bind LPS (122) and is seen to be down-regulated in several viral studies (123-126).

After removal of all anti-viral proteins, enrichment analysis of the remainder produced an interesting result. RNA-binding proteins, particularly spliceosome components, were both up- and down-regulated on IFN-λ3 treatment vs. control. For example, the splicing factor U2AF1 was significantly upregulated on treatment (p = 0.00165). Searching through individual datasets from an in-house database containing a variety of studies and applying Fisher's exact test (see Experimental Procedures) showed a strong tendency toward both up-regulation and down-regulation of proteins that associate with the non-coding RNA NORAD (log p = -5 and -13, respectively) (127). The same pattern applies to proteins shown to bind to the splicing factor U2AF2 (log p = -6 and -9, respectively) (128).

Though our primary intent is to elaborate on IFN-λ3's potential, comparative studies against the best characterized interferon, IFN-α, are essential. Given the known parallelism in broad modes of action between the two IFNs, significant overlaps should be seen in sets of up-/down-regulated proteins upon treatment, offering a simple validation of IFN-λ3's activity. At the same time, and most intriguingly, the comparison would allow us to suggest possible differences in effect. To take advantage of the depth of our data, we constructed a tree depicting all 27 possible differential expression outcomes resulting from 3 pairs of treatment comparisons (i.e. IFN-λ3 vs. Ctrl, IFN-α2a vs. Ctrl, IFN-λ3 vs. IFN-α2a, see Figure 13).

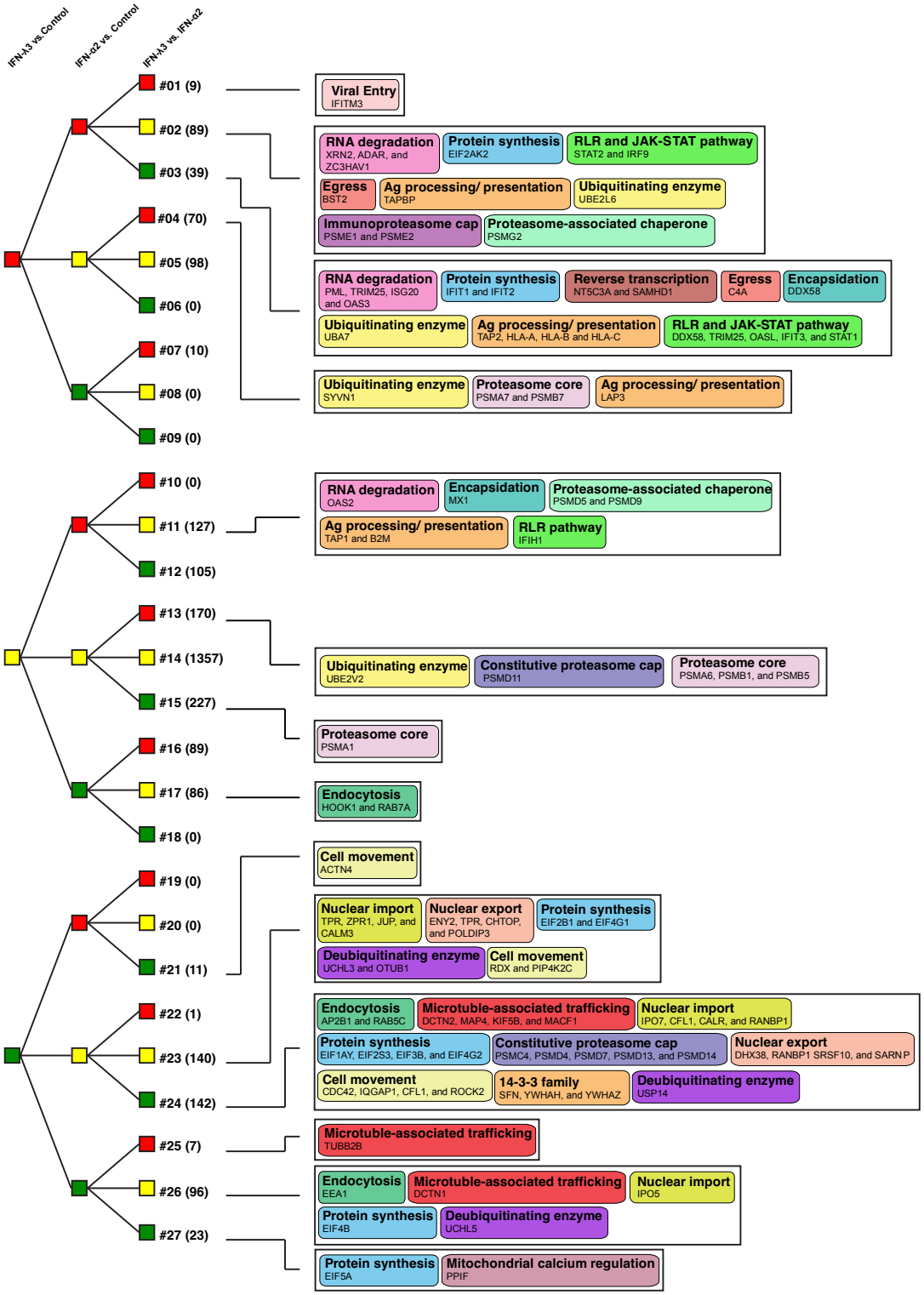

Figure 13. Outcome tree. In order to compare the effects IFN-λ3 with IFN-α2a, we generated a tree representing the 27 possible outcomes. The boxes in red and green represent the group of proteins with significantly up and down-regulated expressions, respectively. Groups of proteins with insignificantly changed expressions are by yellow boxes. As an example, the topmost outcome represents proteins in which IFN-λ3 treatment causes significant upregulation versus control, IFN-α2a treatment causes significant upregulation versus control, and IFN-λ3 treatment causes significant upregulation versus IFN-α2a. The number in parentheses refers to the number of identified proteins in the group. The proteins in each group that might be involved in suppressing HBV replication are shown in colored boxes specifying various processes, particularly antiviral.

A simple comparison between IFN-λ3 vs. IFN-α2a could lead to errors in interpretation. For example, the observation that IFN-λ3 treatment results in up-regulation or down-regulation of a protein vs. IFN-α2a renders an uninteresting result if IFN-λ3 does not have any significant effect vs. Ctrl. This scenario can be seen in outcomes #12 and #16 in Figure 13. Another problem in interpretation arises when both IFNs have the same directional effect on cells but one effect is significantly more potent than the other; this would not be noticed upon mere IFN-λ3 vs. IFN-α2 comparison. This scenario can be seen in outcomes #3 and #25 in Figure 13. The tree shows the number of MS-derived proteins at their appropriate outcome branch points and shows proteins associated with various biological processes (as described in Experimental Procedures) for each outcome. As one simple example of the power of this approach, note that IFITM3 was significantly upregulated upon treatment with both IFNs, however this effect was significantly stronger upon IFN-λ3 treatment (outcome #1). Another example was in outcome #4 where IFN-λ3 treatment caused upregulation of particular proteins involved in antigen processing and presentation (SYVN1, LAP3, PSMA7, and PSMB7), while IFN-α2a did not produce any significant effects. Interestingly, the mirror image of this branch, outcome #24 where IFN-λ3 caused down-regulation while IFN-α2a did not, was also populated with a subset of proteins involved in antigen processing and presentation, specifically those associated with the constitutive proteasome cap (PSMC4, PSMD4, PSMD7, PSMD13, and PSMD14). A priori, one would expect the most interesting outcomes to be found in cases in which IFN-α2a and IFN-λ3 have clearly opposite effects (outcomes #7 and #21). We did not identify proteins clearly related to antiviral processes in these two outcome groups. This reason pointed to broader unbiased analysis. Hence, we performed “Reactome” enrichment analysis against all outcome groups for complete enrichment analysis beyond the aforementioned antiviral processes. The resulting Reactome enrichment groups were subjected to 2-D cluster analysis (Figure 14).

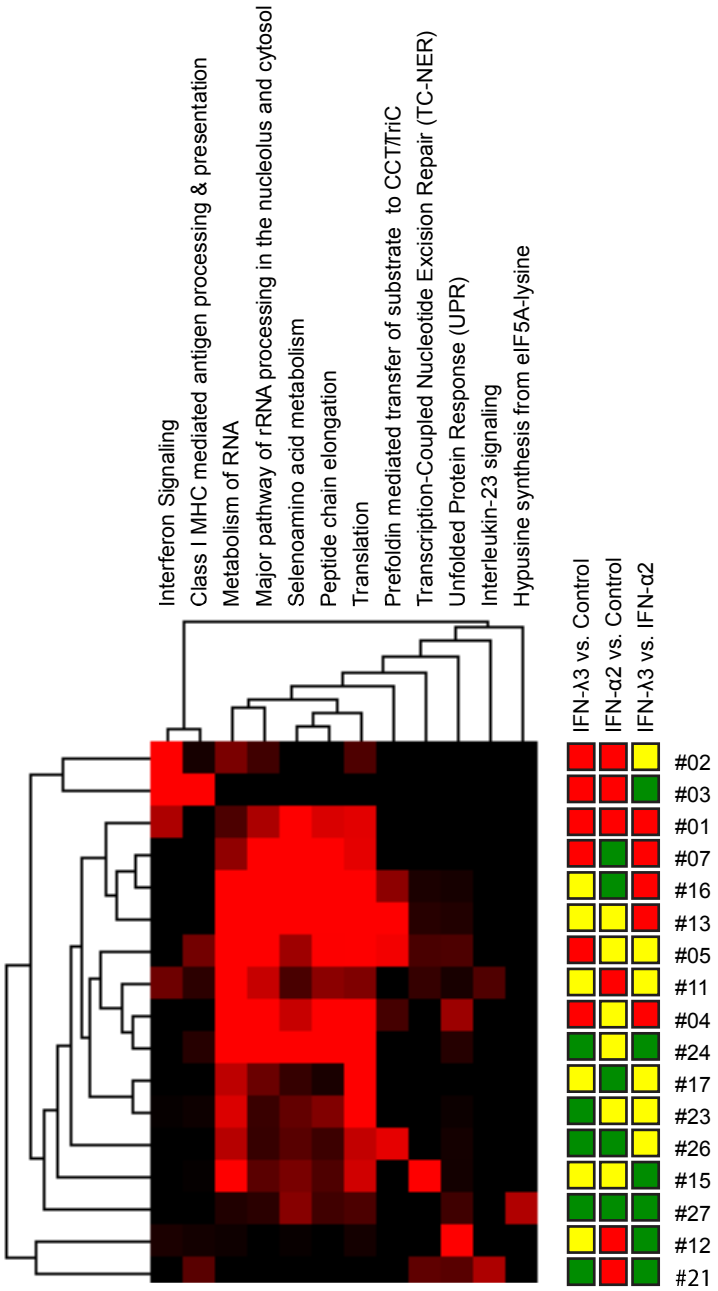

Figure 14. Enrichment heatmap. Reactome enrichment analysis was performed on the tree outcomes that contained at least 9 members, excluding outcome #14 in which no significant alterations were seen on any treatment. Probabilities (Reactome's hypergeometric test, -log(p-value)) were generated for every intersection of these tree outcomes with the specified Reactome groups. This matrix of probabilities was then submitted for two-dimensional cluster analysis using Cluster 3.0 and Java Treeview. The result is displayed as a heatmap. Red color intensity indicates the level of significance.

This analysis offers new insights. Firstly, we note the aforementioned cases in which IFN-λ3 and IFN-α2a showed opposing effects. In outcome #7, where IFN-λ3 exclusively caused upregulation, the 'peptide chain elongation', 'metabolism of RNA', 'major pathway of rRNA processing

in the nucleolus and cytosol', 'selenoamino acid metabolism', and 'translation' terms are highlighted, while in outcome #21, where IFN-λ3 exclusively caused downregulation, the 'interleukin-23 signaling' term is emphasized. Next, we observe that in most cases where proteins were upregulated upon IFN-α2a treatment (outcomes#1, #2, #3, #11, and #21), 'interferon signaling' and/or 'class I MHC mediated antigen processing & presentation' terms were apparent, reinforcing expectations regarding IFN-α's potency on these pathways. Interestingly, specific terms related to 'translation' and 'metabolism of RNA' were significantly associated with 13 out of 17 different outcome groups. To our best knowledge, these biological processes have been not mentioned as consequences of general IFN activation. Finally, enrichment terms that are largely unexplored with regard to IFN treatment include 'transcription-coupled nucleotide excision repair (TC-NER)' (1 significant occurrence), 'interleukin-23 signaling' (1) , 'unfolded protein response (UPR) (2)', 'prefoldin mediated transfer of substrate to CCT/TriC (4)', and 'hypusine synthesis from eIF5A-lysine (1)'. Interestingly, the final enrichment term was only associated with a single case, that of proteins downregulated in all treatment pairs (outcome #27). These results could help point toward differential effects of IFN-λ3 vs. IFN-α2a.

DISCUSSION

HBV infection continues to be a major global health concerns affecting more than 4 billion people worldwide. CHB can develop to liver cirrhosis and hepatocellular carcinoma causing 600,000 deaths each year. Although IFN-α and NAs are used as the first line of treatment for CHB, each drug has some limitations such as undesirable side effects of IFN-α and occurrence of drug-resistant HBV following NAs treatment. The new agents, which overcome these restrictions, are still required in the present. The novel cytokine IFN-λ (type III IFN) is being explored as the new therapeutic drug in several diseases such as viral infections and cancers because it possesses biological activities-like type I IFN including anti-viral, anti-proliferative and immune-modulating effects. Type III IFN has been shown to exert antiviral effects on several viruses including EMCV, IAV, HSV, VSV, HIV, HCV and HBV (17, 60, 66, 67, 70, 78, 116, 129). In clinical trials, peg IFN-λ treatment showed reduced HBV DNA, HBsAg and HBeAg in CHB patients at levels greater than or comparable to those treated with peg IFN-α during on-treatment and at end-of-treatment (9). Although the virological, serological, and biochemical responses of peg IFN-λ at week 24 after treatment were not superior to peg-IFN-α, adverse events associated with drug treatment were mostly seen in patients treated with peg-IFN-α. Numerous HCV studies also illustrate this tendency toward diminished side-effects (13, 14). Another clinical trial demonstrated that patients treated with peg IFN-λ had improved anti-HBV immunity through an increase in poly-functional NK cells and maintenance of both HBV-specific $CD4^+$ and $CD8^+$ T cells, important arms of immunity for viral elimination (8). The mechanisms involved in these immunomodulatory effects remain to be elucidated. At the level of cell culture, only two studies (71, 78) have focused on the effects of IFN-λ treatment of HBV-transfected cells, one of which offers a comparison against a type I IFN, IFN-β. Here, a comparison against IFN-β showed that IFN-β exhibited greater potency in viral elimination at the 6 hour time-point, but potency was equivalent at 24 hours.

In this study, we selected HepG2.2.15 cells as CHB model in vitro because this cell line supports HBV replication and it also secretes HBsAg, HBeAg as well as HBV DNA into the culturing media like natural HBV life cycle. Here, in addition to up-regulation of OAS1, MxA and ISG15 expressions, we first demonstrated that IFN-λ3 exerted its antiviral activities by reducing the expression of HBV RNA transcript (pres1) and replicative intermediate (pgRNA) as well as reducing amount of intracellular HBV DNA in a dose-dependent manner. Our findings were in accord with the results from Robek et al. (71) and Seung-Ho Hong et al. (78), these suggested that all 3 IFN-λ subtypes could suppress HBV replication in vitro. Although the antiviral effects of IFN are dose-

dependent manner, IFN itself has toxicity to cells. IFN-λ3 at 100 ng/ml, used to treat the cells in subsequent experiments, was optimal concentration based on its inhibitory effects on HBV replication with minimal cytotoxicity. In addition, the previous studies showed that this concentration of IFN-λ3 could inhibit HCV (65) and HIV (129) replication in vitro. For time of treatment, 24 hours were chosen from the previous time-course study using microarray approach because it was the time that the expressions of most genes and the maximal magnitude of responses were induced in HCV-infected cells treated with IFN-λ1 (17). This was also the same time that Leiliang Zhang used to investigate the efficiency of IFN-λ3 to inhibit HCV replication in OR6 and JFH1 cells which is the hepatoblastoma harboring HCV RNA (65).

Surprisingly, the effects of IFN-λ treatment have not been studied with high-resolution mass spectrometry to date, possibly because it is assumed that type I and type III IFNs share the same signaling pathways. In fact, modern, deep proteomic studies of the effects of IFN treatment in general are lacking, perhaps because of an underlying assumption that RNA-seq results should parallel those generated via MS. Here, we used a modern high-resolution LC-MS/MS system with upstream high-pH reversed phase fractionation to yield a total of 127,989 peptides (25,181 unique peptides) representing 4,670 proteins. The peptides were labeled with dimethyl isotopes, allowing accurate quantification under different treatments. This study provides the most comprehensive examination of changes in protein abundance under IFN treatments to date.

In order to provide objective measures for study-study comparisons, in the discussion below we perform numerous comparisons between our studies and others with Fisher's exact test (see Experimental Procedures). As expected, canonical IFN-stimulated biological processes were prominent in IFN-λ3 treatment. In particular, proteins significantly upregulated upon IFN-λ3 treatment vs. Ctrl (hereafter λ3/c) overlapped with the GO "antiviral defense" term at p-value = 10^{-14} (with the α/c condition giving p-value = 10^{-12}). Similarly, the λ3/c list significantly overlapped (p-value = 10^{-13}) transcripts whose up/down regulation patterns (i.e. "co-expression") mirror those of RIG-I transcripts reported in the ARCHS4 resource (130); the α/c list gave p-value = 10^{-18}, perhaps illustrating the expected difference in potency. Comparing proteins significantly upregulated in λ3/c against those upregulated in α/c, we derive p = 10^{-138}, a clear demonstration of similarities in effect vs. control. Stepping outside the bounds of our own work, Bolen's transcriptomic comparison of the effects of 5 interferons, including IFN-λ3, on Huh7 cells can be examined against our proteomic results (16). Here, a list of highly upregulated transcripts derived from Bolen's 6, 12, and 24 hour λ3/c time-points significantly intersected with our own λ3/c results (p-value = 10^{-25}). Of interest, the degree of overlap (p-value = 10^{-5}) was less significant when performing the same exercise with down-regulated

transcripts vs. proteins, paralleling the tendency of lower correlation seen in our own qPCR results for a number of down-regulated proteins (Figure 8). Other comparisons illustrating the expected canonical effects would be an α/c result in Huh7 (131) (a λ3/c experiment was not performed) where upregulated transcripts align with our own λ3/c results (p-value = 10^{-30}), and a list of genes likely to be activated by STAT2 based on curated STAT2 chip-seq results that significantly overlaps with our λ3/c results (p-value = 10^{-25}) (132).

In addition to acting on viral replication directly, we propose that the proteolytic pathway may be induced by IFN-λ3 to inhibit HBV replication. The proteasome plays a crucial role in degradation of misfolded, unfolded or damaged proteins which were occurred in the natural state and responding to the oxidative stress. The abnormal proteins were cleaved by protease enzymes into small peptides with 7-8 amino acid in length and further hydrolyzed into shorter fragments to newly synthesize protein or to be chaperoned by HSPs to facilitate antigen presentation in case of viral infection. Like other viral infections, HBV produces and secretes its proteins into the host cells during its propagation and these proteins facilitate the efficiency of HBV replication.

Robek et al. demonstrated that small molecule-based inhibition of proteasome activity could restrain the anti-HBV activity of type I IFN *in vitro*, suggesting that antiviral effects of IFN might relate to the proteasome (133). Yao et al. demonstrated that suppression of HBV replication was accompanied by an increase of 5 proteasome subunits in HepG2.2.15 cells in response to interleukin-4 (IL-4) treatment (134). This implied that IL-4 exerted one of its anti-HBV effects through proteasome pathway to degrade the proteins produced during HBV propagation. Here, we found that some core subunits of proteasome (PSMA7 and PSMB7) were increased their expressions as a result of IFN-λ3 treatment. This suggested that antiviral effects of IFN-λ3, in part, might depend on proteasome by degradation of the essential proteins either viral or host cellular proteins which were required for HBV replication. In our study, we also note up-regulation of immunoproteasome members (cap components PSME1 and PSME2) on IFN-λ3 and IFN-α2a treatment. The immunoproteasome is distinct from the constitutive proteasome in the composition of its catalytic subunits, its cap, and its peptide processing capacity (135). Interestingly, all significantly altered cap components of the constitutive proteasome were downregulated only upon IFN-λ3 treatment, suggesting coordinated modulation towards the antigen processing form of the proteasome on IFN-λ3 treatment. To our knowledge, this is the first report suggesting a shift from proteasome constitutive degradation mode to antigen processing/presentation mode in response to type III IFN treatment. HBV has been termed a “stealth” virus because innate immune responses in chimpanzees are not observed shortly after infection (43). The synthesis of type I IFNs is induced by the activation of RIG-I-like receptor (RLR) signaling pathways in response to viral infection. Previous studies have shown that HBV polymerase

and HBx proteins interfere with the interaction of RIG-I and downstream signaling molecules, resulting in diminished type I IFN production (136-138).

HBV has also been shown to alter RIG-I expression by inducing up-regulation of miR146a, which may directly down-regulate RIG-I and RIG-G transcripts (139). IFN treatment has not previously been shown to up-regulate RIG-I pathway components in HBV infected cells. We found, for the first time, that treating HepG2.2.15 with IFN-λ3 increased the expression of RIG-I. In addition, upon IFN-λ3 treatment, we observed elevated expression of RIG-G, known to enhance the activity of RIG-I, as well as TRIM25 and OASL, which promote the interaction between RIG-I and IPS1 on mitochondria or peroxisomes, leading to increased IFN production (140, 141). We propose that IFN-λ3 restores RIG-I and associated downstream signaling to produce type I IFN in HBV infected cells and likely other viruses. Although we did not find any IFNs in our proteomic work, possibly due to low abundances, qPCR verified increases in type I IFN (IFN-β) and type III IFN (IFN-λ1 and IFN-λ3) upon IFN-λ3 stimulation.

Several biological processes not mentioned above emerged from this work, including the involvement of 14-3-3 proteins, cyclophilin D, calreticulin, and cell motility proteins. These subjects are explored in detail below. In our study, the 14-3-3 proteins YWHAZ, YWHAH, and SFN were found to be down-regulated following IFN-λ3 treatment. Several studies have shown that 14-3-3 proteins may facilitate the replication of viruses (142, 143). The 14-3-3 proteins are highly conserved regulatory molecules having multiple functions, including involvement in signal transduction via kinases and phosphatases, the cell cycle, and apoptosis. These proteins have been shown to play important roles in viral infection. For example, complex formation of cdc25 with the HIV accessory protein Vpr, an event that alters the host cell life cycle, is facilitated by 14-3-3 proteins (142). Also, HCV core protein interacts with 14-3-3 proteins resulting in enhancement of Raf-1 kinase activity together with control of hepatocyte growth (143). Interestingly, sequence analysis revealed a 14-3-3 binding domain in HBx protein (144), suggesting that 14-3-3 proteins could directly interact with HBV. Notably, we could not observe significant alterations in 14-3-3 proteins upon IFN-α2a treatment; the differential effects of IFN-λ vs. IFN-α on 14-3-3 levels would be worthy of further investigation.

The downregulation of cyclophilin D upon IFN-λ3 treatment observed in our work suggests that this molecule may play a role in inhibition of HBV replication. One of the pathways affected by HBx is calcium signaling, as Ca^{2+} is necessary for viral replication and core assembly (145, 146). Calcium ions are the second messenger with various functions in the cell biology. These ions are stored in the mitochondria which acts as the regulator of intracellular calcium signaling. In addition to interference with RIG-I signaling, the HBx protein can interact with and modulate the mitochondrial permeability transition pore (MPTP) leading to the release of mitochondrial calcium into the cytoplasm

(145). The opening of the MPTP anion channel is regulated by cyclophilin D (147), thus downregulation of cyclophilin D would serve to counteract Ca^{2+}-assisted viral replication and core assembly. Increasing levels of cytosolic calcium causes the stimulation of PYK2 kinase, in turn activating Src kinase signal transduction to promote HBV reverse transcription, replication, and core assembly (146, 148). In several studies, cyclosporine A (CsA) was used as an MPTP specific blocker, thus reducing core assembly and inhibiting HBV replication (101, 147, 148). Consistent with CsA treatment, the calcium ion chelating agent BAPTA-AM also suppressed HBV propagation (148).

Calreticulin (CALR), down-regulated upon IFN-λ3 treatment in our study, is an ER calcium-binding chaperone involved in the regulation of calcium homoeostasis, the folding of newly synthesized proteins, nuclear import, and peptide loading on MHC class I (149-151). In HBV-transfected cells, Yue et al. demonstrated that the inhibition of IRF-7 translocation into the nucleus was induced by CALR, resulting in suppression of type I IFN production (152). Moreover, this group showed that CALR inhibited JAK-STAT pathway induction by IFN-α by inhibiting STAT1 phosphorylation, diminishing expression of PKR and OAS. Thus, the observation of downregulation of CALR would be expected to have an anti-viral effect. However, the downregulation of CALR would also seem to interfere with antigen processing/presentation. We note that most antigen processing/presentation molecules were upregulated upon treatment in our work, possibly compensating for this effect. Overall, the observed IFN-λ3-induced downregulation of CALR in our study may have an inhibitory effect on HBV replication.

Enrichment analysis (DAVID) showed that the most significantly down-regulated proteins following IFN-λ3 treatment were involved in cell motility and cell adhesion. We believe these processes could be relevant to the effects of IFN-λ3 treatment on liver cancer. Tan et al. demonstrated that HBV-transfected cells showed morphological changes due to formation of filopodia and lamellipodia, leading to cell migration. Of interest, CHB patients have 5-15 fold increased risk of HCC, a characteristic of which is increased cell motility (153, 154). CDC42, down-regulated on IFN-λ3 treatment, has been reported to control cell proliferation, adhesion, and metastases. High expression of this protein was observed in several types of cancers including HBV-related HCC. Inhibition of CDC42 by CRISPR/Cas9 knockout and treatment with a specific CDC42 inhibitor in HBx-Huh7 cells (155) reduced cell proliferation and promoted apoptosis in these cells. In addition to CDC42 downregulation, we also found that its downstream effectors, actin and IQGAP1, showed decreased expression following IFN-λ3 treatment. Also, proteins involved in cell movement and focal adhesion such as ACTN1, ACTN4, RDX, CFL1, PIP4K2C, and ROCK2 were down-regulated.

We have shown that IFN-λ3's effects were largely in accord with those expected of canonical IFN activity. Nevertheless, our tree and cluster analyses (Figure 13 and 14) highlight a number of

differential effects between IFN-λ3 and IFN-α2a worthy of further investigation. Most obviously, despite the division of treatment outcomes into 27 non-intersecting protein groups, unbiased Reactome enrichment analysis repeatedly elicited an RNA-metabolism/translation theme. This broad theme can be divided into Reactome sub-groups (e.g. metabolism of RNA, major pathway of rRNA processing in the nucleolus and cytosol, translation, transcription-coupled nucleotide excision repair (TC-NER), and peptide chain elongation). However, we could not specifically find IFN-λ3- or IFN-α2a dominant patterns in these sub-groups, suggesting that investigation of this broad theme might best be undertaken at the level of individual proteins. Perhaps the strongest general observation would be a tendency for involvement of ER-associated proteins (GO "establishment of protein localization to endoplasmic reticulum", which is primarily composed of ribosomal proteins) in cases where IFN-λ3 treatment results in significantly greater protein abundance vs. IFN-α2a; in the 5 outcomes where such an effect would be discernable, -log(p) = 4.7, 3.2, 4.8, 8.2, and 5.3. On the other hand, such significance (-log(p) = 4.1) is seen only once out of six outcomes where IFN-α2a treatment results in significantly more abundant protein expression. This result could imply differential regulation of these ER targeting proteins on IFN-λ3 vs. IFN-α2a treatment. Altered regulation of these ER proteins could interfere with viral replication (156, 157). It is interesting to note that some viruses utilize the ER as a replication compartment, whereas others do not. Thus, our work suggests that in addition to IFN's role in regulating ER-targeting, one IFN treatment might be more appropriate than another for particular infections. Of other Reactome groups that emerged during clustering, we find the "hypusine synthesis from eIF5A-lysine" case especially interesting, as it is only associated with a single outcome group, that in which λ3<c, α2a <c, λ3< α2a (i.e. the two IFNs cause downregulation, but IFN-λ3's effect is most potent). Hypusine, a rare amino acid, is apparently found only once in the human proteome, as a modification of eukaryotic initiation factor 5 (eIF5A), with proviral implications for HIV and Ebola (158). Thus, IFN-λ3's antiviral effect may be especially potent in down-regulating hypusination. The case of hypusination also illustrates how IFN-λ3-induced alterations to the RNA-metabolism/translation machinery could target particular viruses.

At the level of individual studies, we note that, in addition to the aforementioned λ3/α2a comparison, Bolen's data (16) also allows a λ3/λ2 comparison; here, upregulated transcripts aligned strongly with our own λ3/c upregulated proteins (p-value = 10^{-27}), suggesting possible differential effects even within the IFN-λ subgroup. As a side note, IFITM3, strongly upregulated in our own λ3/α2a comparison (outcome #1), was the single most significantly upregulated transcript in the λ3/λ2 comparison (p-value = 10^{-10}). Having noted possible IFN-λ3 vs. IFN-α2a differences, we should reiterate the points that: 1) our experimental design did not allow for discrimination of kinetic

effects (e.g. those caused over time by differing receptor/ligand affinities and half-lives) vs. substantial alterations at the level of pathways and 2) the effects of IFN-λ3 and IFN-α2a were indeed substantially similar, especially with regard to canonical IFN effects such as regulation of anti-viral proteins, antigen processing/presentation, and the RIG-I signaling pathway. A recent work does make a strong case for a differential λ3/α2a effect on murine intestinal epithelial cells (159), but the effect is pronounced only upon polarization of cells, and the underlying microarray data does not correlate with our proteomic data. Thorough studies focused on possible differential effects on PTMs may help resolve these questions; the immediate result of IFN-receptor/ligand interaction is, after all, a phosphorylation event. Comprehensive identification of phosphorylation events and other kinds of PTMs will help us to elucidate possible differential effects in different IFN treatment.

In conclusion, our study found that IFN-λ3 exhibited anti-HBV activities by significant inhibition of HBV replication and expression of HBV RNA. We utilized high-throughput quantitative proteomics to obtain a comprehensive understanding of molecular events upon treatment of HepG2.2.15 with IFN-λ3. To our knowledge, in fact, this study is the most comprehensive proteomics-based analysis of IFN treatment to date. For the first time, we reported significant upregulation of immunoproteasome components, restoration of HBV-inhibited RIG-I pathway proteins, as well as a number of proteins not previously associated with IFN-λ3 treatment. Further study of these proteins is required. Clearly, IFN-λ3 exhibited both antiviral and immunomodulatory effects to inhibit HBV replication; therefore, IFN-λ3 is an attractive novel candidate for CHB treatment and the altered proteins might be new therapeutic targets in CHB infection.

REFERENCES

1. Schweitzer, A., Horn, J., Mikolajczyk, R. T., Krause, G., and Ott, J. J. (2015) Estimations of worldwide prevalence of chronic hepatitis B virus infection: a systematic review of data published between 1965 and 2013. *Lancet* 386, 1546-1555

2. Grimm, D., Thimme, R., and Blum, H. E. (2011) HBV life cycle and novel drug targets. *Hepatol Int* 5, 644-653

3. Wright, T. L. (2006) Introduction to chronic hepatitis B infection. *The American journal of gastroenterology* 101 Suppl 1, S1-6

4. (2017) EASL 2017 Clinical Practice Guidelines on the management of hepatitis B virus infection. *Journal of hepatology* 67, 370-398

5. Yuen, M. F., and Lai, C. L. (2011) Treatment of chronic hepatitis B: Evolution over two decades. *J Gastroenterol Hepatol* 26 Suppl 1, 138-143

6. Lau, D. T. Y., and Bleibel, W. (2008) Current Status of Antiviral Therapy for Hepatitis B. *Therapeutic Advances in Gastroenterology* 1, 61-75

7. Fung, J., Lai, C. L., Seto, W. K., and Yuen, M. F. (2011) Nucleoside/nucleotide analogues in the treatment of chronic hepatitis B. *J Antimicrob Chemother* 66, 2715-2725

8. Phillips, S., Mistry, S., Riva, A., Cooksley, H., Hadzhiolova-Lebeau, T., Plavova, S., Katzarov, K., Simonova, M., Zeuzem, S., Woffendin, C., Chen, P.-J., Peng, C.-Y., Chang, T.-T., Lueth, S., De Knegt, R., Choi, M.-S., Wedemeyer, H., Dao, M., Kim, C.-W., Chu, H.-C., Wind-Rotolo, M., Williams, R., Cooney, E., and Chokshi, S. (2017) Peg-Interferon Lambda Treatment Induces Robust Innate and Adaptive Immunity in Chronic Hepatitis B Patients. *Frontiers in Immunology* 8, 621

9. Chan, H. L. Y., Ahn, S. H., Chang, T. T., Peng, C. Y., Wong, D., Coffin, C. S., Lim, S. G., Chen, P. J., Janssen, H. L. A., Marcellin, P., Serfaty, L., Zeuzem, S., Cohen, D., Critelli, L., Xu, D., Wind-Rotolo, M., and Cooney, E. (2016) Peginterferon lambda for the treatment of HBeAg-positive chronic hepatitis B: A randomized phase 2b study (LIRA-B). *Journal of hepatology* 64, 1011-1019

10. Dellgren, C., Gad, H. H., Hamming, O. J., Melchjorsen, J., and Hartmann, R. (2009) Human interferon-lambda3 is a potent member of the type III interferon family. *Genes Immun* 10, 125-131

11. Pestka, S. (1997) The interferon receptors. *Semin Oncol* 24, S9-18-s19-40

12. de Weerd, N. A., Samarajiwa, S. A., and Hertzog, P. J. (2007) Type I Interferon Receptors: Biochemistry and Biological Functions. *Journal of Biological Chemistry* 282, 20053-20057

13. Miller, D. M., Klucher, K. M., Freeman, J. A., Hausman, D. F., Fontana, D., and Williams, D. E. (2009) Interferon lambda as a potential new therapeutic for hepatitis C. *Ann N Y Acad Sci* 1182, 80-87

14. Ramos, E. L. (2010) Preclinical and clinical development of pegylated interferon-lambda 1 in chronic hepatitis C. *J Interferon Cytokine Res* 30, 591-595

15. Jilg, N., Lin, W., Hong, J., Schaefer, E. A., Wolski, D., Meixong, J., Goto, K., Brisac, C., Chusri, P., Fusco, D. N., Chevaliez, S., Luther, J., Kumthip, K., Urban, T. J., Peng, L. F., Lauer, G. M., and Chung, R. T. (2014) Kinetic Differences in the Induction of Interferon Stimulated Genes by Interferon-α and IL28B are altered by Infection with Hepatitis C Virus. *Hepatology (Baltimore, Md.)* 59, 1250-1261

16. Bolen, C. R., Ding, S., Robek, M. D., and Kleinstein, S. H. (2014) Dynamic expression profiling of type I and type III interferon-stimulated hepatocytes reveals a stable hierarchy of gene expression. *Hepatology (Baltimore, Md.)* 59, 1262-1272

17. Marcello, T., Grakoui, A., Barba–Spaeth, G., Machlin, E. S., Kotenko, S. V., Macdonald, M. R., and Rice, C. M. (2006) Interferons α and λ Inhibit Hepatitis C Virus Replication With Distinct Signal Transduction and Gene Regulation Kinetics. *Gastroenterology* 131, 1887-1898

18. Dumoutier, L., Tounsi, A., Michiels, T., Sommereyns, C., Kotenko, S. V., and Renauld, J. C. (2004) Role of the interleukin (IL)-28 receptor tyrosine residues for antiviral and antiproliferative activity of IL-29/interferon-lambda 1: similarities with type I interferon signaling. *J Biol Chem* 279, 32269-32274

19. Donnelly, R. P., Sheikh, F., Kotenko, S. V., and Dickensheets, H. (2004) The expanded family of class II cytokines that share the IL-10 receptor-2 (IL-10R2) chain. *Journal of Leukocyte Biology* 76, 314-321

20. Sells, M. A., Chen, M. L., and Acs, G. (1987) Production of hepatitis B virus particles in Hep G2 cells transfected with cloned hepatitis B virus DNA. *Proc Natl Acad Sci U S A* 84, 1005-1009

21. Witt-Kehati, D., Bitton Alaluf, M., and Shlomai, A. (2016) Advances and Challenges in Studying Hepatitis B Virus In Vitro. *Viruses* 8, 21

22. Verrier, E. R., Colpitts, C. C., Schuster, C., Zeisel, M. B., and Baumert, T. F. (2016) Cell Culture Models for the Investigation of Hepatitis B and D Virus Infection. *Viruses* 8, 261

23. Wang, J., Jiang, D., Zhang, H., Lv, S., Rao, H., Fei, R., and Wei, L. (2009) Proteome responses to stable hepatitis B virus transfection and following interferon alpha treatment in human liver cell line HepG2. *Proteomics* 9, 1672-1682

24. Otsuka, M., Aizaki, H., Kato, N., Suzuki, T., Miyamura, T., Omata, M., and Seki, N. (2003) Differential cellular gene expression induced by hepatitis B and C viruses. *Biochem Biophys Res Commun* 300, 443-447

25. Xin, X. M., Li, G. Q., Guan, X. R., Li, D., Xu, W. Z., Jin, Y. Y., and Gu, H. X. (2008) Combination therapy of siRNAs mediates greater suppression on hepatitis B virus cccDNA in HepG2.2.15 cell. *Hepatogastroenterology* 55, 2178-2183

26. Li, G. Q., Xu, W. Z., Wang, J. X., Deng, W. W., Li, D., and Gu, H. X. (2007) Combination of small interfering RNA and lamivudine on inhibition of human B virus replication in HepG2.2.15 cells. *World J Gastroenterol* 13, 2324-2327

27. Ding, X. R., Yang, J., Sun, D. C., Lou, S. K., and Wang, S. Q. (2008) Whole genome expression profiling of hepatitis B virus-transfected cell line reveals the potential targets of anti-HBV drugs. *Pharmacogenomics J* 8, 61-70

28. Liang, T. J. (2009) Hepatitis B: the virus and disease. *Hepatology (Baltimore, Md.)* 49, S13-21

29. Dienstag, J. L. (2008) Hepatitis B Virus Infection. *New England Journal of Medicine* 359, 1486-1500

30. Ganem, D., and Prince, A. M. (2004) Hepatitis B Virus Infection — Natural History and Clinical Consequences. *New England Journal of Medicine* 350, 1118-1129

31. Lin, X., Robinson, N. J., Thursz, M., Rosenberg, D. M., Weild, A., Pimenta, J. M., and Hall, A. J. (2005) Chronic hepatitis B virus infection in the Asia-Pacific region and Africa: review of disease progression. *J Gastroenterol Hepatol* 20, 833-843

32. Seeger, C., and Mason, W. S. (2000) Hepatitis B Virus Biology. *Microbiology and Molecular Biology Reviews* 64, 51-68

33. Kao, J. H. (2002) Hepatitis B viral genotypes: clinical relevance and molecular characteristics. *J Gastroenterol Hepatol* 17, 643-650

34. Locarnini, S. (2004) Molecular virology of hepatitis B virus. *Semin Liver Dis* 24 Suppl 1, 3-10

35. Locarnini, S., and Zoulim, F. (2010) Molecular genetics of HBV infection. *Antivir Ther* 15 Suppl 3, 3-14

36. Block, T. M., Guo, H., and Guo, J. T. (2007) Molecular virology of hepatitis B virus for clinicians. *Clin Liver Dis* 11, 685-706, vii

37. Yan, H., Liu, Y., Sui, J., and Li, W. (2015) NTCP opens the door for hepatitis B virus infection. *Antiviral research* 121, 24-30

38. Yan, H., Zhong, G., Xu, G., He, W., Jing, Z., Gao, Z., Huang, Y., Qi, Y., Peng, B., Wang, H., Fu, L., Song, M., Chen, P., Gao, W., Ren, B., Sun, Y., Cai, T., Feng, X., Sui, J., and Li, W. (2012) Sodium taurocholate cotransporting polypeptide is a functional receptor for human hepatitis B and D virus. *eLife* 1, e00049

39. Stephanie, S., and Eberhard, H. (2009) HBV Life Cycle: Entry and Morphogenesis. *Viruses* 1

40. Urban, S., Schulze, A., Dandri, M., and Petersen, J. (2010) The replication cycle of hepatitis B virus. *Journal of hepatology* 52, 282-284

41. Bertoletti, A., and Gehring, A. J. (2006) The immune response during hepatitis B virus infection. *J Gen Virol* 87, 1439-1449

42. Tan, A. T., Koh, S., Goh, V., and Bertoletti, A. (2008) Understanding the immunopathogenesis of chronic hepatitis B virus: an Asian prospective. *J Gastroenterol Hepatol* 23, 833-843

43. Wieland, S., Thimme, R., Purcell, R. H., and Chisari, F. V. (2004) Genomic analysis of the host response to hepatitis B virus infection. *Proc Natl Acad Sci U S A* 101, 6669-6674

44. Chang, J. J., and Lewin, S. R. (2007) Immunopathogenesis of hepatitis B virus infection. *Immunol Cell Biol* 85, 16-23

45. Bertoletti, A., Maini, M. K., and Ferrari, C. (2010) The host-pathogen interaction during HBV infection: immunological controversies. *Antivir Ther* 15 Suppl 3, 15-24

46. Zhang, Z., Zhang, J. Y., Wang, L. F., and Wang, F. S. (2012) Immunopathogenesis and prognostic immune markers of chronic hepatitis B virus infection. *J Gastroenterol Hepatol* 27, 223-230

47. Tang, H., Oishi, N., Kaneko, S., and Murakami, S. (2006) Molecular functions and biological roles of hepatitis B virus x protein. *Cancer Sci* 97, 977-983

48. Lok, A. S., and McMahon, B. J. (2007) Chronic hepatitis B. *Hepatology (Baltimore, Md.)* 45, 507-539

49. Samuel, C. E. (2001) Antiviral Actions of Interferons. *Clinical Microbiology Reviews* 14, 778-809

50. Gonzalez-Navajas, J. M., Lee, J., David, M., and Raz, E. (2012) Immunomodulatory functions of type I interferons. *Nat Rev Immunol* 12, 125-135

51. Pedder, S. C. (2003) Pegylation of interferon alfa: structural and pharmacokinetic properties. *Semin Liver Dis* 23 Suppl 1, 19-22

52. Foster, G. R. (2004) Review article: pegylated interferons: chemical and clinical differences. *Aliment Pharmacol Ther* 20, 825-830

53. Papatheodoridis, G. V., Dimou, E., and Papadimitropoulos, V. (2002) Nucleoside analogues for chronic hepatitis B: antiviral efficacy and viral resistance. *The American journal of gastroenterology* 97, 1618-1628

54. Kim, K. H., Kim, N. D., and Seong, B. L. (2010) Discovery and development of anti-HBV agents and their resistance. *Molecules (Basel, Switzerland)* 15, 5878-5908

55. Han, S.-H., and Tran, T. T. (2015) Management of Chronic Hepatitis B: An Overview of Practice Guidelines for Primary Care Providers. *The Journal of the American Board of Family Medicine* 28, 822-837

56. Sundaram, V., and Kowdley, K. (2015) Management of chronic hepatitis B infection. *BMJ : British Medical Journal* 351

57. Dienstag, J. L. (2009) Benefits and risks of nucleoside analog therapy for hepatitis B. *Hepatology (Baltimore, Md.)* 49, S112-121

58. Kotenko, S. V., Gallagher, G., Baurin, V. V., Lewis-Antes, A., Shen, M., Shah, N. K., Langer, J. A., Sheikh, F., Dickensheets, H., and Donnelly, R. P. (2003) IFN-lambdas mediate antiviral protection through a distinct class II cytokine receptor complex. *Nat Immunol* 4, 69-77

59. Sheppard, P., Kindsvogel, W., Xu, W., Henderson, K., Schlutsmeyer, S., Whitmore, T. E., Kuestner, R., Garrigues, U., Birks, C., Roraback, J., Ostrander, C., Dong, D., Shin, J., Presnell, S., Fox, B., Haldeman, B., Cooper, E., Taft, D., Gilbert, T., Grant, F. J., Tackett, M., Krivan, W., McKnight, G., Clegg, C., Foster, D., and Klucher, K. M. (2003) IL-28, IL-29 and their class II cytokine receptor IL-28R. *Nat Immunol* 4, 63-68

60. Donnelly, R. P., and Kotenko, S. V. (2010) Interferon-Lambda: A New Addition to an Old Family. *Journal of Interferon & Cytokine Research* 30, 555-564

61. Hamming, O. J., Gad, H. H., Paludan, S., and Hartmann, R. (2010) Lambda Interferons: New Cytokines with Old Functions. *Pharmaceuticals* 3, 795-809

62. Gad, H. H., Hamming, O. J., and Hartmann, R. (2010) The structure of human interferon lambda and what it has taught us. *J Interferon Cytokine Res* 30, 565-571

63. Iversen, M. B., and Paludan, S. R. (2010) Mechanisms of type III interferon expression. *J Interferon Cytokine Res* 30, 573-578

64. Witte, K., Witte, E., Sabat, R., and Wolk, K. (2010) IL-28A, IL-28B, and IL-29: promising cytokines with type I interferon-like properties. *Cytokine Growth Factor Rev* 21, 237-251

65. Zhang, L., Jilg, N., Shao, R. X., Lin, W., Fusco, D. N., Zhao, H., Goto, K., Peng, L. F., Chen, W. C., and Chung, R. T. (2011) IL28B inhibits hepatitis C virus replication through the JAK-STAT pathway. *Journal of hepatology* 55, 289-298

66. Marcello, T., Grakoui, A., Barba-Spaeth, G., Machlin, E. S., Kotenko, S. V., MacDonald, M. R., and Rice, C. M. (2006) Interferons alpha and lambda inhibit hepatitis C virus replication with distinct signal transduction and gene regulation kinetics. *Gastroenterology* 131, 1887-1898

67. Ank, N., West, H., and Paludan, S. R. (2006) IFN-lambda: novel antiviral cytokines. *J Interferon Cytokine Res* 26, 373-379

68. Diegelmann, J., Beigel, F., Zitzmann, K., Kaul, A., Goke, B., Auernhammer, C. J., Bartenschlager, R., Diepolder, H. M., and Brand, S. (2010) Comparative analysis of the lambda-interferons IL-28A and IL-29 regarding their transcriptome and their antiviral properties against hepatitis C virus. *PLoS One* 5, e15200

69. Donnelly, R. P., and Kotenko, S. V. (2010) Interferon-lambda: a new addition to an old family. *J Interferon Cytokine Res* 30, 555-564

70. Pagliaccetti, N. E., and Robek, M. D. (2010) Interferon-lambda in the immune response to hepatitis B virus and hepatitis C virus. *J Interferon Cytokine Res* 30, 585-590

71. Robek, M. D., Boyd, B. S., and Chisari, F. V. (2005) Lambda interferon inhibits hepatitis B and C virus replication. *Journal of virology* 79, 3851-3854

72. Clark, P. J., Thompson, A. J., and McHutchison, J. G. (2011) IL28B genomic-based treatment paradigms for patients with chronic hepatitis C infection: the future of personalized HCV therapies. *The American journal of gastroenterology* 106, 38-45

73. Jablonowska, E., Piekarska, A., Koslinska-Berkan, E., Omulecka, A., Szymanska, B., and Wojcik, K. (2012) Sustained virologic response and IL28B single-nucleotide polymorphisms in patients with chronic hepatitis C treated with pegylated interferon alfa and ribavirin. *Acta Biochim Pol* 59, 333-337

74. Halfon, P., Bourliere, M., Ouzan, D., Maor, Y., Renou, C., Wartelle, C., Penaranda, G., Tran, A., Botta, D., Oules, V., Castellani, P., Portal, I., Argiro, L., and Dessein, A. (2011) A single IL28B genotype SNP rs12979860 determination predicts treatment response in patients with chronic hepatitis C Genotype 1 virus. *European journal of gastroenterology & hepatology* 23, 931-935

75. Kim, S. U., Song, K. J., Chang, H. Y., Shin, E. C., Park, J. Y., Kim do, Y., Han, K. H., Chon, C. Y., and Ahn, S. H. (2013) Association between IL28B polymorphisms and spontaneous clearance of hepatitis B virus infection. *PLoS One* 8, e69166

76. Martin, M. P., Qi, Y., Goedert, J. J., Hussain, S. K., Kirk, G. D., Keith Hoots, W., Buchbinder, S., Carrington, M., and Thio, C. L. (2010) IL28B Polymorphism Does Not Determine Outcomes of Hepatitis B Virus or HIV Infection. *Journal of Infectious Diseases* 202, 1749-1753

77. Peng, L. J., Guo, J. S., Zhang, Z., Shi, H., Wang, J., and Wang, J. Y. (2012) IL28B rs12979860 polymorphism does not influence outcomes of hepatitis B virus infection. *Tissue Antigens* 79, 302-305

78. Hong, S. H., Cho, O., Kim, K., Shin, H. J., Kotenko, S. V., and Park, S. (2007) Effect of interferon-lambda on replication of hepatitis B virus in human hepatoma cells. *Virus Res* 126, 245-249

79. Muir, A. J., Shiffman, M. L., Zaman, A., Yoffe, B., de la Torre, A., Flamm, S., Gordon, S. C., Marotta, P., Vierling, J. M., Lopez-Talavera, J. C., Byrnes-Blake, K., Fontana, D., Freeman, J., Gray, T., Hausman, D., Hunder, N. N., and Lawitz, E. (2010) Phase 1b study of pegylated interferon lambda 1 with or without ribavirin in patients with chronic genotype 1 hepatitis C virus infection. *Hepatology (Baltimore, Md.)* 52, 822-832

80. Phillips, S., Mistry, S., Riva, A., Cooksley, H., Hadzhiolova-Lebeau, T., Plavova, S., Katzarov, K., Simonova, M., Zeuzem, S., Woffendin, C., Chen, P.-J., Peng, C.-Y., Chang, T.-T., Lueth, S., De Knegt, R., Choi, M.-S., Wedemeyer, H., Dao, M., Kim, C.-W., Chu, H.-C., Wind-Rotolo, M., Williams, R., Cooney, E., and Chokshi, S. (2017) Peg-Interferon Lambda Treatment Induces Robust Innate and Adaptive Immunity in Chronic Hepatitis B Patients. *Frontiers in Immunology* 8

81. Wieland, S. F., Eustaquio, A., Whitten-Bauer, C., Boyd, B., and Chisari, F. V. (2005) Interferon prevents formation of replication-competent hepatitis B virus RNA-containing nucleocapsids. *Proc Natl Acad Sci U S A* 102, 9913-9917

82. Li, J., Lin, S., Chen, Q., Peng, L., Zhai, J., Liu, Y., and Yuan, Z. (2010) Inhibition of hepatitis B virus replication by MyD88 involves accelerated degradation of pregenomic RNA and nuclear retention of pre-S/S RNAs. *Journal of virology* 84, 6387-6399

83. Chen, H., Wang, L. W., Huang, Y. Q., and Gong, Z. J. (2010) Interferon-alpha Induces High Expression of APOBEC3G and STAT-1 in Vitro and in Vivo. *Int J Mol Sci* 11, 3501-3512

84. Gordien, E., Rosmorduc, O., Peltekian, C., Garreau, F., Brechot, C., and Kremsdorf, D. (2001) Inhibition of hepatitis B virus replication by the interferon-inducible MxA protein. *Journal of virology* 75, 2684-2691

85. Xiong, W., Wang, X., Liu, X. Y., Xiang, L., Zheng, L. J., Liu, J. X., and Yuan, Z. H. (2003) Analysis of gene expression in hepatitis B virus transfected cell line induced by interferon. *Sheng Wu Hua Xue Yu Sheng Wu Wu Li Xue Bao (Shanghai)* 35, 1053-1060

86. Gorg, A., Weiss, W., and Dunn, M. J. (2004) Current two-dimensional electrophoresis technology for proteomics. *Proteomics* 4, 3665-3685

87. Tyers, M., and Mann, M. (2003) From genomics to proteomics. *Nature* 422, 193-197

88. Monteoliva, L., and Albar, J. P. (2004) Differential proteomics: an overview of gel and non-gel based approaches. *Briefings in functional genomics & proteomics* 3, 220-239

89. Baggerman, G., Vierstraete, E., De Loof, A., and Schoofs, L. (2005) Gel-based versus gel-free proteomics: a review. *Combinatorial chemistry & high throughput screening* 8, 669-677

90. Scherp, P., Ku, G., Coleman, L., and Kheterpal, I. (2011) Gel-based and gel-free proteomic technologies. *Methods in molecular biology (Clifton, N.J.)* 702, 163-190

91. Baiwir, D., Nanni, P., Müller, S., Smargiasso, N., Morsa, D., De Pauw, E., and Mazzucchelli, G. (2018) Gel-Free Proteomics. In: de Almeida, A. M., Eckersall, D., and Miller, I., eds. *Proteomics in Domestic Animals: from Farm to Systems Biology*, pp. 55-101, Springer International Publishing, Cham

92. Sandberg, A., Branca, R. M. M., Lehtiö, J., and Forshed, J. (2014) Quantitative accuracy in mass spectrometry based proteomics of complex samples: The impact of labeling and precursor interference. *Journal of Proteomics* 96, 133-144

93. Bakalarski, C. E., and Kirkpatrick, D. S. (2016) A Biologist's Field Guide to Multiplexed Quantitative Proteomics. *Molecular & Cellular Proteomics* 15, 1489-1497

94. Chahrour, O., Cobice, D., and Malone, J. (2015) Stable isotope labelling methods in mass spectrometry-based quantitative proteomics. *Journal of pharmaceutical and biomedical analysis* 113, 2-20

95. Li, Z., Adams, R. M., Chourey, K., Hurst, G. B., Hettich, R. L., and Pan, C. (2012) Systematic comparison of label-free, metabolic labeling, and isobaric chemical labeling for quantitative proteomics on LTQ Orbitrap Velos. *Journal of proteome research* 11, 1582-1590

96. Chen, X., Wei, S., Ji, Y., Guo, X., and Yang, F. (2015) Quantitative proteomics using SILAC: Principles, applications, and developments. *Proteomics* 15, 3175-3192

97. Boersema, P. J., Raijmakers, R., Lemeer, S., Mohammed, S., and Heck, A. J. R. (2009) Multiplex peptide stable isotope dimethyl labeling for quantitative proteomics. *Nature Protocols* 4, 484

98. Hsu, J.-L., and Chen, S.-H. (2016) Stable isotope dimethyl labelling for quantitative proteomics and beyond. *Philosophical transactions. Series A, Mathematical, physical, and engineering sciences* 374, 20150364

99. Wang, L. Y., Li, Y. G., Chen, K., Li, K., Qu, J. L., Qin, D. D., and Tang, H. (2012) Stable expression and integrated hepatitis B virus genome in a human hepatoma cell line. *Genet Mol Res* 11, 1442-1448

100. Fang, C., Zhao, C., Liu, X., Yang, P., and Lu, H. (2012) Protein alteration of HepG2.2.15 cells induced by iron overload. *Proteomics* 12, 1378-1390

101. Xie, H. Y., Xia, W. L., Zhang, C. C., Wu, L. M., Ji, H. F., Cheng, Y., and Zheng, S. S. (2007) Evaluation of hepatitis B virus replication and proteomic analysis of HepG2.2.15 cell line after cyclosporine A treatment. *Acta Pharmacol Sin* 28, 975-984

102. Venkatakrishnan, B., and Zlotnick, A. (2016) The Structural Biology of Hepatitis B Virus: Form and Function. *Annual review of virology* 3, 429-451

103. Hu, J., and Liu, K. (2017) Complete and Incomplete Hepatitis B Virus Particles: Formation, Function, and Application. *Viruses* 9, 56

104. Park, I. H., Kwon, Y. C., Ryu, W. S., and Ahn, B. Y. (2014) Inhibition of hepatitis B virus replication by ligand-mediated activation of RNase L. *Antiviral research* 104, 118-127

105. Jeong, G. U., Park, I. H., Ahn, K., and Ahn, B. Y. (2016) Inhibition of hepatitis B virus replication by a dNTPase-dependent function of the host restriction factor SAMHD1. *Virology* 495, 71-78

106. Chen, Z., Zhu, M., Pan, X., Zhu, Y., Yan, H., Jiang, T., Shen, Y., Dong, X., Zheng, N., Lu, J., Ying, S., and Shen, Y. (2014) Inhibition of Hepatitis B virus replication by SAMHD1. *Biochem Biophys Res Commun* 450, 1462-1468

107. Sommer, A. F., Riviere, L., Qu, B., Schott, K., Riess, M., Ni, Y., Shepard, C., Schnellbacher, E., Finkernagel, M., Himmelsbach, K., Welzel, K., Kettern, N., Donnerhak, C., Munk, C., Flory, E., Liese, J., Kim, B., Urban, S., and Konig, R. (2016) Restrictive influence of SAMHD1 on Hepatitis B Virus life cycle. *Sci Rep* 6, 26616

108. Lu, X., Wang, J., Jin, X., Huang, Y., Zeng, W., and Zhu, J. (2015) IFN-CSP Inhibiting Hepatitis B Virus in HepG2.2.15 Cells Involves JAK-STAT Signal Pathway. *BioMed Research International* 2015, 8

109. Robek, M. D., Boyd, B. S., Wieland, S. F., and Chisari, F. V. (2004) Signal transduction pathways that inhibit hepatitis B virus replication. *Proc Natl Acad Sci U S A* 101, 1743-1747

110. Amini-Bavil-Olyaee, S., Choi, Y. J., Lee, J. H., Shi, M., Huang, I. C., Farzan, M., and Jung, J. U. (2013) The antiviral effector IFITM3 disrupts intracellular cholesterol homeostasis to block viral entry. *Cell host & microbe* 13, 452-464

111. Macovei, A., Petrareanu, C., Lazar, C., Florian, P., and Branza-Nichita, N. (2013) Regulation of Hepatitis B Virus Infection by Rab5, Rab7, and the Endolysosomal Compartment. *Journal of virology* 87, 6415-6427

112. Kann, M., Schmitz, A., and Rabe, B. (2007) Intracellular transport of hepatitis B virus. *World J Gastroenterol* 13, 39-47

113. Osseman, Q., and Kann, M. (2017) Intracytoplasmic Transport of Hepatitis B Virus Capsids. *Methods in molecular biology (Clifton, N.J.)* 1540, 37-51

114. Gallucci, L., and Kann, M. (2017) Nuclear Import of Hepatitis B Virus Capsids and Genome. *Viruses* 9, 21

115. Sadler, A. J., and Williams, B. R. G. (2008) Interferon-inducible antiviral effectors. *Nature reviews. Immunology* 8, 559-568

116. Schoggins, J. W., and Rice, C. M. (2011) Interferon-stimulated genes and their antiviral effector functions. *Current opinion in virology* 1, 519-525

117. Pei, R., Qin, B., Zhang, X., Zhu, W., Kemper, T., Ma, Z., Trippler, M., Schlaak, J., Chen, X., and Lu, M. (2014) Interferon-induced proteins with tetratricopeptide repeats 1 and 2 are cellular factors that limit hepatitis B virus replication. *J Innate Immun* 6, 182-191

118. Sato, S., Li, K., Kameyama, T., Hayashi, T., Ishida, Y., Murakami, S., Watanabe, T., Iijima, S., Sakurai, Y., Watashi, K., Tsutsumi, S., Sato, Y., Akita, H., Wakita, T., Rice, C. M., Harashima, H., Kohara, M., Tanaka, Y., and Takaoka, A. (2015) The RNA sensor RIG-I dually functions as an innate sensor and direct antiviral factor for hepatitis B virus. *Immunity* 42, 123-132

119. Ryoo, J., Choi, J., Oh, C., Kim, S., Seo, M., Kim, S. Y., Seo, D., Kim, J., White, T. E., Brandariz-Nunez, A., Diaz-Griffero, F., Yun, C. H., Hollenbaugh, J. A., Kim, B., Baek, D., and Ahn, K. (2014) The ribonuclease activity of SAMHD1 is required for HIV-1 restriction. *Nat Med* 20, 936-941

120. Fu, Y., Gaelings, L., Soderholm, S., Belanov, S., Nandania, J., Nyman, T. A., Matikainen, S., Anders, S., Velagapudi, V., and Kainov, D. E. (2016) JNJ872 inhibits influenza A virus replication without altering cellular antiviral responses. *Antiviral research* 133, 23-31

121. Wang, X., Li, Y., Li, L. F., Shen, L., Zhang, L., Yu, J., Luo, Y., Sun, Y., Li, S., and Qiu, H. J. (2016) RNA interference screening of interferon-stimulated genes with antiviral activities against classical swine fever virus using a reporter virus. *Antiviral research* 128, 49-56

122. Meng, G., Zhao, Y., Bai, X., Liu, Y., Green, T. J., Luo, M., and Zheng, X. (2010) Structure of human stabilin-1 interacting chitinase-like protein (SI-CLP) reveals a saccharide-binding cleft with lower sugar-binding selectivity. *J Biol Chem* 285, 39898-39904

123. Rubins, K. H., Hensley, L. E., Wahl-Jensen, V., Daddario DiCaprio, K. M., Young, H. A., Reed, D. S., Jahrling, P. B., Brown, P. O., Relman, D. A., and Geisbert, T. W. (2007) The temporal program of peripheral blood gene expression in the response of nonhuman primates to Ebola hemorrhagic fever. *Genome Biology* 8, R174-R174

124. Zapata, J. C., Carrion, R., Jr., Patterson, J. L., Crasta, O., Zhang, Y., Mani, S., Jett, M., Poonia, B., Djavani, M., White, D. M., Lukashevich, I. S., and Salvato, M. S. (2013) Transcriptome analysis of human peripheral blood mononuclear cells exposed to Lassa virus and to the attenuated Mopeia/Lassa reassortant 29 (ML29), a vaccine candidate. *PLoS Negl Trop Dis* 7, e2406

125. Ioannidis, I., McNally, B., Willette, M., Peeples, M. E., Chaussabel, D., Durbin, J. E., Ramilo, O., Mejias, A., and Flano, E. (2012) Plasticity and virus specificity of the airway epithelial cell immune response during respiratory virus infection. *Journal of virology* 86, 5422-5436

126. Mitchell, H. D., Eisfeld, A. J., Sims, A. C., McDermott, J. E., Matzke, M. M., Webb-Robertson, B. J., Tilton, S. C., Tchitchek, N., Josset, L., Li, C., Ellis, A. L., Chang, J. H., Heegel, R. A., Luna, M. L., Schepmoes, A. A., Shukla, A. K., Metz, T. O., Neumann, G., Benecke, A. G., Smith, R. D., Baric,

R. S., Kawaoka, Y., Katze, M. G., and Waters, K. M. (2013) A network integration approach to predict conserved regulators related to pathogenicity of influenza and SARS-CoV respiratory viruses. *PLoS One* 8, e69374

127. Lee, S., Kopp, F., Chang, T. C., Sataluri, A., Chen, B., Sivakumar, S., Yu, H., Xie, Y., and Mendell, J. T. (2016) Noncoding RNA NORAD Regulates Genomic Stability by Sequestering PUMILIO Proteins. *Cell* 164, 69-80

128. Whisenant, T. C., Peralta, E. R., Aarreberg, L. D., Gao, N. J., Head, S. R., Ordoukhanian, P., Williamson, J. R., and Salomon, D. R. (2015) The Activation-Induced Assembly of an RNA/Protein Interactome Centered on the Splicing Factor U2AF2 Regulates Gene Expression in Human CD4 T Cells. *PLoS One* 10, e0144409

129. Liu, M. Q., Zhou, D. J., Wang, X., Zhou, W., Ye, L., Li, J. L., Wang, Y. Z., and Ho, W. Z. (2012) IFN-lambda3 inhibits HIV infection of macrophages through the JAK-STAT pathway. *PLoS One* 7, e35902

130. Lachmann, A., Torre, D., Keenan, A. B., Jagodnik, K. M., Lee, H. J., Silverstein, M. C., Wang, L., Ma, and ayan, A. (2017) Massive Mining of Publicly Available RNA-seq Data from Human and Mouse. *bioRxiv*

131. Maiwald, T., Schneider, A., Busch, H., Sahle, S., Gretz, N., Weiss, T. S., Kummer, U., and Klingmuller, U. (2010) Combining theoretical analysis and experimental data generation reveals IRF9 as a crucial factor for accelerating interferon alpha-induced early antiviral signalling. *Febs j* 277, 4741-4754

132. Rouillard, A. D., Gundersen, G. W., Fernandez, N. F., Wang, Z., Monteiro, C. D., McDermott, M. G., and Ma'ayan, A. (2016) The harmonizome: a collection of processed datasets gathered to serve and mine knowledge about genes and proteins. *Database (Oxford)* 2016

133. Robek, M. D., Wieland, S. F., and Chisari, F. V. (2002) Inhibition of hepatitis B virus replication by interferon requires proteasome activity. *Journal of virology* 76, 3570-3574

134. Yao, Y., Li, J., Lu, Z., Tong, A., Wang, W., Su, X., Zhou, Y., Mu, B., Zhou, S., Li, X., Chen, L., Gou, L., Song, H., Yang, J., and Wei, Y. (2011) Proteomic analysis of the interleukin-4 (IL-4) response in hepatitis B virus-positive human hepatocelluar carcinoma cell line HepG2.2.15. *Electrophoresis* 32, 2004-2012

135. Ferrington, D. A., and Gregerson, D. S. (2012) Immunoproteasomes: structure, function, and antigen presentation. *Prog Mol Biol Transl Sci* 109, 75-112

136. Yu, S., Chen, J., Wu, M., Chen, H., Kato, N., and Yuan, Z. (2010) Hepatitis B virus polymerase inhibits RIG-I- and Toll-like receptor 3-mediated beta interferon induction in human hepatocytes

through interference with interferon regulatory factor 3 activation and dampening of the interaction between TBK1/IKKepsilon and DDX3. *J Gen Virol* 91, 2080-2090

137. Jiang, J., and Tang, H. (2010) Mechanism of inhibiting type I interferon induction by hepatitis B virus X protein. *Protein Cell* 1, 1106-1117

138. Kumar, M., Jung, S. Y., Hodgson, A. J., Madden, C. R., Qin, J., and Slagle, B. L. (2011) Hepatitis B Virus Regulatory HBx Protein Binds to Adaptor Protein IPS-1 and Inhibits the Activation of Beta Interferon. *Journal of virology* 85, 987-995

139. Hou, Z., Zhang, J., Han, Q., Su, C., Qu, J., Xu, D., Zhang, C., and Tian, Z. (2016) Hepatitis B virus inhibits intrinsic RIG-I and RIG-G immune signaling via inducing miR146a. *Sci Rep* 6, 26150

140. Zhu, J., Zhang, Y., Ghosh, A., Cuevas, R. A., Forero, A., Dhar, J., Ibsen, M. S., Schmid-Burgk, J. L., Schmidt, T., Ganapathiraju, M. K., Fujita, T., Hartmann, R., Barik, S., Hornung, V., Coyne, C. B., and Sarkar, S. N. (2014) Antiviral activity of human OASL protein is mediated by enhancing signaling of the RIG-I RNA sensor. *Immunity* 40, 936-948

141. Gack, M. U., Shin, Y. C., Joo, C. H., Urano, T., Liang, C., Sun, L., Takeuchi, O., Akira, S., Chen, Z., Inoue, S., and Jung, J. U. (2007) TRIM25 RING-finger E3 ubiquitin ligase is essential for RIG-I-mediated antiviral activity. *Nature* 446, 916-920

142. Kino, T., Gragerov, A., Valentin, A., Tsopanomihalou, M., Ilyina-Gragerova, G., Erwin-Cohen, R., Chrousos, G. P., and Pavlakis, G. N. (2005) Vpr protein of human immunodeficiency virus type 1 binds to 14-3-3 proteins and facilitates complex formation with Cdc25C: implications for cell cycle arrest. *Journal of virology* 79, 2780-2787

143. Aoki, H., Hayashi, J., Moriyama, M., Arakawa, Y., and Hino, O. (2000) Hepatitis C virus core protein interacts with 14-3-3 protein and activates the kinase Raf-1. *Journal of virology* 74, 1736-1741

144. Fu, H., Subramanian, R. R., and Masters, S. C. (2000) 14-3-3 proteins: structure, function, and regulation. *Annu Rev Pharmacol Toxicol* 40, 617-647

145. Yang, B., and Bouchard, M. J. (2012) The hepatitis B virus X protein elevates cytosolic calcium signals by modulating mitochondrial calcium uptake. *Journal of virology* 86, 313-327

146. Bouchard, M. J., Wang, L. H., and Schneider, R. J. (2001) Calcium signaling by HBx protein in hepatitis B virus DNA replication. *Science* 294, 2376-2378

147. Xia, W. L., Shen, Y., and Zheng, S. S. (2005) Inhibitory effect of cyclosporine A on hepatitis B virus replication in vitro and its possible mechanisms. *Hepatobiliary Pancreat Dis Int* 4, 18-22

148. Choi, Y., Gyoo Park, S., Yoo, J. H., and Jung, G. (2005) Calcium ions affect the hepatitis B virus core assembly. *Virology* 332, 454-463

149. Coppolino, M. G., and Dedhar, S. (1998) Calreticulin. *Int J Biochem Cell Biol* 30, 553-558

150. Raghavan, M., Wijeyesakere, S. J., Peters, L. R., and Del Cid, N. (2013) Calreticulin in the immune system: ins and outs. *Trends Immunol* 34, 13-21

151. Michalak, M., Corbett, E. F., Mesaeli, N., Nakamura, K., and Opas, M. (1999) Calreticulin: one protein, one gene, many functions. *Biochem J* 344 Pt 2, 281-292

152. Yue, X., Wang, H., Zhao, F., Liu, S., Wu, J., Ren, W., and Zhu, Y. (2012) Hepatitis B virus-induced calreticulin protein is involved in IFN resistance. *J Immunol* 189, 279-286

153. Arjonen, A., Kaukonen, R., and Ivaska, J. (2011) Filopodia and adhesion in cancer cell motility. *Cell Adhesion & Migration* 5, 421-430

154. Zhao, R., Wang, T. Z., Kong, D., Zhang, L., Meng, H. X., Jiang, Y., Wu, Y. Q., Yu, Z. X., and Jin, X. M. (2011) Hepatoma cell line HepG2.2.15 demonstrates distinct biological features compared with parental HepG2. *World J Gastroenterol* 17, 1152-1159

155. Xu, Y., Qi, Y., Luo, J., Yang, J., Xie, Q., Deng, C., Su, N., Wei, W., Shi, D., Xu, F., Li, X., and Xu, P. (2017) Hepatitis B Virus X Protein Stimulates Proliferation, Wound Closure and Inhibits Apoptosis of HuH-7 Cells via CDC42. *International Journal of Molecular Sciences* 18, 586

156. Romero-Brey, I., and Bartenschlager, R. (2016) Endoplasmic Reticulum: The Favorite Intracellular Niche for Viral Replication and Assembly. *Viruses* 8, 160

157. Inoue, T., and Tsai, B. (2013) How Viruses Use the Endoplasmic Reticulum for Entry, Replication, and Assembly. *Cold Spring Harbor Perspectives in Biology* 5, a013250

158. Olsen, M. E., and Connor, J. H. (2017) Hypusination of eIF5A as a Target for Antiviral Therapy. *DNA Cell Biol* 36, 198-201

159. Selvakumar, T. A., Bhushal, S., Kalinke, U., Wirth, D., Hauser, H., Koster, M., and Hornef, M. W. (2017) Identification of a Predominantly Interferon-lambda-Induced Transcriptional Profile in Murine Intestinal Epithelial Cells. *Front Immunol* 8, 1302

Output จากโครงการวิจัยที่ได้รับทุนจาก สกว.

1. ผลงานตีพิมพ์ในวารสารวิชาการนานาชาติ (ระบุชื่อผู้แต่ง ชื่อเรื่อง ชื่อวารสาร ปี เล่มที่ เลขที่ และหน้า) พร้อมแจ้งสถานะของการตีพิมพ์ เช่น submitted, accepted, in press, published

   1.1 Makjaroen, J., Somparn, P., Hodge, K., Poomipak, W., Hirankarn, N., and **Pisitkun, T**. (2018) Comprehensive proteomics identification of IFN-lambda3-regulated anti-viral proteins in HBV-transfected cells. Molecular and Cellular Proteomics, In press.

   1.2 Medvar, B., Sarkar, A., Knepper, M., and **Pisitkun, T**. (2018) Sequence-Based Searching of Custom Proteome and Transcriptome Databases. Physiological Reports, In press.

2. การนำผลงานวิจัยไปใช้ประโยชน์

   - เชิงพาณิชย์ (มีการนำไปผลิต/ขาย/ก่อให้เกิดรายได้ หรือมีการนำไปประยุกต์ใช้โดยภาคธุรกิจ/บุคคลทั่วไป)
   - เชิงนโยบาย (มีการกำหนดนโยบายอิงงานวิจัย/เกิดมาตรการใหม่/เปลี่ยนแปลงระเบียบข้อบังคับหรือวิธีทำงาน)
   - เชิงสาธารณะ (มีเครือข่ายความร่วมมือ/สร้างกระแสความสนใจในวงกว้าง)
   - เชิงวิชาการ (มีการพัฒนาการเรียนการสอน/สร้างนักวิจัยใหม่)

   ส่วนหนึ่งของผลงานวิจัยนี้เป็นวิทยานิพนธ์ของนิสิตในการกำกับดูแลของผู้วิจัย โดยผู้วิจัยได้สอนความรู้พื้นฐาน, ทักษะในการทำวิจัย, กระบวนการคิดแบบเชิงระบบ, การวิเคราะห์และการแก้ไขปัญหาต่างๆแก่นิสิตผ่านการทำวิจัยนี้ โดยผู้วิจัยคาดหวังว่าเมื่อนิสิตจบการศึกษาไปจะสามารถเป็นนักวิจัยที่ดี, มีทักษะ และสามารถต่อยอดงานวิจัยนี้หรือสามารถทำงานวิจัยเรื่องอื่นได้อย่างมีประสิทธิภาพ นอกจากนี้ผู้วิจัยยังได้พัฒนาเครื่องมือที่ใช้สืบค้นในระดับทรานสคิปและโปรตีน โดยใช้ลำดับนิวคลีโอไทด์หรือลำดับกรดอะมิโน แทนการใช้สัญลักษณ์ยีน ซึ่งการใช้เครื่องมือนี้จะทำให้การวิเคราะห์ข้อมูลเชิงโอมิกส์ถูกต้องแม่นยำมากกว่าวิธีการสืบค้นแบบเดิม

3. อื่นๆ (เช่น ผลงานตีพิมพ์ในวารสารวิชาการในประเทศ การเสนอผลงานในที่ประชุมวิชาการ หนังสือ การจดสิทธิบัตร)

   3.1 Jiradej Makjaroen, Poorichaya Somparn, Kenneth Hodge, Witthaya Poomisak, Nattiya Hirankarn, and Trairak Pisitkun. Comphehensive proteomics identification of IFN-λ3-regulated anti-viral proteins in HBV-transfected cells. Cancer Precision Medicine Academic Conference, Nov 15-16, 2017. (Poster presentation)

   3.2 Jiradej Makjaroen, Poorichaya Somparn, Kenneth Hodge, Witthaya Poomisak, Nattiya Hirankarn, and Trairak Pisitkun. Comphehensive proteomics identification of IFN-λ3-

regulated anti-viral proteins in HBV-transfected cells. The 34th Annual Meeting AAIAT 2018, Mar 28-30, 2018. (Oral presentation)

3.3 Jiradej Makjaroen, Poorichaya Somparn, Kenneth Hodge, Witthaya Poomisak, Nattiya Hirankarn, and Trairak Pisitkun. Comphehensive proteomics identification of IFN-λ3-regulated anti-viral proteins in HBV-transfected cells. The Federation of Immunological Societies of Asia-Oceania (FIMSA 2018), Nov 10-13, 2018. (Poster presentation)

ภาคผนวก

Supplementary Table: Sequences of primers and probe

Primer	Sequence
preS1	F: 5′-GGGTCACCATATTCTTGGGAAC-3′ R: 5′-CCTGAGCCTGAGGGCTCCAC-3′
pgRNA	F: 5′-CTCAATCTCGGGAACCTCAATGT-3′ R: 5′-TGGATAAAACCTAGCAGGCATAAT-3′
OAS1	F: 5′-AGCCTCATCCGCCTAGTCAA-3′ R: 5′-CCTCGCTCCCAAGCATAGAC-3′
MX1	F: 5′-TGGTGTCGACATACCGGAAGA-3′ R: 5′-CCTTGCATGAGAGCAGTGATG-3′
ISG15	F: 5′-CGCAGATCACCCAGAAGATT-3′ R: 5′-GCCCTTGTTATTCCTCACCA-3′
TBK1	F: 5'-AGCGGCAGAGTTAGGTGAAA-3' R: 5'-CCAGTGATCCACCTGGAGAT-3'
DDX58	F: 5′-GCCATTACACTGTGCTTGGAGA-3' R: 5′-CCAGTTGCAATATCCTCCACCA-3'
IFNB	F: 5′-TGGGAGGCTTGAATACTGCCTCAA-3′ R: 5′-TCCTTGGCCTTCAGGTAATGCAGA-3′
IFNL1	F: 5'-CGCCTTGGAAGAGTCACTCA-3' R: 5'-GAAGCCTCAGGTCCCAATTC-3'
IFNL3	F: 5'-AGTTCCGGGCCTGTATCCAG-3' R: 5'-GAGCCGGTACAGCCAATGGT-3'
SFN	F: 5′-AAGAAGCGCATCATTGACTCAGCC-3′ R: 5′-TGTTGGCGATCTCGTAGTGGAAGA-3′
YWHAH	F: 5′-TGCAGAACTGGATACGCTGAGTGA-3′ R: 5′-TCACCCTGCATGTCTGAAGTCCAT-3′
CRT	F: 5'-AAGTTCTACGGTGACGAGGAG-3' R: 5'-GTCGATGTTCTGCTCATGTTTC-3'

Supplementary Table (Continued): Sequences of primers and probe

Primer	Sequence
Bst2	F: 5'-CCGTCCTGCTCGGCTTT-3'
	R: 5'-CCGCTCAGAACTGATGAGATCA-3'
IFIT3	F: 5'-GAACATGCTGACCAAGCAGA-3'
	R: 5'-CAGTTGTGTCCACCCTTCCT-3'
IFITM3	F: 5'-ATGTCGTCTGGTCCCTGTTC-3'
	R: 5'-GTCATGAGGATGCCCAGAAT-3'
GAPDH	F: 5'-AGATCCCTCCAAAATCAAGTGG-3'
	R: 5'-GGCAGAGATGATGACCCTTTT-3'
KRT8	F: 5'-TCTGGGATGCAGAACATGAG-3'
	R: 5'-CTCCTGTTCCCAGTGCTACC-3'
PGK2	F: 5'-AAGTCAGCCATGTCAGCACTG-3'
	R: 5'-GCCTGCTGCTTGTCCATTACA-3'
TRIM21	F: 5'-AAGCTCCAGGTGGCATTAGG-3'
	R: 5'-ACTGTTTTCTTCCAGTCTGCTCT-3'
SAMHD1	F: 5'-TCACAGGCGCATTACTGCC-3'
	R: 5'-GGATTTGAACCAATCGCTGGA-3'
TRIM25	F: 5'-AAAGCCACCAGCTCACATCCGA-3'
	R: 5'-CGGTGTTGTAGTCCAGGATGA-3'
EIFAK2	F: 5'-ATGATGGAAAGCGAACAAGG-3'
	R: 5'-TTCTCTGGGCTTTTCTTCCA-3'
OAS3	F: 5'-CCCTGGTCTGAGACTCACGTTT-3'
	R: 5'-GACTTGTGGCTTGGGTTTGAC-3'
OASL	F: 5'-CGTGAAACATCGGCCAACTAAG-3'
	R: 5'-GTACCCATTTCCCAGGCATAGA-3'

Reagents

Culturing media and reagents involving in cell stimulation and viability assay

1.) **Complete DMEM (100 ml)** (Store at 4°C)

Incomplete DMEM	90	ml
FBS	10	ml
5000 U/ml Penicillin/Streptomycin	1	ml
100X MEM-NEAA	1	ml

2.) **1X PBS pH 7.4**

PBS	1	pouch
Type I water	1	liter

PBS powder was dissolved in distilled water, sterilized this solution by autoclaving at 121°C for 15 minutes and stored at room temperature.

3.) **0.1% BSA** (Store at 4°C)

BSA	0.01	g
Sterile PBS	10	ml

4.) **5 mg/ml MTT solution**

MTT	50	mg
Sterile PBS	10	ml

MTT was dissolved in sterile PBS and filtrated by 0.2 μM acrodisc syringe filter. This solution was kept at 4°C with light protection.

Mastermixes for reverse transcription and quantitative real-time PCR

1.) **Mastermix for cDNA synthesis (1 reaction)**

RNase free water	5.5	μl
10X RT buffer	3	μl
25 mM $MgCl_2$	6.6	μl

10 mM dNTPs	2	µl
50 M Random hexamer	0.5	µl
20 U/µl RNase inhibitor	0.6	µl
50 U/µl Multiscribe	0.25	µl
RNA 200 ng/µl	11.5	µl

2.) Mastermix for qPCR using SYBR green (1 reaction)

Power SYBR Green PCR Master Mix	10	µl
RNase-free water	7	µl
20 µM forward primer	0.5	µl
20 µM reverse primer	0.5	µl
50 ng/µl of cDNA or DNA	2	µl

3.) Mastermix for qPCR using probe (1 reaction)

TaqMan Universal PCR Master Mix	10	µl
RNase-free water	6.8	µl
20 µM forward primer	0.5	µl
20 µM reverse primer	0.5	µl
20 µM probe	0.2	µl
50 ng/µl of cDNA	2	µl

Reagents in SDS-PAGE preparation

1.) 1.5 M Tris-HCl pH 8.8

Tris base	181.7	g

This agent was dissolved in 750 ml of type I water and then adjusted pH to 8.8 by HCl. The final volume of this solution was adjusted to 1,000 ml with type I water. This solution was kept at 4^{o}C.

2.) 1 M Tris-HCl pH 6.8

Tris base	121.1	g

This chemical was combined with 750 ml of type I water followed by pH adjustment to pH 6.8 using HCl. The volume was adjusted to 1,000 ml by type I water and this solution was stored at 4°C.

3.) 10% SDS

SDS	10	g
Milli Q	100	ml

4.) 10% APS

Ammonium persulfate	0.1	g
Milli Q	1	ml

This solution should be fresh preparation.

Buffer for running SDS-PAGE

1.) 10X SDS-PAGE running buffer

Glycine	144	g
Tris base	30.2	g
SDS	10	g

All chemicals were dissolved in Milli Q and adjusted to final volume of 1,000 ml with MilliQ. This buffer was kept at room temperature.

2.) 1X SDS-PAGE running buffer

10X SDS-PAGE running buffer	100	ml
Milli Q	900	ml

Reagents and buffers in western blotting assay

1.) Laemmli buffer (2X)

10% (w/v) SDS	4	ml
Glycerol	2	ml
1 M Tris-HCl (pH 6.8)	1.2	ml

Milli Q	2.8	ml

After combination of all agents, bromophenol blue was added to the solution with final concentration 0.02% (w/v). This buffer was stored at -20^{o}C until use. 30 mg of DTT was added to 1 ml of this buffer prior to use.

2.) 12.5% SDS-PAGE (1 gel)

Milli Q	4,175	µl
40% Acrylamide gel	3,125	µl
1.5 M Tris-HCl pH 8.8	2.5	ml
10% SDS	100	µl
10% APS	100	µl
TEMED	5	µl

3.) 4% Stacking gel (1 gel)

Milli Q	3,650	µl
40% Acrylamide gel	625	µl
1 M Tris-HCl pH 6.8	625	µl
10% SDS	50	µl
10% APS	50	µl
TEMED	6	µl

4.) 1X Transfer buffer

Trans-Blot Turbo 5X Transfer buffer	20	ml
Ethanol	20	ml
Type I water	60	ml

5.) 10X TBS

Tris base	60.5	g
NaCl	88.7	g

Both Tris base and NaCl were dissolve in 1,000 ml of type I water and this buffer was kept at room temperature.

6.) 1X TBST

10X TBS	100	ml
Tween 20	1	ml

Both solutions were mixed and adjusted volume to 1,000 ml with Milli Q. This buffer was kept at room temperature.

Reagents for in-solution digestion

1.) Lysis buffer (Store at -20^{o}C)

Sodium deoxycholate	13.6	g
1 M triethylammonium bicarbonate (TEAB)	0.5	g
Distilled water	25	ml
100X Protease inhibitor cocktail		

2.) 25 mM TEAB

1 M TEAB	100	mg
Type I water	10	ml

3.) 100 mM DTT

DTT	10	ml
25 mM TEAB	0.05	g

4.) 100 mM IA

Iodoacetamide	10	ml
25 mM TEAB	72.07	g

5.) Trypsin solution

Trypsin

Suspension buffer

Reagents for in-solution dimethyl labeling

1.) 100 mM TEAB

1 M TEAB	1	ml
Type I water	9	ml

2.) 4% CH2O

37% CH2O	10.81	µl
Type I water	89.19	µl

3.) 4% CD2O

20% CD2O	20	µl
Type I water	80	µl

4.) 4% 13CD2O

20% 13CD2O	20	µl
Type I water	80	µl

5.) 0.6 M NaBH3CN

NaBH3CN	7.54	mg
Type I water	200	µl

6.) 0.6 M NaBD3CN

NaBD3CN	3.95	mg
Type I water	100	µl

7.) 1% Ammonia solution

25% Ammonia solution	20	µl
Type I water	480	µl

Reagents for LC-MS/MS

1.) Buffer A (0.1% in 5% ACN)

Acetonitrile	1	ml
50% Formic acid	40	µl
LC-MS grade water	19	ml

2.) Buffer B (0.1% FA in 100% ACN)

Acetonitrile	20	ml
50% Formic acid	40	µl

3.) 25 fmol BSA standard

1 pmol of digested BSA	5	µl
0.1% FA in LC-MS grade water	195	µl

4.) Blank

0.1% FA in LC-MS grade water	200	µl

Manuscript proof 1

Comprehensive Proteomics Identification of IFN-λ3-regulated Antiviral Proteins In HBV-transfected Cells*[S]

Jiradej Makjaroen‡§¶, Poorichaya Somparn§¶, Kenneth Hodge¶, Witthaya Poomipak¶, Nattiya Hirankarn§**, and Trairak Pisitkun¶‖**

Interferon lambda (IFN-λ) is a relatively unexplored, yet promising antiviral agent. IFN-λ has recently been tested in clinical trials of chronic hepatitis B virus infection (CHB), with the advantage that side effects may be limited compared with IFN-α, as IFN-λ receptors are found only in epithelial cells. To date, IFN-λ's downstream signaling pathway remains largely unelucidated, particularly via proteomics methods. Here, we report that IFN-λ3 inhibits HBV replication in HepG2.2.15 cells, reducing levels of both HBV transcripts and intracellular HBV DNA. Quantitative proteomic analysis of HBV-transfected cells was performed following 24-hour IFN-λ3 treatment, with parallel IFN-α2a and PBS treatments for comparison using a dimethyl labeling method. The depth of the study allowed us to map the induction of antiviral proteins to multiple points of the viral life cycle, as well as facilitating the identification of antiviral proteins not previously known to be elicited upon HBV infection (*e.g.* IFITM3, XRN2, and NT5C3A). This study also shows up-regulation of many effectors involved in antigen processing/presentation indicating that this cytokine exerted immunomodulatory effects through several essential molecules for these processes. Interestingly, the 2 subunits of the immunoproteasome cap (PSME1 and PSME2) were up-regulated whereas cap components of the constitutive proteasome were down-regulated upon both IFN treatments, suggesting coordinated modulation toward the antigen processing/presentation mode. Furthermore, in addition to confirming canonical activation of interferon-stimulated gene (ISG) transcription through the JAK-STAT pathway, we reveal that IFN-λ3 restored levels of RIG-I and RIG-G, proteins known to be suppressed by HBV. Enrichment analysis demonstrated that several biological processes including RNA metabolism, translation, and ER-targeting were differentially regulated upon treatment with IFN-λ3 *versus* IFN-α2a. Our proteomic data suggests that IFN-λ3 regulates an array of cellular processes to control HBV replication. ***Molecular & Cellular Proteomics 17: 1–19, 2018. DOI: 10.1074/mcp.RA118.000735.***

AQ: A

Chronic hepatitis B (CHB)[1] is a major health problem worldwide, affecting 240 million people throughout the world with a prevalence in Africa and South-East Asia (1). Chronic HBV-infected individuals mostly acquire the virus at a young age through vertical transmission or contact with the blood or other body fluids of an infected person. CHB eventually progresses to severe and high-mortality liver diseases including liver cirrhosis and hepatocellular carcinoma (HCC) resulting in 600,000 deaths annually (2, 3).

Fn1, AQ:B-F

Current therapeutic agents for CHB are interferon (IFN)-α and nucleos(t)ide analogs (NAs) (4–6). IFN-α is a cytokine that possesses antiviral and immunomodulatory effects, which promotes control and eradication of viral infection. The advantages of using IFN-α for CHB treatment are the decreased incidence of viral resistance following this treatment and the finite duration of therapy with a higher rate of seroconversion of viral antigens, *i.e.* HBeAg and HBsAg, compared with NAs. However, the drawbacks of IFN-α treatment are its inconvenient route of administration and its adverse effects such as influenza-like symptoms, nausea, vomiting, cytopenia, and psychiatric disorders. Regarding the latter agent, NAs against CHB, the lack of a 3′-hydroxyl group in these compounds allows competitive incorporation into the viral genome resulting in termination of viral replication (7). Although NAs can directly suppress HBV replication and have fewer unfavorable side effects compared with IFN-α, CHB patients usually require a long-term treatment of these agents, thus increasing the chance of the emergence of viral resistance. In addition, the low rate of HBeAg and HBsAg seroconversion is another limitation of NAs. Therefore, new drugs that overcome restrictions of current antiHBV treatments are still needed.

From the ‡Medical Microbiology Interdisciplinary Program, Graduate School, Chulalongkorn University, Bangkok, Thailand; §Center of Excellence in Immunology and Immune-mediated Diseases, Department of Microbiology, Faculty of Medicine, Chulalongkorn University, Bangkok, Thailand; ¶Center of Excellence in Systems Biology, Research affairs, Faculty of Medicine, Chulalongkorn University, Bangkok, Thailand

Received March 14, 2018, and in revised form, June 10, 2018
Published, MCP Papers in Press, August 10, 2018, DOI 10.1074/mcp.RA118.000735

Several lines of reasoning suggest that IFN-λ could have a superior combination of efficacy and reduced side-effects. IFN-λ or type III IFN is a cytokine in the class II cytokine family that has recently been used in clinical trials of CHB treatment (8, 9). IFN-λ has 4 subtypes, namely IFN-λ1, -λ2, -λ3, and –λ4. IFN-λ3 was shown to have superior antiviral potency compared with other IFN-λ subtypes (10). IFN-λ receptor is composed of an IFNLR1 and IL10R2 dimer; hence upon ligand binding, the receptor activates both IFN and IL-10-like signaling pathways. The type I IFN-receptors also form a heterodimer (IFNAR1 and IFNAR2), however, the sequences of all these receptors do diverge, particularly at the C terminus (11, 12). IFNLR1 is expressed only in epithelial cells including hepatocytes in contrast to IFN-α receptor, which is widely expressed in many cell types throughout the body; thus IFN-λ treatment results in fewer side-effects when compared with IFN-α treatment (9, 13, 14). IFN-λ has been shown to activate the JAK/STAT pathway, inducing formation of the ISGF3 transcription complex, leading to expression of interferon-stimulated genes (ISGs) in similar fashion to type I IFN, but with a different temporal profile compared with those induced by type I IFN (15–17). A limited number of reports regarding IL-10-like signaling pathways have been published, with evidence of STAT3/5 biological activities (18, 19). In fact, no reports have comprehensively investigated the downstream molecular signaling effects of IFN-λ.

To better understand molecular mechanisms underlying direct antiviral and immunomodulatory effects of IFN-λ3, a comprehensive catalogue of protein effectors regulated by IFN-λ3 was compiled using quantitative proteomics analysis in the well-established HBV-transfected hepatocellular carcinoma cell line model viz. HepG2.2.15 cells (20). HepG2.2.15 cells have been widely used as a model of chronic hepatitis B because they support HBV replication and virion secretion (21–27). These new findings could improve the treatment strategy of HBV infection and expand potential applications of IFN-λ3.

EXPERIMENTAL PROCEDURES

Experimental Design and Statistical Rationale—Mixing of dimethyl-labeled samples corresponding to IFN-λ3, IFN-α2a, and control (PBS) treatments were performed at $n = 5$ *versus* the typical $n = 3$ to emphasize depth. Only biological replicates were performed. The normality of all proteomics, western-blotting and qPCR data was evaluated with the Shapiro-Wilk test. In all cases, the unpaired Student's *t* test or one-way ANOVA was selected when the distribution of the data was normal; otherwise the Mann-Whitney *U* test was applied. For proteomic analysis, peak intensity log2 ratios (L/M, L/H, M/H) were compared against a value of 0 (no change, log2(1)). Significance was based on the following criterion: p value < 0.05 or cases where proteins were detected in only one condition making standard statistical analysis inapplicable, with the requirement that these proteins must be identified in at least 4 of 5 experiments. Proteins not fulfilling the above criteria as well as those appearing in fewer than 3 experiments, were excluded from downstream analysis. Regarding western-blotting and qPCR experiments, $n = 3$ was set. One-way ANOVA was performed for these experiments with p value < 0.05 considered significant. In the case of DAVID enrichment analysis, all proteins identified by mass spectrometry were input as background. When Fisher-based enrichment analysis was performed against an in-house database of proteomic/transcriptomic studies, resulting log (p values) were conservatively adjusted by subtracting the log value corresponding to the total of all possible study/study combinations in the database.

Cell Culture and Cell Stimulation—HepG2.2.15 cells are stable HBV-transfected cells derived from a hepatoblastoma HepG2 cell line (20). These cells contain a plasmid which expresses the complete genome of HBV, which integrates into host cellular DNA (20, 28). Because HBV within HepG2.2.15 replicates and secretes HBsAg, HBeAg and HBV DNA into the culture media, HepG2.2.15 has been widely used as a model of chronic hepatitis B (22, 28). The HepG2.2.15 cell line was kindly provided from Professor Antonio Bertoletti (Singapore Institute for Clinical Sciences, A*Star). These cells were maintained in Dulbecco's Modified Eagle's Medium (DMEM; Gibco) supplemented with 10% Fetal Bovine Serum (FBS; Gibco), 1% MEM Non-Essential Amino Acids (MEM-NEAA; Gibco), 1% Penicillin/Streptomycin (Gibco) and Geneticin (G418; Gibco) at a final concentration of 150 μg/ml. The cultured cells were grown in a humidified incubator at 37 °C with 5% CO_2. One million HepG2.2.15 cells were seeded into 6-well plates with 1 ml media and maintained in complete DMEM for 24 h. For determining the effects of IFN-λ3 on HBV replication, these cells were left untreated or treated with 1, 10, 100 or 1000 ng/ml of IFN-λ3 (5259-IL-025, R&D Systems) and incubated for another 24 h. For proteomics analysis, HepG2.2.15 cells were plated at 5×10^6 cells in T-75 flasks and grown in complete DMEM for 24 h at 37 °C. These cells were subsequently cultured in media with 100 ng/ml of IFN-λ3 or 100 ng/ml of IFN-α2a (11100–1, pbl assay science) or PBS (control) for another 24 h. For further qPCR experiments with an optimized concentration of IFN-λ3, HepG2.2.15 cells were stimulated with or without 100 ng/ml of IFN-λ3 for 0, 8, 16, and 24 h.

RNA Isolation, Reverse Transcription, and qPCR for Gene Expression—TRIzol Reagent (Thermo) was used to extract total RNA as specified in the accompanying manual. Complementary DNA (cDNA) synthesis was carried out using the Taqman Reverse transcription kit (Applied Biosystems). Conditions for reverse transcription were as specified in the manual. Relative gene expression was measured with the ABI Prism 7500 sequence detection system (Applied Biosystems). All primers and probes were designed with the "primer express 3" program (Applied Biosystems), and are shown in supplemental Table S1. To monitor gene amplification, the intensity of fluorescence from the 18S housekeeping gene was monitored via Taqman probe whereas all target gene levels were monitored via SYBR green dye (Applied Biosystems). To test the specificity of SYBR green dye, melting curve analysis was conducted for all target genes. The condition of amplification for both target and housekeeping genes was 1 cycle at 95 °C for 5 min followed by 40 cycles at 95 °C for 15 s and 60 °C for 1 min. Relative gene expression was calculated with the 2^{-ddCt} method. The Student's *t* test and one-way ANOVA were used to compare the relative expressions of target genes in cells treated with various doses of IFN-λ3. A p value less than 0.05 was considered significant.

[1] The abbreviations used are: HBV, hepatitis B virus; CHB, chronic hepatitis B; HCC, hepatocellular carcinoma; pgRNA, pregenomic RNA; IFN-α2a, interferon-alpha2a; IFN-λ3, interferon-lambda3; ISG, interferon-stimulated gene; SDC, sodium deoxycholate; qPCR, quantitative polymerase chain reaction; GO, Gene Ontology; FDR, false discovery rate.

DNA Extraction and Absolute qPCR—After trypsinization and PBS-washing, cellular DNA was extracted using the QIAamp DNA Blood Mini Kit (Qiagen) according to manufacturer's instructions. Quantification of HBV viral load was performed by absolute quantitative real-time PCR using the ABI Prism 7500 sequence detection system (Applied Biosystems). For ease of plasmid amplification, we used plasmids containing only the HBV gene preS1 as a surrogate marker for HBV DNA (preS1 was chosen because it is highly conserved across all HBV genotypes). First, preS1 plasmids were extracted from *E. coli* transformants with the GeneJET Plasmid Miniprep Kit (Fermentas). The concentration of extracted plasmids was measured by spectrophotometer (Nanodrop, Thermo) and copy/μl was determined. The plasmid concentration was adjusted and diluted in a range of 10^7, 10^6, 10^5, 10^4, 10^3, and 10^2 copy/μl. These concentrations were used to construct a standard curve. Both standard and sample *pres1* were amplified at the same time using conditions described above. The fluorescent intensities were specified as C_t values. For standards, C_t values at the above concentrations were used to plot a standard curve. This curve and sample C_t values were used to calculate the amount of HBV DNA in the samples. The Student's *t* test and one-way ANOVA were used to compare viral loads in cells treated with various levels of IFN-λ3, as well as untreated cells. A *p* value less than 0.05 was considered significant.

MTT Assay—HepG2.2.15 cells were seeded in 96-well plates at a density of 1×10^4 cells per well and incubated for 24 h. The culture media was removed and replaced with fresh complete media in the absence or presence of IFN-λ3 (1, 10, 100 and 1000 ng/ml). The cells were further incubated for 24 h followed by addition of 10 μl 5 mg/ml MTT (Sigma) solution in each well with gentle shaking. After 4h incubation, the resulting purple formazan crystals were dissolved with dimethyl sulfoxide (DMSO, Riedel-deHaën) and subsequently measured with ELISA plate reader (Thermo) at wavelength 570 nm. The absorbance values of cells treated with each concentration of drug were compared with that of control (untreated) cells and % cell viability was calculated. This experiment was performed in triplicate.

Protein Extraction and In-solution Digestion—After trypsinization, the cells were lysed with 5% sodium deoxycholate (SDC) and 1X protease inhibitor (Thermo) mixture, followed by sonication. All cell debris was removed by centrifugation and supernatant protein concentrations of each sample were measured via BCA Protein Assay (Thermo). Equal amounts of protein from treated and untreated HepG2.2.15 were reduced and alkylated by dithiothreitol (DTT) treatment for 30 min at 37 °C and iodoacetamide (IA) treatment for 30 min at room temperature in the dark, respectively. These samples were further quenched with DTT at least 15 min at room temperature before incubating with trypsin at a ratio of 1:50 at 37 °C overnight. These mixtures were incubated with 0.5% trifluoroacetic acid (TFA) for 30 min and then centrifuged to remove SDC precipitate. The amount of tryptic peptide of each sample was determined with the Pierce Quantitative Fluorometric Peptide Assay (Thermo).

Dimethyl Labeling and Fractionation—Peptides from IFN-λ3 treated, IFN-α2a treated, and untreated HepG2.2.15 were labeled with light reagents (formaldehyde and cyanoborohydride), medium reagents (formaldehyde-d2 and cyanoborohydride), and heavy reagents (deuterated and ^{13}C-labeled formaldehyde and cyanoborodeuteride), respectively, for an hour at room temperature. Ammonia solution and formic acid (FA) were sequentially used to stop the reaction. Labeling efficiency was tested, and we found that greater than 99% of peptides were labeled (data not shown). After combining these three samples, the mixed labeled-peptides were dried in a SpeedVac centrifuge at room temperature. Next, the pooled peptides were separated into 10 fractions to reduce complexity using the Pierce High pH Reversed-Phase Peptide Fractionation Kit (Thermo). Eluates of each fraction were dried in a SpeedVac centrifuge before LC-MS/MS analysis.

LC-MS/MS and Analysis—The fractionated samples were resuspended in 0.1% FA (Sigma) to a final volume of 15 μl prior to MS injection. The peptides were then analyzed via an EASY-nLC1000 system (Thermo) coupled to a Q-Exactive Orbitrap Plus mass spectrometer (Thermo) equipped with a nano-electrospray ion source (Thermo). The peptides were eluted in 5–40% acetonitrile in 0.1% FA for 70 min followed by 40–95% acetonitrile in 0.1% FA for 20 min at a flow rate of 300 nl/min. The MS methods included a full MS scan at a resolution of 70,000 followed by 10 data-dependent MS2 scans at a resolution of 17,500. The normalized collision energy of HCD fragmentation was set at 32%. An MS scan range of 350 to 1400 *m/z* was selected and precursor ions with unassigned charge states, a charge state of +1, or a charge state of greater than +8 were excluded. A dynamic exclusion of 30 s was used. The peaklist-generating software used in this study was Proteome Discoverer™ Software 2.1 (Thermo). The SEQUEST-HT search engine was employed in data processing. MS raw data files were searched against the Human Swiss-Prot Database (20,219 proteins, June 2017) and the Hepatitis B Virus Swiss-Prot Database (225 proteins, June 2017), as well as a list of common protein contaminants (www.thegpm.org/crap/). The following parameters were set for the search: (1) digestion enzyme: trypsin; (2) maximum allowance for missed cleavages: 2; (3) maximum of modifications: 4; (4) fixed modifications: carbamidomethylation of cysteine (+57.02146 Da), as well as light, medium, and heavy dimethylation of N termini and lysine (+28.031300, +32.056407, and +36.075670 Da); (5) variable modifications: oxidation of methionine (+15.99491 Da). The mass tolerances for precursor and fragment ions were set to 10 ppm and 0.02 Da, respectively. Known contaminant ions were excluded. The Proteome Discoverer decoy database together with the Percolator algorithm were used to calculate the false positive discovery rate of the identified peptides based on Q-values which were set to 1%. The Precursor Ions Quantifier node in Proteome Discoverer™ Software was employed to quantify the relative MS signal intensities of dimethyl labeled-peptides. The control channels were used as denominators to generate abundance ratios of IFN-λ3/control and IFN-α2a/control. Log2 of the normalized ratio was used to calculate the mean and standard deviation of fold change across all five biological replicates. When these ratios were found in less than three experiments, the relevant proteins were excluded. Significantly differentially regulated proteins were determined by Mann-Whitney *U* test and unpaired *t*-tests with *p* value < 0.05 considered significant.

Bioinformatics—We compiled a list of defense response to virus using a variety of resources as follows. The online resource Database for Annotation, Visualization and Integrated Discovery (DAVID, v6.8, https://david.ncifcrf.gov/) and Reactome (https://reactome.org/) were employed to classify the proteins regulated by IFN-λ3 into functional categories using all proteins identified by MS as background (for DAVID). We used terms such as "antiviral," "antigen processing/presentation" to help extract a custom list of broad antiviral proteins. Additionally, the list contains proteins involved in the HBV life-cycle that were derived from manual literature curation. Further analysis of up/downregulated proteins was performed against an in-house database currently under assembly. The goal is simply to expand on DAVID's method by emphasizing data sets from individual MS and RNA-seq studies. Probabilities presented here are generated using Fisher's exact test with a background proteome size of 10,000 and are unadjusted. For consistency, lists of proteins with altered expression in our own HBV work are generated by filtering out all cases where differential expression is not accompanied by a *p* value < 0.05 (*i.e.* fold-change is not a factor); the lists are then subjected to Fisher analysis.

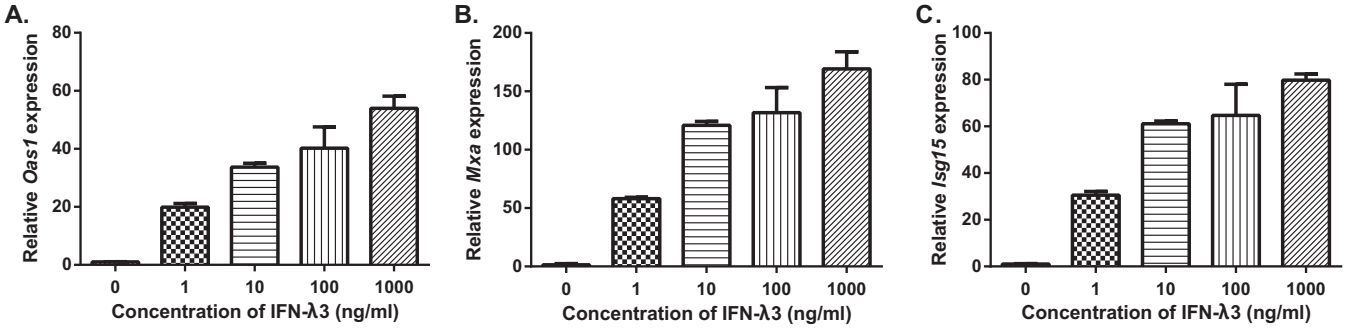

FIG. 1. **Relative quantification of ISG transcripts in HepG2.** 2.15 treated with IFN-λ3 for 24 h. The relative expression of *OAS1* (*A*), *MxA* (*B*) and *ISG15* (C*)* genes in HepG2.2.15 cells 24h post-stimulation with different doses of IFN-λ3 is shown using Mean ± S.E. As with type I IFNs, all 3 ISGs were significantly elevated by IFN-λ3 treatment ($p < 0.001$) at all doses compared with a control (PBS). These experiments were performed in triplicate. AQ: J

Western Blotting for MS Confirmation—Fifteen milligrams of protein from IFN-λ3-treated and untreated HepG2.2.15 was subjected to SDS-PAGE (10%) electrophoresis. Proteins were transferred onto nitrocellulose membranes (Bio-Rad) using the Trans-Blot Turbo Transfer System (Bio-Rad). The membranes were blocked with Odyssey Blocking Buffer (LICOR-Biosciences) for an hour at room temperature, washed three times with TBST and probed with anti-OAS3 (ab64163, abcam), anti-SAMHD1 (#12361, CST), anti-STAT1 (#9175, CST), or anti-GAPDH (#5174, CST) antibodies at 4 °C overnight. After washing three times with TBST, the probed membranes were incubated with IRDye 680RD secondary antibody (LICOR-Biosciences) at 1:10,000 dilution for 1 h in the dark followed by three washes with TBST. The membranes were visualized using Odyssey CLx (LICOR-Biosciences).

Data Deposition—The mass spectrometry proteomics data, including annotated spectra for all modified peptides and proteins identified on the basis of a single peptide, have been deposited to: (1) the ProteomeXchange Consortium via the PRoteomics IDEntifications (PRIDE) partner repository with the data set identifier PXD007896 and (2) the MS-Viewer (http://msviewer.ucsf.edu/prospector/cgi-bin/msform.cgi?form=msviewer) with the following keys: dhjzinh2g0, tjnx2fzkzu, 3xzzxfanwm, ac4wmxx0tv, and ao9nga6qqm.

RESULTS

Validation of Responses to IFN-λ3 Treatment in HBV-transfected Hepatocellular Carcinoma Cell Line Model—HepG2.2.15 is a hepatocellular carcinoma cell line that contains a stable HBV expression plasmid that has been validated as an HBV infection model in previous reports (20, 28). The response to type III IFN treatment in HepG2.2.15 cells has not been reported. To determine whether HepG2.2.15 cells respond to IFN-λ3, we performed qPCR to investigate the expression of the classical ISGs, namely *OAS1*, *MxA* and *ISG15* in HepG2.2.15 cells treated with various amounts of IFN-λ3 for 24h. Fig. 1 shows that IFN-λ3 could significantly increase the expression of these 3 ISGs in a dose-dependent manner. These results indicated that HepG2.2.15 cells responded to IFN-λ3 stimulation. F1

For thoroughness, we investigated the anti-HBV effects of IFN-λ3 by determining the differential changes at 3 points in the viral life-cycle including the levels of *pres1* (typically used as a representative gene for HBV transcripts, given its high conservation across all genotypes), replicative intermediate pre-genomic RNA (pgRNA), and intracellular HBV DNA (both rcDNA and cccDNA). qPCR was performed on HepG2.2.15 RNA following treatment with various amounts of IFN-λ3 for 24 h. As shown in Fig. 2*A* and 2*B*, IFN-λ3 reduced both *pres1* and pgRNA expression compared with control in a dose-dependent manner. Measurement of intracellular HBV DNA showed that copy numbers of virus in IFNλ3-treated HepG2.2.15 cells were diminished in a dose-dependent manner relative to control (Fig. 2*C*). The reduction reached significant levels when the doses of IFN-λ3 were 100 ng/ml (p value = 0.04) and 1,000 ng/ml (p value = 0.0134). Collectively, these results indicated that IFN-λ3 inhibits HBV replication in HepG2.2.15 at the given time point. F2

Before we investigated the cellular response to IFN-λ3, the toxicity of this drug was considered. The MTT cytotoxicity assay was performed to determine HepG2.2.15 viability under distinct concentrations of IFN-λ3. The percentage of viable cells is illustrated in Fig. 3. The increasing doses of IFN-λ3 significantly promoted cell death only at the highest dose in this experiment, where the viable HepG2.2.15 cells reduced to 84%. Thus, we settled on 100 ng/ml of IFN-λ3 for further experiments because this dose showed the ability to significantly inhibit HBV replication with minimal cytotoxicity on HepG2.2.15 cells. F3

Quantitative Proteomics Analysis of IFN-λ3 Responses in HepG2.2.15—Fig. 4 shows the schematic workflow of this study. Briefly, IFN-λ3-treated, IFN-α2a-treated, and untreated HepG2.2.15 cells were lysed and digested with trypsin. The tryptic peptides of these groups were labeled with light, medium, and heavy dimethyl reagents and then fractionated for subsequent LC-MS/MS analysis. In total, 4670 proteins were identified at a false discovery rate (FDR) of less than 1%, with 1471 proteins identified based on a single peptide (all information regarding peptide sequences assigned and protein identifications are supplied in supplemental Table S2 and S3). For the IFN-λ3 treatment condition, 2904 proteins were identified in at least 3 of 5 replicates allowing evaluation of significance, shown in the corresponding volcano plot (Fig. 5). Seven hundred thirty-seven proteins showed significant F4 ZSI F5

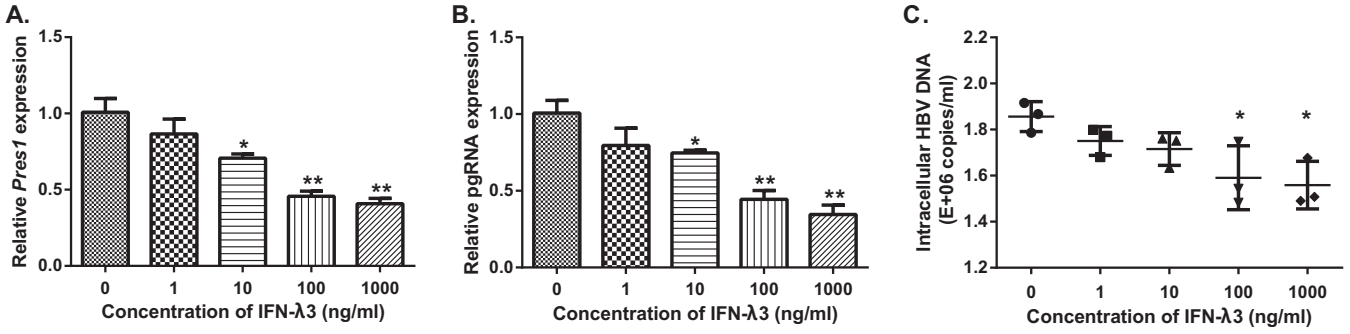

FIG. 2. **Effects of IFN-λ3 on HBV replication.** HepG2.2.15 cells were incubated with IFN-λ3 (1, 10, 100 and 1000 ng/ml) or treated with PBS for 24 h. The relative transcript expression and the amount of HBV DNA are shown as Mean ± S.E. IFN-λ3 significantly inhibited *pres1* and pgRNA expression at doses equal to or greater than 10 ng/ml (*A* and *B*). IFN-λ3 significantly suppressed viral propagation at doses equal to or greater than 100 ng/ml (*C*). These experiments were performed in triplicate. (* represents a *p* value less than 0.05 and ** represents a *p* value less than 0.01).

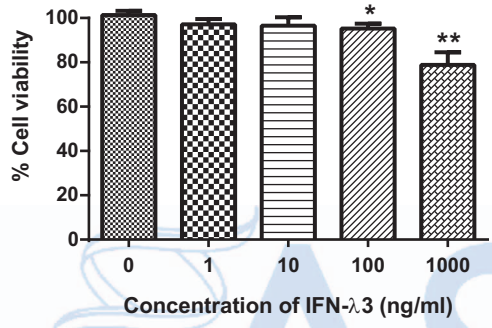

FIG. 3. **IFN-λ3 cytotoxicity assay.** The viability of HepG2.2.15 after IFN-λ3 treatment was determined by MTT assay. The percentage of cell viability is shown as Mean ± S.E. IFN-λ3 showed minimal effect on cell viability when the doses were less than 1,000 ng/ml. These experiments were performed in triplicate.

changes in abundance, with a slight bias toward down-regulated proteins in response to IFN-λ3 stimulation (see Fig. 5). T1 Table I displays a list of significantly regulated proteins with $\log_2$(IFN-λ3/Ctrl) ratios of greater than 1 . We should point out that our primary intention in this work is to explore IFN-λ3 effects on HepG2.2.15 cells; the effects of IFN-α2a would be secondary, for the sake of comparison with IFN-λ3 effects, and will be presented at the last part of the Results section. All ZSI data can be accessed from supplemental Table S4.

All HBV proteins were identified in this study. However, calculation of significance could not be performed because of absence in multiple MS runs, except for putative X-Core fused ZSI protein (which showed no significant change), see supplemental Table S4. Based on spectral counts, all the HBV peptides were apparently expressed at very low levels relative to the entire HepG2.2.15 proteome (below 1 ppm, see in PRIDE partner repository as mentioned in Data Deposition). This finding is in agreement with a previous study that specifically examined intracellular HBV proteins in HepG2.2.15 cells but found them to be undetectable (29). Note that all HBV proteins, except HBV pol and HBx, are secreted (30–32), likely causing intracellular levels of these proteins to be scarce.

To confirm the results from MS analysis, three proteins known to be differentially regulated in response to HBV infection, namely 2′-5′-oligoadenylate synthase 3 (OAS3) (33), Sterile α motif (SAM) and histidine/aspartate (HD)-containing protein 1 (SAMHD1) (34–36), and signal transducer and activator of transcription 1 (STAT1) (37, 38) were selected for validation by Western blot analysis. Consistent with MS results, OAS3, SAMHD1 and STAT1 were up-regulated as a F6 result of IFN-λ3 treatment (Fig. 6).

To further explore the possible roles of transcriptional regulation for significantly altered proteins, we selected several proteins involved in antiviral processes for qPCR analysis. Fig. F7 7 show that up-regulation was seen at both protein and RNA expression levels without exception. However, no clear pattern emerged when downregulated proteins were examined for transcript levels.

Bioinformatics Analysis and Antiviral/Immunomodulatory Process Mapping—The DAVID bioinformatics tool was used to classify and cluster significant functions of all up and down-regulated proteins. Upon IFN-λ3 treatment, we found several biological processes expected to be canonically regulated on general IFN stimulation, such as immune response and viral infection defense. Additionally, however, several biological processes not previously emphasized upon interferon stimulation emerged from this work, including metabolism of RNA, major pathway of rRNA processing in the nucleolus and cytosol, selenoamino acid metabolism, peptide chain elongation, translation, prefoldin mediated transfer of substrate to CCT/TriC, transcription-coupled nucleotide excision repair (TC-NER), unfolded protein response (UPR), interleukin-23 signaling, and hypusine synthesis from eIF5A-lysine.

Following enrichment analysis, we conducted a protein-by-protein search for relevance to the viral processes. We manually searched the viral literature, as well as using DAVID's antiviral defense groups and antigen processing/presentation groups, to construct a map of points at which these proteins may partake in viral processes (Fig. 8) (as described under F8 Experimental Procedures). We also built a map displaying

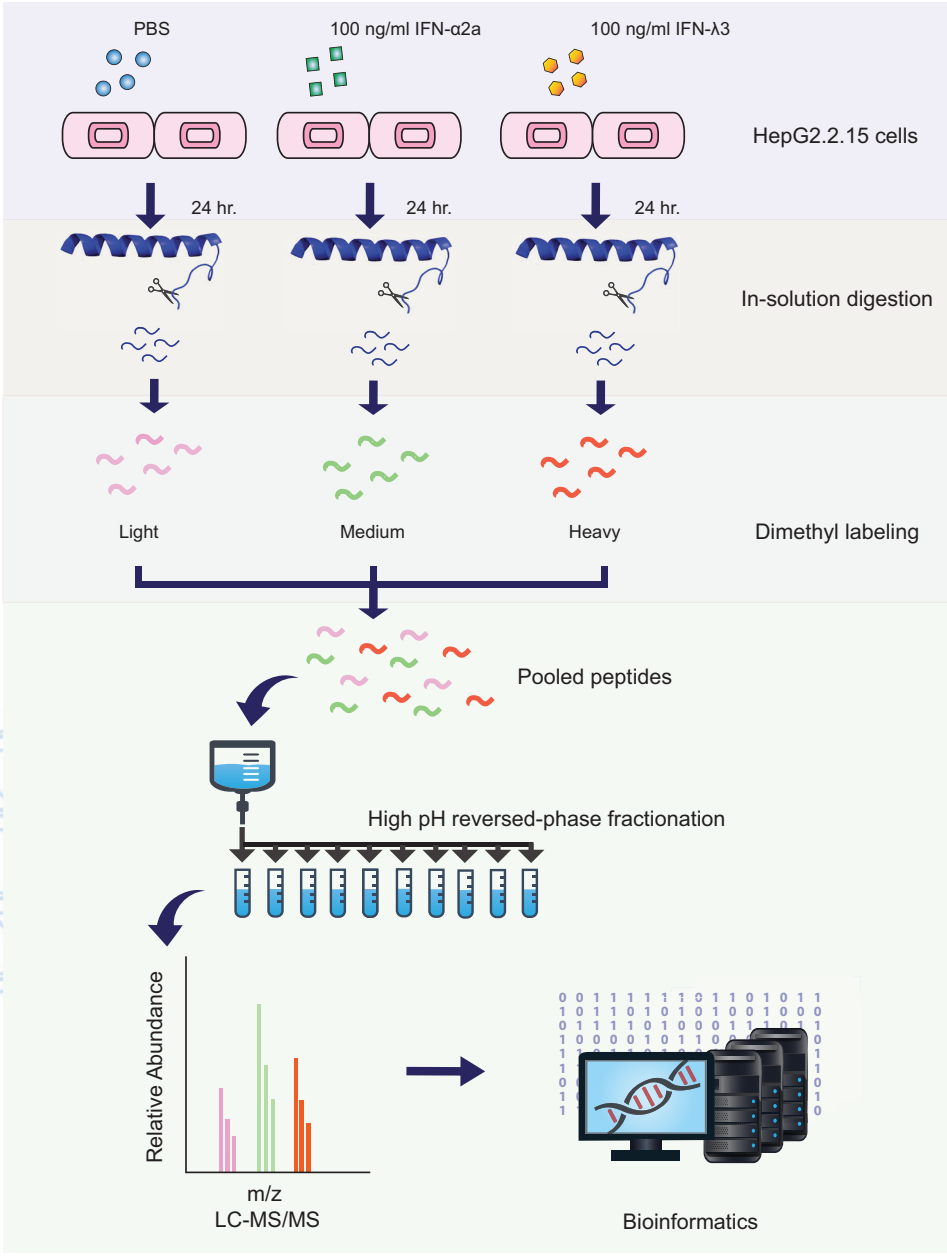

FIG. 4. **Quantitative proteomic workflow.** HepG2.2.15 cells were treated with 100 ng/ml of IFN-λ3 and IFN-α2a and PBS for 24 h. Cell lysates of each group were digested and then labeled with different dimethyl reagents. After combining the 3 samples, these peptides were fractionated and then analyzed by LC-MS/MS.

steps at which IFN-λ3 treatment could promote antigen processing and presentation of viral proteins. Finally, we constructed a map that highlights points at which IFN-λ3 stimulation may heighten expression of proteins in the RIG-I pathway that have been shown to be inhibited via HBV infection. Unless otherwise stated, we found no proteins that contradict the patterns that we report below.

Regarding the HBV life cycle, we identified many proteins which may be involved at numerous points (Fig. 8). At the early steps of viral attachment, entry, and cytosolic release from endosomes (Fig. 8, step 1 and 2), we detected an increased expression of IFITM3, known to alter intracellular cholesterol homeostasis, preventing viral fusion with endosomes in at least 4 out of 7 of the Baltimore viral groups (39). RAB5C and RAB7A, proteins previously implicated in viral trafficking (Fig. 8, step 2), were downregulated upon IFN-λ3 treatment (40), though RAB7A did not reach statistical significance. Two other trafficking proteins not mentioned in the viral literature, AP2B1 and EEA1, were significantly downregulated. Regarding cytosolic-to-nuclear transport of the HBV capsid along microtubules (Fig. 8, step 4), we found that several molecules involved in microtubule assembly and func-

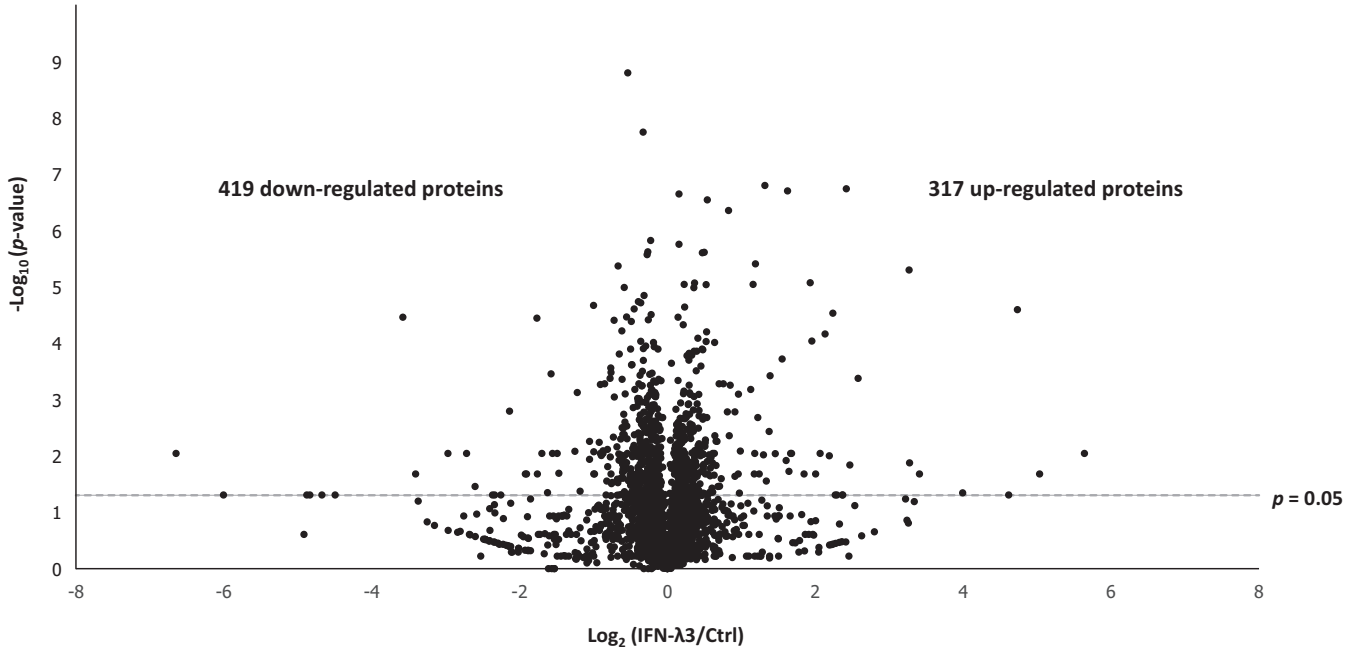

FIG. 5. **Volcano plot.** Volcano plot shows the distribution of identified proteins according to *p* value and fold change, indicating significance with a dashed line (p value < 0.05).

tion evinced decreased expression after IFN-λ3 treatment, consistent with the literature. These proteins were DCTN1, DCTN2, KIF5B, MAP4, and MACF1 (41, 42). For nuclear import (Fig. 8, step 5), all identified proteins known to play roles herein (42, 43) were found to decrease because of IFN-λ3 stimulation (IPO5, IPO7, CALR, CALM, RANBP1, and TPR). Within the nucleus (Fig. 8, step 7), all identified ISG products shown previously to limit or degrade viral mRNA (44–46) were observed to be upregulated: ADAR1, OAS3, ISG20, PML, XRN2, ZC3HAV1, and TRIM25. At the level of RNA export (Fig. 8, step 8), ENY2 and CALR were downregulated. Regarding translation (Fig. 8, step 9), antiviral proteins (EIF2AK2, IFIT1, and IFIT2) involved in protein synthesis increased in treated cells, as shown in previous work with type I IFN treatment (44, 46, 47). In addition, almost all identified translation initiation factors (EIF1AY, EIF2S3, EIF2B1, EIF3B, EIF4G1, EIF4B, EIF4G2, and EIF5A) decreased in this study. Encapsidation follows translation of viral proteins (Fig. 8, step 10). Interestingly, RIG-I was up-regulated and has been shown to interfere with the interaction between pgRNA and HBV polymerase, required for encapsidation (48). Other effects of RIG-I up-regulation are discussed below. Reverse transcription, which occurs within the capsid (Fig. 8, step 11), has been demonstrated to be inhibited by SAMHD1 (HBV and HIV) (35, 49) and NT5C3A (IAV and CSFV) (50, 51); these proteins were up-regulated in our study upon treatment. Proteins that might interfere with viral assembly (Fig. 8, step 12.1) were not identified in this study. Finally, at the egress step (Fig. 8, step 13), two up-regulated proteins thought to play a role in inhibiting HBV export, BST2 and C4A, were detected after IFN-λ3 stimulation.

Regarding antigen processing and presentation, we identified 22 proteins that are involved in this process (Fig. 9). F9 Among proteins in the degradation-related ubiquitination cascade, we found only up-regulation, specifically UBA7 (E1), UBE2L6 (E2), and SYVN1 (E3) after IFN-λ3 stimulation. Two ubiquitination enzymes were downregulated but have not been reported to instigate degradation. All deubiquitinating enzymes (DUBs) identified in this study, *i.e.* USP14, UCHL3, UCHL5, and OTUB1, decreased because of IFN-λ3 treatment. Downstream of these processes, core proteasome components, PSMA7, PSMB7, and PSMG2, were up-regulated with no exceptions. Importantly, both cap components (PSME1 and PSME2) associated with the immunoproteasome were up-regulated, whereas all significantly altered cap components of the constitutive proteasome were downregulated. Evidence of possible post-proteasome processing was seen in the up-regulation of a cytosol aminopeptidase, LAP3. Next, we saw up-regulation of proteins involved in transport of peptides from the cytosol to the ER as well as assembly of peptide-HLA class I complexes; these proteins included TAP2, TAPBP, HLA-A, HLA-B, and HLA-C. Other proteins involved in the above step did not reach statistical significance but tended to increase expression following IFN-λ3 treatment; TAP1, PDIA3 (ERP57), and B2M. CALR, a player in this process, was downregulated, the reasons for which will be discussed later.

One of the important functions of the innate immune response against HBV is the sensing of viral RNA, leading to IFN activation, which includes components such as toll-like receptors, RIG-I, and MDA5. Here, we saw significant up-regulation of RIG-I upon treatment, which could counteract the

TABLE I

A list of significantly upregulated (A) and downregulated (B) proteins with log_2(IFN-λ3/Control) ratios of greater than 1

A.

Accession number	Description	Gene ID	Average Log_2 ratios	Pathway
O14879	Interferon-induced protein with tetratricopeptide repeats 3	IFIT3	4.74	Antiviral defense (Inhibit viral protein synthesis)
Q96AZ6	Interferon-stimulated gene 20 kDa protein	ISG20	3.28	Antiviral defense (Degrade viral RNA)
P05161	Ubiquitin-like protein ISG15	ISG15	3.27	Antiviral defense
Q15646	2′-5′-oligoadenylate synthase-like protein	OASL	2.58	RLR signaling pathway
O95786	Probable ATP-dependent RNA helicase DDX58	DDX58	2.47	RLR signaling pathway
Q9Y6K5	2′-5′-oligoadenylate synthase 3	OAS3	2.42	Antiviral defense (Degrade viral RNA)
Q29960	HLA class I histocompatibility antigen, Cw-16 alpha chain	HLA-C	2.24	Antigen processing and presentation
P09914	Interferon-induced protein with tetratricopeptide repeats 1	IFIT1	2.19	Antiviral defense (Inhibit viral protein synthesis)
P42224	Signal transducer and activator of transcription 1-alpha/beta	STAT1	2.13	Type I and III IFN signaling
Q63HN8	Isoform 2 of E3 ubiquitin-protein ligase RNF213	RNF213	1.95	Ubiquitin proteasome pathway
Q01628	Interferon-induced transmembrane protein 3	IFITM3	1.93	Antiviral defense (Inhibit viral entry)
P52630	Signal transducer and activator of transcription 2	STAT2	1.65	Type I and III IFN signaling
P29590	Protein PML	PML	1.63	Antiviral defense (Inhibit viral transcription)
P28838	Cytosol aminopeptidase	LAP3	1.61	Antigen processing and presentation
Q10589	Bone marrow stromal antigen 2	BST2	1.55	Antiviral defense (Inhibit viral egress)
Q6IA86	Isoform 6 of Elongator complex protein 2	ELP2	1.46	Regulation of transcription
Q08380	Galectin-3-binding protein	LGALS3BP	1.39	Cell adhesion
Q9H0P0	Cytosolic 5′-nucleotidase 3A	NT5C3A	1.38	Antiviral defense (Inhibit reverse transcription)
P35527	Keratin, type I cytoskeletal 9	KRT9	1.34	Intermediate filament organization
P41226	Ubiquitin-like modifier-activating enzyme 7	UBA7	1.32	Ubiquitin proteasome pathway
Q9Y3Z3	Deoxynucleoside triphosphate triphosphohydrolase SAMHD1	SAMHD1	1.19	Antiviral defense (Inhibit reverse transcription)
Q9BQE5	Apolipoprotein L2	APOL2	1.22	Movement of lipids in the cytoplasm
P01892	HLA class I histocompatibility antigen, A-2 alpha chain	HLA-A	1.16	Antigen processing and presentation
Q9Y6A9	Signal peptidase complex subunit 1	SPCS1	1.13	Proteolysis

B.

Q9BX93	Group XIIB secretory phospholipase A2-like protein	PLA2G12B	-1.05	Lipid catabolic process
Q15427	Splicing factor 3b subunit 4	SF3B4	−1.05	mRNA processing
Q9NPA8	Transcription and mRNA export factor ENY2	ENY2	−1.18	Regulation of transcription
P62158	Calmodulin	CALM3	−1.22	Regulation of synaptic vesicle exocytosis
O75410	Isoform 2 of Transforming acidic coiled-coil-containing protein 1	TACC1	−1.25	Cell proliferation
O75438	Isoform 2 of NADH dehydrogenase [ubiquinone] 1 beta subcomplex subunit 1	NDUFB1	−1.47	Mitochondrial electron transport, NADH to ubiquinone
Q12929	Epidermal growth factor receptor kinase substrate 8	EPS8	−1.57	Actin polymerization-dependent cell motility
Q9NZD2	Glycolipid transfer protein	GLTP	-1.62	Intermembrane lipid transfer
Q13126	Isoform 2 of S-methyl-5′-thioadenosine phosphorylase	MTAP	−1.76	Nucleobase-containing compound metabolic process
Q58FF7	Putative heat shock protein HSP 90-beta-3	HSP90AB3P	−3.58	Protein folding and response to stress

known suppression of RIG-I by HBV. Enhancers of RIG-I activity, such as OASL, TRIM25, and IFIT3 (RIG-G) were also significantly up-regulated. Increased levels of type I and III IFNs, which are activated by RIG-I, would be expected, but were not observed via MS. However, qPCR work confirmed significant up-regulation of these IFNs at the transcript level (Fig. 10). It is likely that the increase in IFN I and III gene expression because of RIG-I up-regulation could lead to more production of IFNs at the protein level and in turn activate IFN receptors as positive feedback. All three canonical ISGF3 components (STAT1, STAT2, and IRF9) downstream from IFN receptor activation were up-regulated, probably as a result of both initial IFN-λ3 treatment and further generation of type I and III IFNs (Fig. 11).

We found several likely antiviral proteins that do not conveniently fit into the above viral processes. Firstly, three 14-3-3 proteins (YWHAZ, YWHAH, and SFN) were found to be downregulated following IFN-λ3 treatment. Another downregulated protein of interest was cyclophilin D (PPIF). Finally, CHID1 was the single most up-regulated protein in our study on IFN-λ3 treatment. Though not prominent in the viral literature, CHID1 is known to bind LPS (52) and is seen to be downregulated in several viral studies (53–56).

After removal of all antiviral proteins, enrichment analysis of the remainder produced an interesting result. RNA-binding proteins, particularly spliceosome components, were both up and downregulated on IFN-λ3 treatment *versus* control. For

COLOR

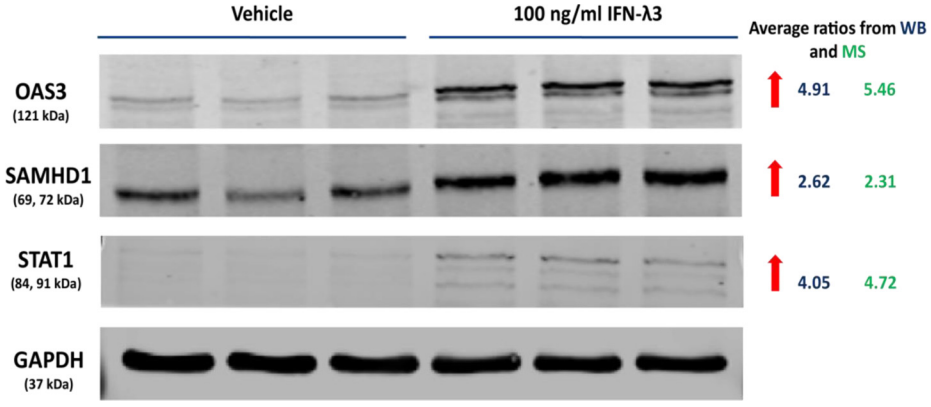

FIG. 6. **Validation of altered proteins by immunoblotting assay.** SDS-PAGE was performed on treated and untreated lysates, followed by membrane transfer and incubation with anti-OAS3, anti-SAMHD1, anti-STAT1, and anti-GAPDH overnight. The proteins of interest were visualized using the LI-COR Odyssey system. Consistent with proteomic results, the expression of OAS3, SAMHD1 and STAT1 increased after IFN-λ3 treatment. These experiments were performed in triplicate.

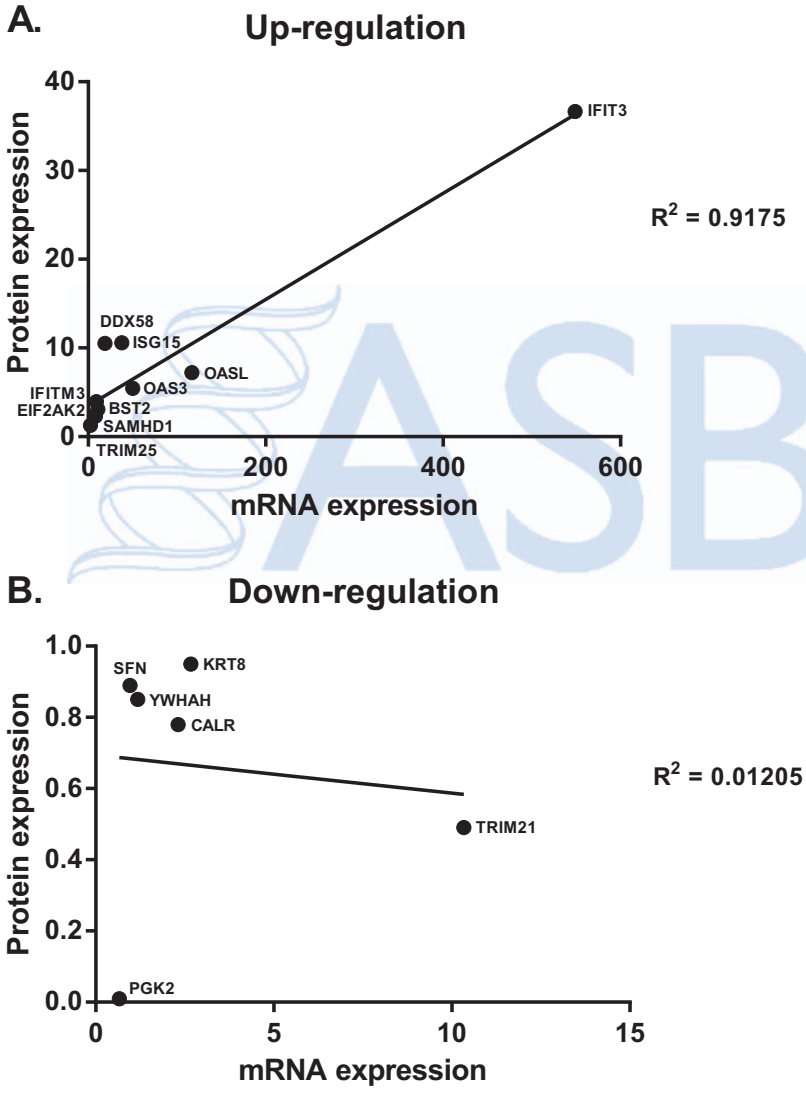

FIG. 7. **Correlation of mRNA and protein levels of up- and down-regulated proteins.** Various up and downregulated proteins were selected to investigate their transcript expressions by qPCR. Clear correlations between protein and mRNA expression were seen in up-regulated proteins (*A*) but not in downregulated proteins (*B*).

example, the splicing factor U2AF1 was significantly up-regulated on treatment ($p = 0.00165$). Searching through individual data sets from an in-house database containing a variety of studies and applying Fisher's exact test (see Experimental Procedures) showed a strong tendency toward both up-regulation and down-regulation of proteins that associate with the non-coding RNA NORAD (log $p = -5$ and -13, respectively) (57). The same pattern applies to proteins shown to bind to the splicing factor U2AF2 (log $p = -6$ and -9, respectively) (58).

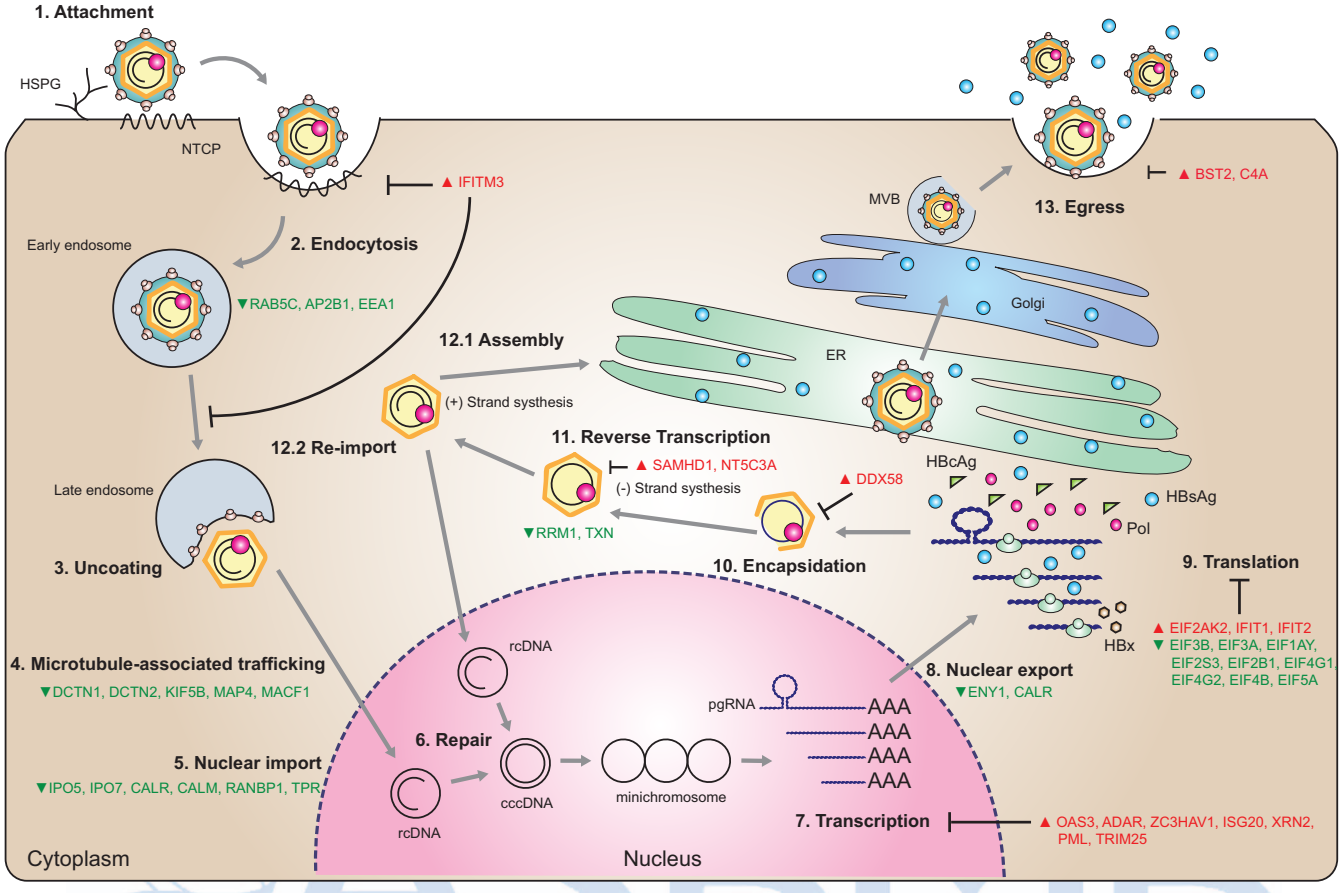

FIG. 8. **Illustration of HBV life-cycle mapped to antiviral proteins that were identified in this study.** Antiviral proteins and host cellular factors of interest identified in this study were mapped into the HBV-life cycle. These proteins were identified at most steps of HBV replication. Proteins in red and green text represent up and downregulated proteins, respectively.

COLOR

Though our primary intent is to elaborate on IFN-λ3's potential, comparative studies against the best characterized interferon, IFN-α, are essential. Given the known parallelism in broad modes of action between the two IFNs, significant overlaps should be seen in sets of up/downregulated proteins upon treatment, offering a simple validation of IFN-λ3's activity. At the same time, and most intriguingly, the comparison would allow us to suggest possible differences in effect. To take advantage of the depth of our data, we constructed a tree depicting all 27 possible differential expression outcomes resulting from 3 pairs of treatment comparisons (*i.e.* IFN-λ3 *versus* Ctrl, IFN-α2a *versus* Ctrl, IFN-λ3 *versus* IFN-α2a, see Fig. 12). A simple comparison between IFN-λ3 *versus* IFN-α2a could lead to errors in interpretation. For example, the observation that IFN-λ3 treatment results in up-regulation or down-regulation of a protein *versus* IFN-α2a renders an uninteresting result if IFN-λ3 does not have any significant effect *versus* Ctrl. This scenario can be seen in outcomes #12 and #16 in Fig. 12. Another problem in interpretation arises when both IFNs have the same directional effect on cells but one effect is significantly more potent than the other; this would not be noticed upon mere IFN-λ3 *versus* IFN-α2 comparison. This scenario can be seen in outcomes #3 and #25 in Fig. 12. The tree shows the number of MS-derived proteins at their appropriate outcome branch points and shows proteins associated with various biological processes (as described under "Experimental procedures") for each outcome. As one simple example of the power of this approach, note that IFITM3 was significantly up-regulated upon treatment with both IFNs, however this effect was significantly stronger upon IFN-λ3 treatment (outcome #1). Another example was in outcome #4 where IFN-λ3 treatment caused up-regulation of proteins involved in antigen processing and presentation (SYVN1, LAP3, PSMA7, and PSMB7), whereas IFN-α2a did not produce any significant effects. Interestingly, the mirror image of this branch, outcome #24 where IFN-λ3 caused down-regulation whereas IFN-α2a did not, was also populated with a subset of proteins involved in antigen processing and presentation, specifically those associated with the constitutive proteasome cap (PSMC4, PSMD4, PSMD7, PSMD13, and PSMD14). A priori, one would expect the most interesting outcomes to be found in cases in which IFN-α2a and IFN-λ3 have clearly opposite effects (outcomes #7 and #21). We did not identify proteins clearly related to antiviral processes in these two

F12

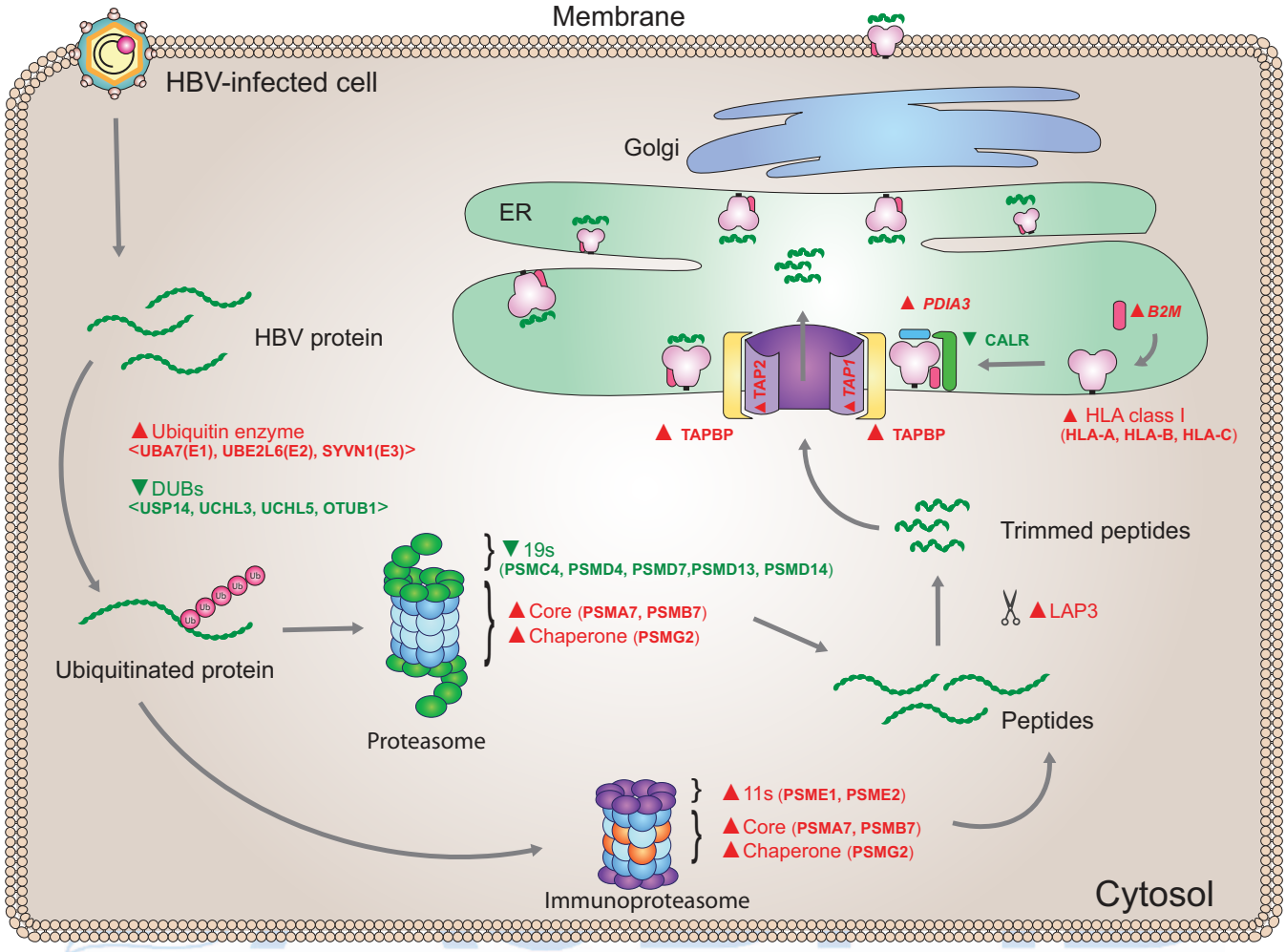

FIG. 9. **IFN-λ3 enhanced antigen processing/presentation.** IFN-λ3 not only up-regulated HLA class I expression but it also increased the expression of other effector molecules involved in antigen processing and antigen presentation. Ubiquitinating enzymes that promote protein degradation were found to be up-regulated whereas deubiquitinating enzymes known to remove ubiquitin were found to decrease after IFN-λ3 treatment. Although all identified subunits of the constitutive proteasome cap were downregulated, the 2 subunits of the immunoproteasome cap as well as some subunits of the proteasome core were elevated in expression. Several effector molecules involved in peptide loading on class I HLA as shown in red text were upregulated with the exception of CALR, which was downregulated as shown in green text. The italic red text represents proteins with increased expression levels that failed to reach statistical significance.

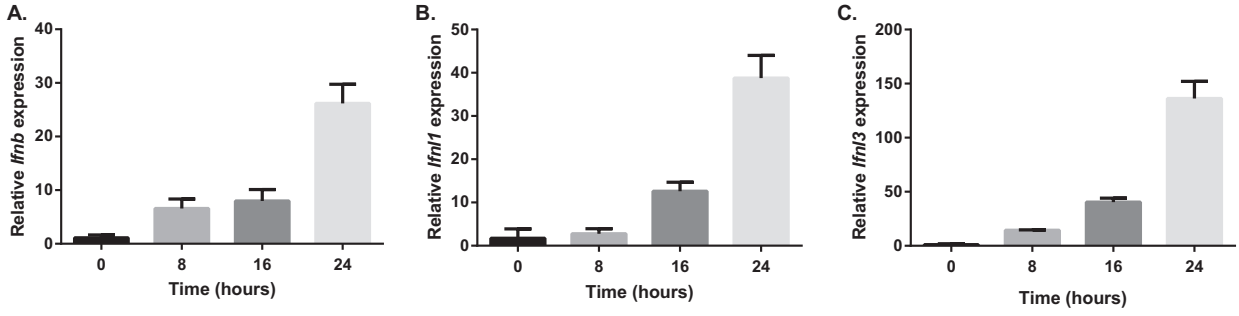

FIG. 10. **qPCR analysis of *Ifn* genes.** Total RNA of HepG2.2.15 cells treated with IFN-λ3 for 8, 16, and 24 h or left untreated was extracted and then converted to cDNA. The expression levels of *Ifnb*, *Ifnl1*, and *Ifnl3* (*A*, *B*, and *C*) were found to be up-regulated in a time-dependent manner after IFN-λ3 treatment.

outcome groups. This reason pointed to broader unbiased analysis. Hence, we performed "Reactome" enrichment analysis against all outcome groups for complete enrichment analysis beyond the aforementioned antiviral processes. The resulting Reactome enrichment groups were subjected to 2-D cluster analysis (Fig. 13 and underlying data in supplemental

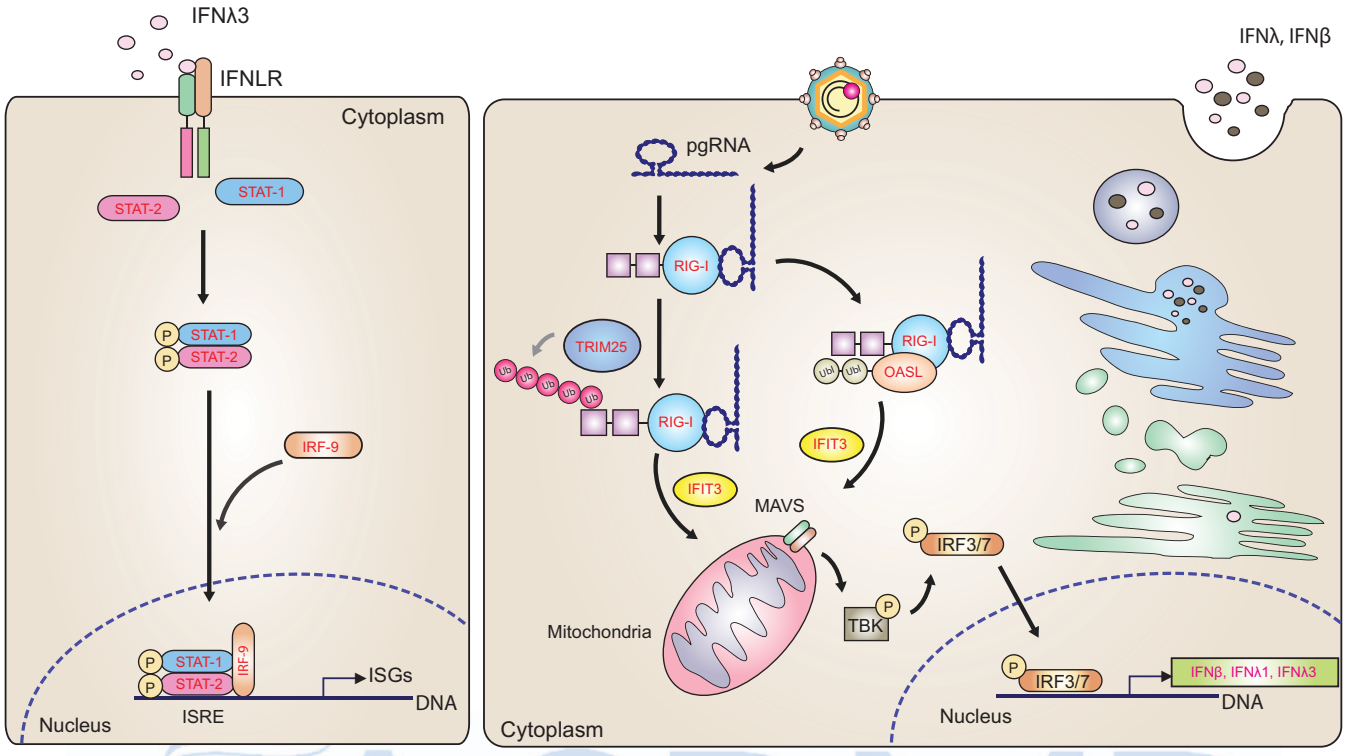

FIG. 11. **IFN-λ3 rescued the RIG-I signaling pathway.** IFN-λ3 up-regulated the expression of *Ddx58* and *Ifit3*, which have been reported to be suppressed by HBV. IFN-λ3 also elevated the expression of OASL and TRIM25. These proteins promote type I and type III IFN production. These IFNs, in turn, activate the JAK-STAT pathway and induce the expression of ISGs. It is likely, then, that IFN-λ3 provides positive feedback to amplify ISG expression to control HBV replication. Proteins in red text represent up-regulated proteins, whereas the pink text represents the upregulated transcripts.

Table S4). This analysis offers new insights. Firstly, we note the aforementioned cases in which IFN-λ3 and IFN-α2a showed opposing effects. In outcome #7, where IFN-λ3 exclusively caused up-regulation, the "peptide chain elongation," "metabolism of RNA," "major pathway of rRNA processing in the nucleolus and cytosol," "selenoamino acid metabolism," and "translation" terms are highlighted, whereas in outcome #21, where IFN-λ3 exclusively caused down-regulation, the "Interleukin-23 signaling" term is emphasized. Next, we observe that in most cases where proteins were up-regulated upon IFN-α2a treatment (outcomes#1, #2, #3, #11, and #21), "interferon signaling" and/or "class I MHC mediated antigen processing & presentation" terms were apparent, reinforcing expectations regarding IFN-α's potency on these pathways. Interestingly, specific terms related to "translation" and "metabolism of RNA" were significantly associated with 13 out of 17 different outcome groups. To our best knowledge, these biological processes have been not mentioned as consequences of general IFN activation. Finally, enrichment terms that are largely unexplored with regard to IFN treatment include "transcription-coupled nucleotide excision repair (TC-NER)" (1 significant occurrence), "interleukin-23 signaling" (1), "unfolded protein response (UPR) (2)," "prefoldin mediated transfer of substrate to CCT/TriC (4)," and "hypusine synthesis from eIF5A-lysine (1)." Interestingly, the final enrichment term was only associated with a single case, that of proteins downregulated in all treatment pairs (outcome #27). These results could help point toward differential effects of IFN-λ3 *versus* IFN-α2a.

DISCUSSION

Type III IFN has been shown to exert antiviral effects on several viruses including EMCV, IAV, HSV, VSV, HIV, HCV, and HBV (17, 46, 59–64). In clinical trials, peg IFN-λ treatment showed reduced HBV DNA, HBsAg and HBeAg in CHB patients at levels greater than or comparable to those treated with peg IFN-α during on-treatment and at end-of-treatment (9). Although the virological, serological, and biochemical responses of peg IFN-λ at week 24 after treatment were not superior to peg-IFN-α, adverse events associated with drug treatment were mostly seen in patients treated with peg-IFN-α. Numerous HCV studies also illustrate this tendency toward diminished side-effects (13, 14). Another clinical trial demonstrated that patients treated with peg IFN-λ had improved anti-HBV immunity through an increase in poly-functional NK cells and maintenance of both HBV-specific $CD4^+$ and $CD8^+$ T cells, important arms of immunity for viral elimination (8). The mechanisms involved in these immunomodulatory effects remain to be elucidated. At the level of cell culture, only two studies (59, 65) have focused on the effects

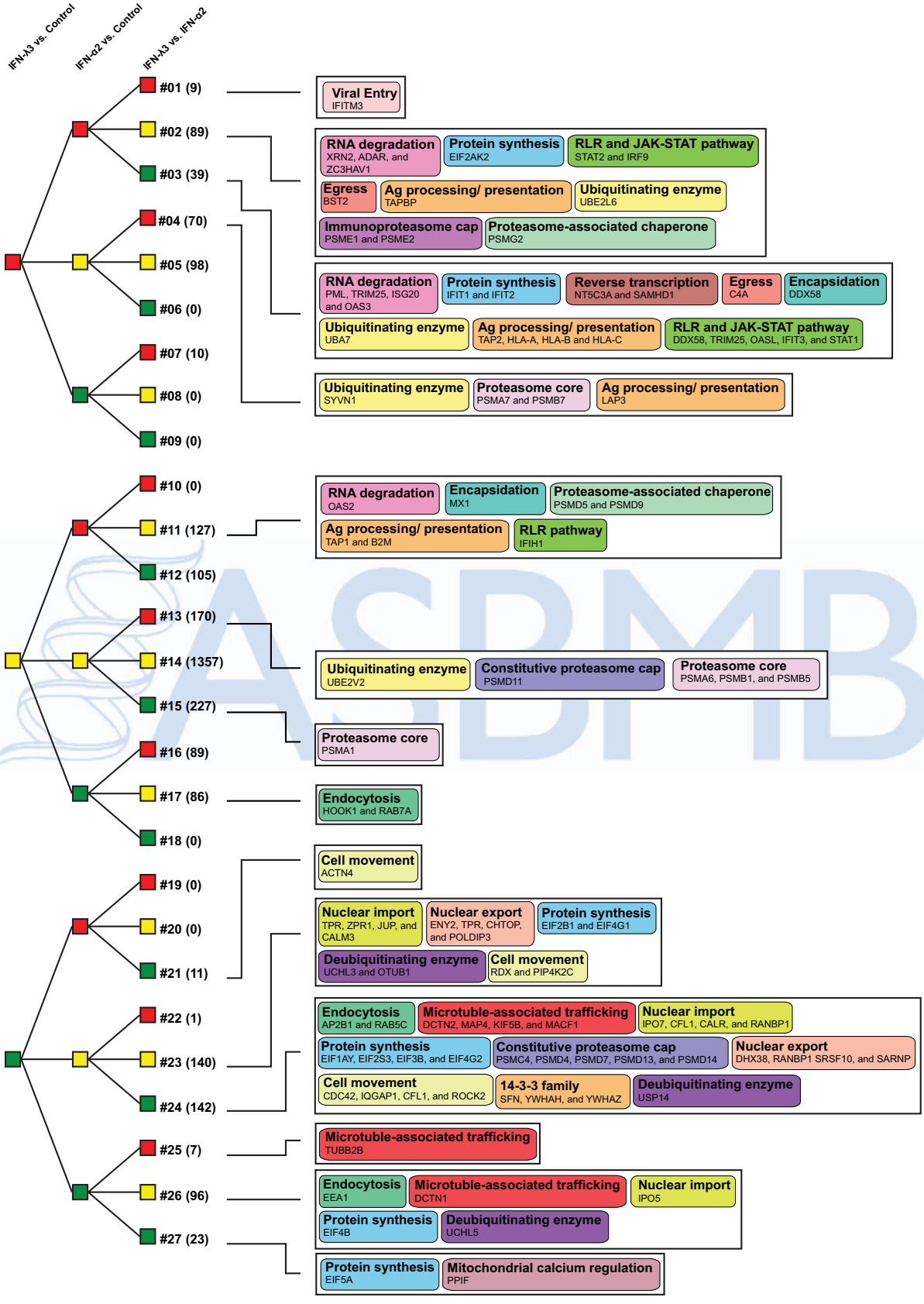
IFN-λ3 vs. Control
IFN-α2 vs. Control
IFN-λ3 vs. IFN-α2
#01 (9)
#02 (89)
#03 (39)
#04 (70)
#05 (98)
#06 (0)
#07 (10)
#08 (0)
#09 (0)
#10 (0)
#11 (127)
#12 (105)
#13 (170)
#14 (1357)
#15 (227)
#16 (89)
#17 (86)
#18 (0)
#19 (0)
#20 (0)
#21 (11)
#22 (1)
#23 (140)
#24 (142)
#25 (7)
#26 (96)
#27 (23)
Viral Entry
IFITM3
RNA degradation
XRN2, ADAR, and ZC3HAV1
Protein synthesis
EIF2AK2
RLR and JAK-STAT pathway
STAT2 and IRF9
Egress
BST2
Ag processing/ presentation
TAPBP
Ubiquitinating enzyme
UBE2L6
Immunoproteasome cap
PSME1 and PSME2
Proteasome-associated chaperone
PSMG2
RNA degradation
PML, TRIM25, ISG20 and OAS3
Protein synthesis
IFIT1 and IFIT2
Reverse transcription
NT5C3A and SAMHD1
Egress
C4A
Encapsidation
DDX58
Ubiquitinating enzyme
UBA7
Ag processing/ presentation
TAP2, HLA-A, HLA-B and HLA-C
RLR and JAK-STAT pathway
DDX58, TRIM25, OASL, IFIT3, and STAT1
Ubiquitinating enzyme
SYVN1
Proteasome core
PSMA7 and PSMB7
Ag processing/ presentation
LAP3
RNA degradation
OAS2
Encapsidation
MX1
Proteasome-associated chaperone
PSMD5 and PSMD9
Ag processing/ presentation
TAP1 and B2M
RLR pathway
IFIH1
Ubiquitinating enzyme
UBE2V2
Constitutive proteasome cap
PSMD11
Proteasome core
PSMA6, PSMB1, and PSMB5
Proteasome core
PSMA1
Endocytosis
HOOK1 and RAB7A
Cell movement
ACTN4
Nuclear import
TPR, ZPR1, JUP, and CALM3
Nuclear export
ENY2, TPR, CHTOP, and POLDIP3
Protein synthesis
EIF2B1 and EIF4G1
Deubiquitinating enzyme
UCHL3 and OTUB1
Cell movement
RDX and PIP4K2C
Endocytosis
AP2B1 and RAB5C
Microtuble-associated trafficking
DCTN2, MAP4, KIF5B, and MACF1
Nuclear import
IPO7, CFL1, CALR, and RANBP1
Protein synthesis
EIF1AY, EIF2S3, EIF3B, and EIF4G2
Constitutive proteasome cap
PSMC4, PSMD4, PSMD7, PSMD13, and PSMD14
Nuclear export
DHX38, RANBP1 SRSF10, and SARNP
Cell movement
CDC42, IQGAP1, CFL1, and ROCK2
14-3-3 family
SFN, YWHAH, and YWHAZ
Deubiquitinating enzyme
USP14
Microtuble-associated trafficking
TUBB2B
Endocytosis
EEA1
Microtuble-associated trafficking
DCTN1
Nuclear import
IPO5
Protein synthesis
EIF4B
Deubiquitinating enzyme
UCHL5
Protein synthesis
EIF5A
Mitochondrial calcium regulation
PPIF

COLOR

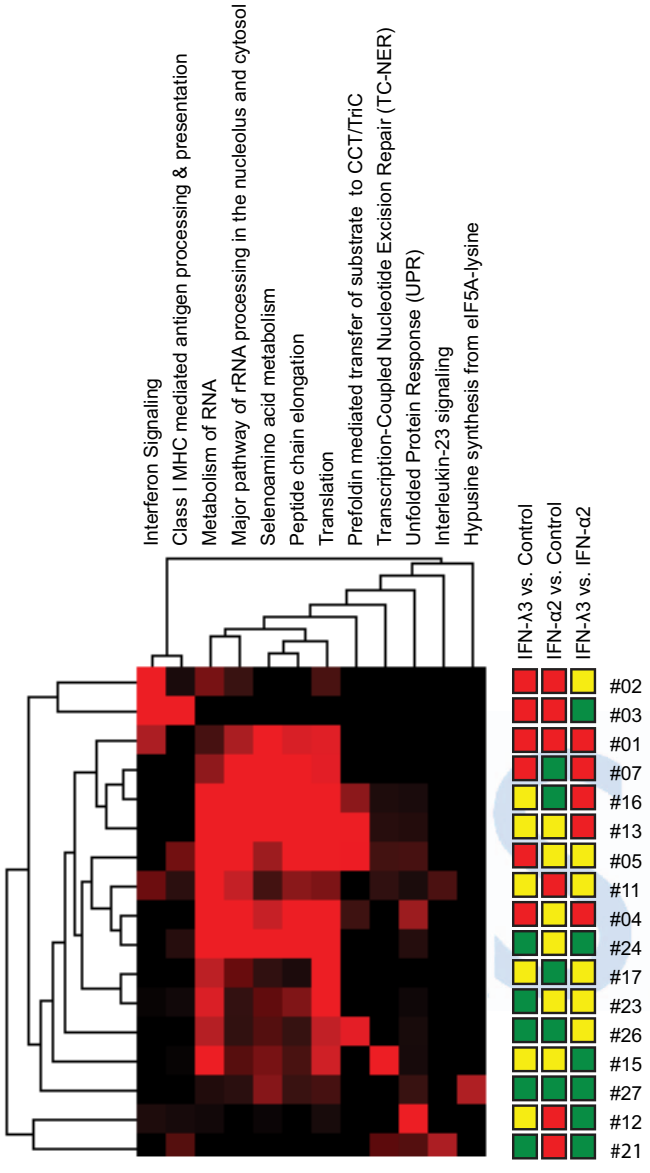

FIG. 13. **Enrichment heatmap.** Reactome enrichment analysis was performed on the tree outcomes that contained at least 9 members, excluding outcome #14 in which no significant alterations were seen on any treatment. Probabilities (Reactome's hypergeometric test, -log(*p* value)) were generated for every intersection of these tree outcomes with the specified Reactome groups. This matrix of probabilities was then submitted for two-dimensional cluster analysis using Cluster 3.0 and Java Treeview. The result is displayed as a heatmap. Red color intensity indicates the level of significance.

of IFN-λ treatment of HBV-transfected cells, one of which offers a comparison against a type I IFN, IFN-β. Here, a comparison against IFN-β showed that IFN-β exhibited greater potency in viral elimination at the 6 h time point, but potency was equivalent at 24 h.

Surprisingly, the effects of IFN-λ treatment have not been studied with high-resolution mass spectrometry to date, possibly because it is assumed that type I and type III IFNs share the same signaling pathways. In fact, modern, deep proteomic studies of the effects of IFN treatment in general are lacking, perhaps because of an underlying assumption that RNA-seq results should parallel those generated via MS. Here, we used a modern high-resolution LC-MS/MS system with upstream high-pH reversed phase fractionation to yield a total of 127,989 peptides (25,181 unique peptides) representing 4670 proteins. The peptides were labeled with dimethyl isotopes, allowing accurate quantification under different treatments. This study provides the most comprehensive examination of changes in protein abundance under IFN treatments to date.

To provide objective measures for study-study comparisons, in the discussion below we perform numerous comparisons between our studies and others with Fisher's exact test (see "Experimental procedures"). As expected, canonical IFN-stimulated biological processes were prominent in IFN-λ3 treatment. Proteins significantly up-regulated upon IFN-λ3 treatment *versus* Ctrl (hereafter λ3/c) overlapped with the GO "antiviral defense" term at p value $= 10^{-14}$ (with the α/c condition giving p value $= 10^{-12}$). Similarly, the λ3/c list significantly overlapped (p value $= 10^{-13}$) transcripts whose up/down-regulation patterns (*i.e.* "co-expression") mirror those of RIG-I transcripts reported in the ARCHS4 resource (66); the α/c list gave p value $= 10^{-18}$, perhaps illustrating the expected difference in potency. Comparing proteins significantly up-regulated in λ3/c against those up-regulated in α/c, we derive $p = 10^{-138}$, a clear demonstration of similarities in effect *versus* control. Stepping outside the bounds of our own work, Bolen's transcriptomic comparison of the effects of 5 interferons, including IFN-λ3, on Huh7 cells can be examined against our proteomic results (16). Here, a list of highly up-regulated transcripts derived from Bolen's 6, 12, and 24 h λ3/c time-points significantly intersected with our own λ3/c results (p value $= 10^{-25}$). Of interest, the degree of overlap (p value $= 10^{-5}$) was less significant when performing the same exercise with downregulated transcripts *versus* proteins, paralleling the tendency of lower correlation seen in our own qPCR results for several down-regulated proteins (Fig. 7).

FIG. 12. **Outcome tree.** To compare the effects of IFN-λ3, IFN-α2a, and PBS control, we generated a tree representing the 27 possible outcomes. The boxes in red and green represent proteins that are significantly up- and downregulated, respectively. Groups of proteins with insignificantly changed expression are represented by yellow boxes. As an example, the topmost outcome represents proteins in which IFN-λ3 treatment causes significant up-regulation *versus* control, IFN-α2a treatment causes significant up-regulation *versus* control, and IFN-λ3 treatment causes significant up-regulation *versus* IFN-α2a. The number in parentheses refers to the number of identified proteins in the group. The proteins in each group that might be involved in suppressing HBV replication are shown in colored boxes specifying various processes, particularly antiviral.

Other comparisons illustrating the expected canonical effects would be an α/c result in Huh7 (67) (a λ3/c experiment was not performed) where up-regulated transcripts align with our own λ3/c results (p value = 10^{-30}), and a list of genes likely to be activated by STAT2 based on curated STAT2 chip-seq results that significantly overlaps with our λ3/c results (p value = 10^{-25}) (68).

In addition to acting on viral replication directly, we propose that the proteolytic pathway may be induced by IFN-λ3 to inhibit HBV replication. Robek *et al.* demonstrated that small molecule-based inhibition of proteasome activity could restrain the anti-HBV activity of type I IFN *in vitro*, suggesting that antiviral effects of IFN might relate to the proteasome (69). Yao *et al.* demonstrated that suppression of HBV replication was accompanied by an increase of 5 proteasome subunits in HepG2.2.15 cells in response to interleukin-4 (IL-4) treatment (70). In our study, we also note up-regulation of immunoproteasome members (cap components PSME1 and PSME2) on IFN-λ3 and IFN-α2a treatment. The immunoproteasome is distinct from the constitutive proteasome in the composition of its catalytic subunits, its cap, and its peptide processing capacity (71). Interestingly, all significantly altered cap components of the constitutive proteasome were down-regulated only upon IFN-λ3 treatment, suggesting coordinated modulation toward the antigen processing form of the proteasome on IFN-λ3 treatment. To our knowledge, this is the first report suggesting a shift from proteasome constitutive degradation mode to antigen processing/presentation mode in response to type III IFN treatment. HBV has been termed a "stealth" virus because innate immune responses in chimpanzees are not observed shortly after infection (72). The synthesis of type I IFNs is induced by the activation of RIG-I-like receptor (RLR) signaling pathways in response to viral infection. Previous studies have shown that HBV polymerase and HBx proteins interfere with the interaction of RIG-I and downstream signaling molecules, resulting in diminished type I IFN production (73–75).

HBV has also been shown to alter RIG-I expression by inducing up-regulation of miR146a, which may directly down-regulate RIG-I and RIG-G transcripts (76). IFN treatment has not previously been shown to upregulate RIG-I pathway components in HBV infected cells. We found, for the first time, that treating HepG2.2.15 with IFN-λ3 increased the expression of RIG-I. In addition, upon IFN-λ3 treatment, we observed elevated expression of RIG-G, known to enhance the activity of RIG-I, as well as TRIM25 and OASL, which promote the interaction between RIG-I and IPS1 on mitochondria or peroxisomes, leading to increased IFN production (77, 78). We propose that IFN-λ3 restores RIG-I and associated downstream signaling to produce type I IFN in HBV infected cells and likely other viruses. Although we did not find any IFNs in our proteomic work, possibly because of low abundances, qPCR verified increases in type I IFN (IFN-β) and type III IFN (IFN-λ1 and IFN-λ3) upon IFN-λ3 stimulation.

Several biological processes not mentioned above emerged from this work, including the involvement of 14-3-3 proteins, cyclophilin D, calreticulin, and cell motility proteins. These subjects are explored in detail below. In our study, the 14-3-3 proteins YWHAZ, YWHAH, and SFN were found to be down-regulated following IFN-λ3 treatment. Several studies have shown that 14-3-3 proteins may facilitate the replication of viruses (79, 80). The 14-3-3 proteins are highly conserved regulatory molecules having multiple functions, including involvement in signal transduction via kinases and phosphatases, the cell cycle, and apoptosis. These proteins have been shown to play important roles in viral infection. For example, complex formation of cdc25 with the HIV accessory protein Vpr, an event that alters the host cell life cycle, is facilitated by 14-3-3 proteins (79). Also, HCV core protein interacts with 14-3-3 proteins resulting in enhancement of Raf-1 kinase activity together with control of hepatocyte growth (80). Interestingly, sequence analysis revealed a 14-3-3 binding domain in HBx protein (81), suggesting that 14-3-3 proteins could directly interact with HBV. Notably, we could not observe significant alterations in 14-3-3 proteins upon IFN-α2a treatment; the differential effects of IFN-λ *versus* IFN-α on 14-3-3 levels would be worthy of further investigation.

The down-regulation of cyclophilin D upon IFN-λ3 treatment observed in our work suggests that this molecule may play a role in inhibition of HBV replication. One of the pathways affected by HBx is calcium signaling, as Ca^{2+} is necessary for viral replication and core assembly (82, 83). In addition to interference with RIG-I signaling, the HBx protein can interact with and modulate the mitochondrial permeability transition pore (MPTP) leading to the release of mitochondrial calcium into the cytoplasm (82). The opening of the MPTP anion channel is regulated by cyclophilin D (84), thus down-regulation of cyclophilin D would serve to counteract Ca^{2+}-assisted viral replication and core assembly. Increasing levels of cytosolic calcium causes the stimulation of PYK2 kinase, in turn activating Src kinase signal transduction to promote HBV reverse transcription, replication, and core assembly (83, 85). In several studies, cyclosporine A (CsA) was used as an MPTP specific blocker, thus reducing core assembly and inhibiting HBV replication (30, 84, 85). Consistent with CsA treatment, the calcium ion chelating agent BAPTA-AM also suppressed HBV propagation (85).

Calreticulin (CALR), downregulated upon IFN-λ3 treatment in our study, is an ER calcium-binding chaperone involved in the regulation of calcium homoeostasis, the folding of newly synthesized proteins, nuclear import, and peptide loading on MHC class I (86–88). In HBV-transfected cells, Yue *et al.* demonstrated that the inhibition of IRF-7 translocation into the nucleus was induced by CALR, resulting in suppression of type I IFN production (89). Moreover, this group showed that CALR inhibited JAK-STAT pathway induction by IFN-α by inhibiting STAT1 phosphorylation, diminishing expression of PKR and OAS. Thus, the observation of down-regulation of

CALR would be expected to have an antiviral effect. However, the down-regulation of CALR would also seem to interfere with antigen processing/presentation. We note that most antigen processing/presentation molecules were up-regulated upon treatment in our work, possibly compensating for this effect. Overall, the observed IFN-λ3-induced down-regulation of CALR in our study may have an inhibitory effect on HBV replication.

Enrichment analysis (DAVID) showed that the most significantly downregulated proteins following IFN-λ3 treatment were involved in cell motility and cell adhesion. We believe these processes could be relevant to the effects of IFN-λ3 treatment on liver cancer. Tan *et al.* demonstrated that HBV-transfected cells showed morphological changes because of formation of filopodia and lamellipodia, leading to cell migration. Of interest, CHB patients have 5–15-fold increased risk of HCC, a characteristic of which is increased cell motility (90, 91). CDC42, downregulated on IFN-λ3 treatment, has been reported to control cell proliferation, adhesion, and metastases. High expression of this protein was observed in several types of cancers including HBV-related HCC. Inhibition of CDC42 by CRISPR/Cas9 knockout and treatment with a specific CDC42 inhibitor in HBx-Huh7 cells (92) reduced cell proliferation and promoted apoptosis in these cells. In addition to CDC42 down-regulation, we also found that its downstream effectors, actin and IQGAP1, showed decreased expression following IFN-λ3 treatment. Also, proteins involved in cell movement and focal adhesion such as ACTN1, ACTN4, RDX, CFL1, PIP4K2C, and ROCK2 were downregulated.

We have shown that IFN-λ3's effects were largely in accord with those expected of canonical IFN activity. Nevertheless, our tree and cluster analyses (Fig. 12 and 13) highlight several differential effects between IFN-λ3 and IFN-α2a worthy of further investigation. Most obviously, despite the division of treatment outcomes into 27 non-intersecting protein groups, unbiased Reactome enrichment analysis repeatedly elicited an RNA-metabolism/translation theme. This broad theme can be divided into Reactome sub-groups (*e.g.* metabolism of RNA, major pathway of rRNA processing in the nucleolus and cytosol, translation, transcription-coupled nucleotide excision repair (TC-NER), and peptide chain elongation). However, we could not specifically find IFN-λ3- or IFN-α2a dominant patterns in these sub-groups, suggesting that investigation of this broad theme might best be undertaken at the level of individual proteins. Perhaps the strongest general observation would be a tendency for involvement of ER-associated proteins (GO "establishment of protein localization to endoplasmic reticulum," which is primarily composed of ribosomal proteins) in cases where IFN-λ3 treatment results in significantly greater protein abundance *versus* IFN-α2a; in the 5 outcomes where such an effect would be discernable, -log(p) = 4.7, 3.2, 4.8, 8.2, and 5.3. On the other hand, such significance (-log(p) = 4.1) is seen only once out of six outcomes where IFN-α2a treatment results in significantly more abundant protein expression. This result could imply differential regulation of these ER targeting proteins on IFN-λ3 *versus* IFN-α2a treatment. Altered regulation of these ER proteins could interfere with viral replication (93, 94). It is interesting to note that some viruses utilize the ER as a replication compartment, whereas others do not. Thus, our work suggests that in addition to IFN's role in regulating ER-targeting, one IFN treatment might be more appropriate than another for infections. Of other Reactome groups that emerged during clustering, we find the "hypusine synthesis from eIF5A-lysine" case especially interesting, as it is only associated with a single outcome group, that in which λ3<c, α2a <c, λ3< α2a (*i.e.* the two IFNs cause down-regulation, but IFN-λ3's effect is most potent). Hypusine, a rare amino acid, is apparently found only once in the human proteome, as a modification of eukaryotic initiation factor 5 (eIF5A), with proviral implications for HIV and Ebola (95). Thus, IFN-λ3's antiviral effect may be especially potent in downregulating hypusination. The case of hypusination also illustrates how IFN-λ3-induced alterations to the RNA-metabolism/translation machinery could target viruses.

At the level of individual studies, we note that, in addition to the aforementioned λ3/α2a comparison, Bolen's data (16) also allows a λ3/λ2 comparison; here, up-regulated transcripts aligned strongly with our own λ3/c up-regulated proteins (p value = 10^{-27}), suggesting possible differential effects even within the IFN-λ subgroup. As a side note, IFITM3, strongly up-regulated in our own λ3/α2a comparison (outcome #1), was the single most significantly up-regulated transcript in the λ3/λ2 comparison (p value = 10^{-10}). Having noted possible IFN-λ3 *versus* IFN-α2a differences, we should reiterate the points that: 1) our experimental design did not allow for discrimination of kinetic effects (*e.g.* those caused over time by differing receptor/ligand affinities and half-lives) *versus* substantial alterations at the level of pathways and 2) the effects of IFN-λ3 and IFN-α2a were indeed substantially similar, especially with regard to canonical IFN effects such as regulation of antiviral proteins, antigen processing/presentation, and the RIG-I signaling pathway. A recent work does make a strong case for a differential λ3/α2a effect on murine intestinal epithelial cells (96), but the effect is pronounced only on polarization of cells, and the underlying microarray data does not correlate with our proteomic data. Thorough studies focused on possible differential effects on PTMs may help resolve these questions; the immediate result of IFN-receptor/ligand interaction is, after all, a phosphorylation event. Comprehensive identification of phosphorylation events and other kinds of PTMs will help us to elucidate possible differential effects in different IFN treatment.

In conclusion, our study found that IFN-λ3 exhibited anti-HBV activities by significant inhibition of HBV replication and expression of HBV RNA. We used high-throughput quantitative proteomics to obtain a comprehensive understanding of molecular events upon treatment of HepG2.2.15 with IFN-λ3.

To our knowledge, in fact, this study is the most comprehensive proteomics-based analysis of IFN treatment to date. For the first time, we reported significant up-regulation of immunoproteasome components, restoration of HBV-inhibited RIG-I pathway proteins, as well as several proteins not previously associated with IFN-λ3 treatment. Further study of these proteins is required. Clearly, IFN-λ3 exhibited both antiviral and immunomodulatory effects to inhibit HBV replication; therefore, IFN-λ3 is an attractive novel candidate for CHB treatment and the altered proteins might be new therapeutic targets in CHB infection.

Acknowledgments—●●●.

* This work was supported by Chulalongkorn Academic Advancement into Its 2nd Century (CUAASC) Project, Thailand Research Fund (TRF) for Research Career Development Grant (RSA 5880014), Government Budget to Chulalongkorn University (Fiscal year 2015), The 100th Anniversary Chulalongkorn University Fund for Doctoral Scholarship, The 90th Anniversary Chulalongkorn University Fund (Ratchadaphiseksomphot Endowment Fund), Center of Excellence in Systems Biology, and Center of Excellence in Immunology and Immune-mediated Diseases. KH's research is supported by Rachadapisek Sompot Fund for Postdoctoral Fellowship, Chulalongkorn University.

ZSI

S This article contains supplemental Tables.

‖ To whom correspondence should be addressed: Center of Excellence in Systems Biology, Research Affairs, Faculty of Medicine, Chulalongkorn University, Bangkok, Thailand. Tel.: 6692-537-0549; Fax: 662-652-4927; E-mail: pisitkut@nhlbi.nih.gov.

** These authors contributed equally to this work.

Author contributions: TP and NH conceived the study. JM, PS, and WP performed the study. JM, KH and TP drafted the manuscript. JM, KH, NH and TP discussed/interpreted results. All authors read and approved the final manuscript.

REFERENCES

1. Schweitzer, A., Horn, J., Mikolajczyk, R. T., Krause, G., and Ott, J. J. (2015) Estimations of worldwide prevalence of chronic hepatitis B virus infection: a systematic review of data published between 1965 and 2013. *Lancet* **386,** 1546–1555
2. Grimm, D., Thimme, R., and Blum, H. E. (2011) HBV life cycle and novel drug targets. *Hepatol. Int.* **5,** 644–653
3. Wright, T. L. (2006) Introduction to chronic hepatitis B infection. *Am. J. Gastroenterol.* **101,** S1–6
4. (2017) EASL 2017 Clinical Practice Guidelines on the management of hepatitis B virus infection. *J. Hepatol.* **67,** 370–398
5. Yuen, M. F., and Lai, C. L. (2011) Treatment of chronic hepatitis B: Evolution over two decades. *J. Gastroenterol. Hepatol.* **26,** 138–143
6. Lau, D. T. Y., and Bleibel, W. (2008) Current status of antiviral therapy for Hepatitis B. *Therap. Adv. Gastroenterol.* **1,** 61–75
7. Fung, J., Lai, C. L., Seto, W. K., and Yuen, M. F. (2011) Nucleoside/nucleotide analogues in the treatment of chronic hepatitis B. *J. Antimicrobial Chemother.* **66,** 2715–2725
8. Phillips, S., Mistry, S., Riva, A., Cooksley, H., Hadzhiolova-Lebeau, T., Plavova, S., Katzarov, K., Simonova, M., Zeuzem, S., Woffendin, C., Chen, P.-J., Peng, C.-Y., Chang, T.-T., Lueth, S., De Knegt, R., Choi, M.-S., Wedemeyer, H., Dao, M., Kim, C.-W., Chu, H.-C., Wind-Rotolo, M., Williams, R., Cooney, E., and Chokshi, S. (2017) Peg-interferon lambda treatment induces robust innate and adaptive immunity in chronic Hepatitis B patients. *Front. Immunol.* **8,** 621
9. Chan, H. L. Y., Ahn, S. H., Chang, T. T., Peng, C. Y., Wong, D., Coffin, C. S., Lim, S. G., Chen, P. J., Janssen, H. L. A., Marcellin, P., Serfaty, L., Zeuzem, S., Cohen, D., Critelli, L., Xu, D., Wind-Rotolo, M., and Cooney, E. (2016) Peginterferon lambda for the treatment of HBeAg-positive chronic hepatitis B: A randomized phase 2b study (LIRA-B). *J. Hepatol.* **64,** 1011–1019
10. Dellgren, C., Gad, H. H., Hamming, O. J., Melchjorsen, J., and Hartmann, R. (2009) Human interferon-lambda3 is a potent member of the type III interferon family. *Genes Immunity* **10,** 125–131
11. Pestka, S. (1997) The interferon receptors. *Sem. Oncol.* **24,** S9–18-S19–40
12. de Weerd, N. A., Samarajiwa, S. A., and Hertzog, P. J. (2007) Type I Interferon Receptors: Biochemistry and Biological Functions. *J. Biol. Chem.* **282,** 20053–20057
13. Miller, D. M., Klucher, K. M., Freeman, J. A., Hausman, D. F., Fontana, D., and Williams, D. E. (2009) Interferon lambda as a potential new therapeutic for hepatitis C. *Ann. N.Y. Acad. Sci.* **1182,** 80–87
14. Ramos, E. L. (2010) Preclinical and clinical development of pegylated interferon-lambda 1 in chronic hepatitis C. *J. Interferon Cytokine Res.* **30,** 591–595
15. Jilg, N., Lin, W., Hong, J., Schaefer, E. A., Wolski, D., Meixong, J., Goto, K., Brisac, C., Chusri, P., Fusco, D. N., Chevaliez, S., Luther, J., Kumthip, K., Urban, T. J., Peng, L. F., Lauer, G. M., and Chung, R. T. (2014) Kinetic Differences in the Induction of Interferon Stimulated Genes by Interferon-α and IL28B are altered by Infection with Hepatitis C Virus. *Hepatology* **59,** 1250–1261
16. Bolen, C. R., Ding, S., Robek, M. D., and Kleinstein, S. H. (2014) Dynamic expression profiling of type I and type III interferon-stimulated hepatocytes reveals a stable hierarchy of gene expression. *Hepatology* **59,** 1262–1272
17. Marcello, T., Grakoui, A., Barba Spaeth –G, Machlin, E. S., Kotenko, S. V., Macdonald, M. R., and Rice, C. M. (2006) Interferons α and λ inhibit Hepatitis C virus replication with distinct signal transduction and gene regulation kinetics. *Gastroenterology* **131,** 1887–1898
18. Dumoutier, L., Tounsi, A., Michiels, T., Sommereyns, C., Kotenko, S. V., and Renauld, J. C. (2004) Role of the interleukin (IL)-28 receptor tyrosine residues for antiviral and antiproliferative activity of IL-29/interferon-lambda 1: similarities with type I interferon signaling. *J. Biol. Chem.* **279,** 32269–32274
19. Donnelly, R. P., Sheikh, F., Kotenko, S. V., and Dickensheets, H. (2004) The expanded family of class II cytokines that share the IL-10 receptor-2 (IL-10R2) chain. *J. Leukocyte Biol.* **76,** 314–321
20. Sells, M. A., Chen, M. L., and Acs, G. (1987) Production of hepatitis B virus particles in Hep G2 cells transfected with cloned hepatitis B virus DNA. *Proc. Natl. Acad. Sci. U.S.A.* **84,** 1005–1009
21. Witt-Kehati, D., Bitton Alaluf, M., and Shlomai, A. (2016) Advances and challenges in studying Hepatitis B virus in vitro. *Viruses* **8,** 21
22. Verrier, E. R., Colpitts, C. C., Schuster, C., Zeisel, M. B., and Baumert, T. F. (2016) Cell culture models for the investigation of Hepatitis B and D virus infection. *Viruses* **8,** 261
23. Wang, J., Jiang, D., Zhang, H., Lv, S., Rao, H., Fei, R., and Wei, L. (2009) Proteome responses to stable hepatitis B virus transfection and following interferon alpha treatment in human liver cell line HepG2. *Proteomics* **9,** 1672–1682
24. Otsuka, M., Aizaki, H., Kato, N., Suzuki, T., Miyamura, T., Omata, M., and Seki, N. (2003) Differential cellular gene expression induced by hepatitis B and C viruses. *Biochem. Biophys. Res. Commun.* **300,** 443–447
25. Xin, X. M., Li, G. Q., Guan, X. R., Li, D., Xu, W. Z., Jin, Y. Y., and Gu, H. X. (2008) Combination therapy of siRNAs mediates greater suppression on hepatitis B virus cccDNA in HepG2.2.15 cell. *Hepato-gastroenterology* **55,** 2178–2183
26. Li, G. Q., Xu, W. Z., Wang, J. X., Deng, W. W., Li, D., and Gu, H. X. (2007) Combination of small interfering RNA and lamivudine on inhibition of human B virus replication in HepG2.2.15 cells. *World J. Gastroenterol.* **13,** 2324–2327
27. Ding, X. R., Yang, J., Sun, D. C., Lou, S. K., and Wang, S. Q. (2008) Whole genome expression profiling of hepatitis B virus-transfected cell line reveals the potential targets of anti-HBV drugs. *Pharmacogenomics J.* **8,** 61–70
28. Wang, L. Y., Li, Y. G., Chen, K., Li, K., Qu, J. L., Qin, D. D., and Tang, H. (2012) Stable expression and integrated hepatitis B virus genome in a human hepatoma cell line. *Gen. Mol. Res.* **11,** 1442–1448
29. Fang, C., Zhao, C., Liu, X., Yang, P., and Lu, H. (2012) Protein alteration of HepG2.2.15 cells induced by iron overload. *Proteomics* **12,** 1378–1390
30. Xie, H. Y., Xia, W. L., Zhang, C. C., Wu, L. M., Ji, H. F., Cheng, Y., and Zheng, S. S. (2007) Evaluation of hepatitis B virus replication and pro-

teomic analysis of HepG2.2.15 cell line after cyclosporine A treatment. *Acta Pharmacol. Sinica* **28,** 975–984

31. Venkatakrishnan, B., and Zlotnick, A. (2016) The Structural Biology of Hepatitis B Virus: Form and Function. *Ann. Rev. Virol.* **3,** 429–451
32. Hu, J., and Liu, K. (2017) Complete and Incomplete Hepatitis B Virus Particles: Formation, Function, and Application. *Viruses* **9,** 56
33. Park, I. H., Kwon, Y. C., Ryu, W. S., and Ahn, B. Y. (2014) Inhibition of hepatitis B virus replication by ligand-mediated activation of RNase L. *Antiviral Res.* **104,** 118–127
34. Jeong, G. U., Park, I. H., Ahn, K., and Ahn, B. Y. (2016) Inhibition of hepatitis B virus replication by a dNTPase-dependent function of the host restriction factor SAMHD1. *Virology* **495,** 71–78
35. Chen, Z., Zhu, M., Pan, X., Zhu, Y., Yan, H., Jiang, T., Shen, Y., Dong, X., Zheng, N., Lu, J., Ying, S., and Shen, Y. (2014) Inhibition of Hepatitis B virus replication by SAMHD1. *Biochem. Biophys. Res. Commun.* **450,** 1462–1468
36. Sommer, A. F., Riviere, L., Qu, B., Schott, K., Riess, M., Ni, Y., Shepard, C., Schnellbacher, E., Finkernagel, M., Himmelsbach, K., Welzel, K., Kettern, N., Donnerhak, C., Munk, C., Flory, E., Liese, J., Kim, B., Urban, S., and Konig, R. (2016) Restrictive influence of SAMHD1 on Hepatitis B Virus life cycle. *Sci. Rep.* **6,** 26616
37. Lu, X., Wang, J., Jin, X., Huang, Y., Zeng, W., and Zhu, J. (2015) IFN-CSP Inhibiting Hepatitis B Virus in HepG2.2.15 Cells Involves JAK-STAT Signal Pathway. *BioMed Res. Int.* **2015,** 8
38. Robek, M. D., Boyd, B. S., Wieland, S. F., and Chisari, F. V. (2004) Signal transduction pathways that inhibit hepatitis B virus replication. *Proc. Natl. Acad. Sci. U.S.A.* **101,** 1743–1747
39. Amini-Bavil-Olyaee, S., Choi, Y. J., Lee, J. H., Shi, M., Huang, I. C., Farzan, M., and Jung, J. U. (2013) The antiviral effector IFITM3 disrupts intracellular cholesterol homeostasis to block viral entry. *Cell Host Microbe* **13,** 452–464
40. Macovei, A., Petrareanu, C., Lazar, C., Florian, P., and Branza-Nichita, N. (2013) Regulation of Hepatitis B Virus Infection by Rab5, Rab7, and the Endolysosomal Compartment. *J. Virol.* **87,** 6415–6427
41. Kann, M., Schmitz, A., and Rabe, B. (2007) Intracellular transport of hepatitis B virus. *World J. Gastroenterol.* **13,** 39–47
42. Osseman, Q., and Kann, M. (2017) Intracytoplasmic transport of Hepatitis B virus capsids. *Methods Mol. Biol.* **1540,** 37–51
43. Gallucci, L., and Kann, M. (2017) Nuclear import of Hepatitis B virus capsids and genome. *Viruses* **9,** 21
44. Samuel, C. E. (2001) Antiviral actions of interferons. *Clin. Microbiol. Rev*. **14,** 778–809
45. Sadler, A. J., and Williams, B. R. G. (2008) Interferon-inducible antiviral effectors. *Nature reviews. Immunology* **8,** 559–568
46. Schoggins, J. W., and Rice, C. M. (2011) Interferon-stimulated genes and their antiviral effector functions. *Curr. Opinion Virol.* **1,** 519–525
47. Pei, R., Qin, B., Zhang, X., Zhu, W., Kemper, T., Ma, Z., Trippler, M., Schlaak, J., Chen, X., and Lu, M. (2014) Interferon-induced proteins with tetratricopeptide repeats 1 and 2 are cellular factors that limit hepatitis B virus replication. *J. Innate Immunity* **6,** 182–191
48. Sato, S., Li, K., Kameyama, T., Hayashi, T., Ishida, Y., Murakami, S., Watanabe, T., Iijima, S., Sakurai, Y., Watashi, K., Tsutsumi, S., Sato, Y., Akita, H., Wakita, T., Rice, C. M., Harashima, H., Kohara, M., Tanaka, Y., and Takaoka, A. (2015) The RNA sensor RIG-I dually functions as an innate sensor and direct antiviral factor for hepatitis B virus. *Immunity* **42,** 123–132
49. Ryoo, J., Choi, J., Oh, C., Kim, S., Seo, M., Kim, S. Y., Seo, D., Kim, J., White, T. E., Brandariz-Nunez, A., Diaz-Griffero, F., Yun, C. H., Hollenbaugh, J. A., Kim, B., Baek, D., and Ahn, K. (2014) The ribonuclease activity of SAMHD1 is required for HIV-1 restriction. *Nat. Med.* **20,** 936–941
50. Fu, Y., Gaelings, L., Soderholm, S., Belanov, S., Nandania, J., Nyman, T. A., Matikainen, S., Anders, S., Velagapudi, V., and Kainov, D. E. (2016) JNJ872 inhibits influenza A virus replication without altering cellular antiviral responses. *Antiviral Res.* **133,** 23–31
51. Wang, X., Li, Y., Li, L. F., Shen, L., Zhang, L., Yu, J., Luo, Y., Sun, Y., Li, S., and Qiu, H. J. (2016) RNA interference screening of interferon-stimulated genes with antiviral activities against classical swine fever virus using a reporter virus. *Antiviral Res.***128,** 49–56
52. Meng, G., Zhao, Y., Bai, X., Liu, Y., Green, T. J., Luo, M., and Zheng, X. (2010) Structure of human stabilin-1 interacting chitinase-like protein (SI-CLP) reveals a saccharide-binding cleft with lower sugar-binding selectivity. *J. Biol. Chem.* **285,** 39898–39904
53. Rubins, K. H., Hensley, L. E., Wahl-Jensen, V., Daddario DiCaprio, K. M., Young, H. A., Reed, D. S., Jahrling, P. B., Brown, P. O., Relman, D. A., and Geisbert, T. W. (2007) The temporal program of peripheral blood gene expression in the response of nonhuman primates to Ebola hemorrhagic fever. *Gen. Biol.* **8,** R174–R174
54. Zapata, J. C., Carrion, R., Jr, Patterson, J. L., Crasta, O., Zhang, Y., Mani, S., Jett, M., Poonia, B., Djavani, M., White, D. M., Lukashevich, I. S., and Salvato, M. S. (2013) Transcriptome analysis of human peripheral blood mononuclear cells exposed to Lassa virus and to the attenuated Mopeia/Lassa reassortant 29 (ML29), a vaccine candidate. *PLoS Neglected Tropical Dis.* **7,** e2406
55. Ioannidis, I., McNally, B., Willette, M., Peeples, M. E., Chaussabel, D., Durbin, J. E., Ramilo, O., Mejias, A., and Flano, E. (2012) Plasticity and virus specificity of the airway epithelial cell immune response during respiratory virus infection. *J. Virol.* **86,** 5422–5436
56. Mitchell, H. D., Eisfeld, A. J., Sims, A. C., McDermott, J. E., Matzke, M. M., Webb-Robertson, B. J., Tilton, S. C., Tchitchek, N., Josset, L., Li, C., Ellis, A. L., Chang, J. H., Heegel, R. A., Luna, M. L., Schepmoes, A. A., Shukla, A. K., Metz, T. O., Neumann, G., Benecke, A. G., Smith, R. D., Baric, R. S., Kawaoka, Y., Katze, M. G., and Waters, K. M. (2013) A network integration approach to predict conserved regulators related to pathogenicity of influenza and SARS-CoV respiratory viruses. *PloS ONE* **8,** e69374
57. Lee, S., Kopp, F., Chang, T. C., Sataluri, A., Chen, B., Sivakumar, S., Yu, H., Xie, Y., and Mendell, J. T. (2016) Noncoding RNA NORAD Regulates Genomic Stability by Sequestering PUMILIO Proteins. *Cell* **164,** 69–80
58. Whisenant, T. C., Peralta, E. R., Aarreberg, L. D., Gao, N. J., Head, S. R., Ordoukhanian, P., Williamson, J. R., and Salomon, D. R. (2015) The Activation-Induced Assembly of an RNA/Protein Interactome Centered on the Splicing Factor U2AF2 Regulates Gene Expression in Human CD4 T Cells. *PloS ONE* **10,** e0144409
59. Hong, S. H., Cho, O., Kim, K., Shin, H. J., Kotenko, S. V., and Park, S. (2007) Effect of interferon-lambda on replication of hepatitis B virus in human hepatoma cells. *Virus Res.* **126,** 245–249
60. Liu, M. Q., Zhou, D. J., Wang, X., Zhou, W., Ye, L., Li, J. L., Wang, Y. Z., and Ho, W. Z. (2012) IFN-lambda3 inhibits HIV infection of macrophages through the JAK-STAT pathway. *PloS ONE* **7,** e35902
61. Ank, N., West, H., and Paludan, S. R. (2006) IFN-lambda: novel antiviral cytokines. *J. Interferon Cytokine Res* **26,** 373–379
62. Pagliaccetti, N. E., and Robek, M. D. (2010) Interferon-lambda in the immune response to hepatitis B virus and hepatitis C virus. *J. Interferon Cytokine Res* **30,** 585–590
63. Donnelly, R. P., and Kotenko, S. V. (2010) Interferon-Lambda: A New Addition to an Old Family. *J. Interferon Cytokine Res.* **30,** 555–564
64. Marcello, T., Grakoui, A., Barba-Spaeth, G., Machlin, E. S., Kotenko, S. V., MacDonald, M. R., and Rice, C. M. (2006) Interferons alpha and lambda inhibit hepatitis C virus replication with distinct signal transduction and gene regulation kinetics. *Gastroenterology* **131,** 1887–1898
65. Robek, M. D., Boyd, B. S., and Chisari, F. V. (2005) Lambda interferon inhibits hepatitis B and C virus replication. *J. Virol.* **79,** 3851–3854
66. Lachmann, A., Torre, D., Keenan, A. B., Jagodnik, K. M., Lee, H. J., Silverstein, M. C., Wang, L., Ma and ayan, A. (2017) Massive mining of publicly available RNA-seq data from human and mouse. *bioRxiv* **AQ: H**
67. Maiwald, T., Schneider, A., Busch, H., Sahle, S., Gretz, N., Weiss, T. S., Kummer, U., and Klingmuller, U. (2010) Combining theoretical analysis and experimental data generation reveals IRF9 as a crucial factor for accelerating interferon alpha-induced early antiviral signalling. *FEBS J.* **277,** 4741–4754
68. Rouillard, A. D., Gundersen, G. W., Fernandez, N. F., Wang, Z., Monteiro, C. D., McDermott, M. G., and Ma'ayan, A. (2016) The harmonizome: a collection of processed data sets gathered to serve and mine knowledge about genes and proteins. *Database* **AQ: I**
69. Robek, M. D., Wieland, S. F., and Chisari, F. V. (2002) Inhibition of hepatitis B virus replication by interferon requires proteasome activity. *J. Virol.* **76,** 3570–3574
70. Yao, Y., Li, J., Lu, Z., Tong, A., Wang, W., Su, X., Zhou, Y., Mu, B., Zhou, S., Li, X., Chen, L., Gou, L., Song, H., Yang, J., and Wei, Y. (2011) Proteomic analysis of the interleukin-4 (IL-4) response in hepatitis B

virus-positive human hepatocelluar carcinoma cell line HepG2.2.15. *Electrophoresis* **32,** 2004–2012

71. Ferrington, D. A., and Gregerson, D. S. (2012) Immunoproteasomes: structure, function, and antigen presentation. *Progress Mol. Biol. Translational Sci.* **109,** 75–112
72. Wieland, S., Thimme, R., Purcell, R. H., and Chisari, F. V. (2004) Genomic analysis of the host response to hepatitis B virus infection. *Proc. Natl. Acad. Sci. U.S.A.* **101,** 6669–6674
73. Yu, S., Chen, J., Wu, M., Chen, H., Kato, N., and Yuan, Z. (2010) Hepatitis B virus polymerase inhibits RIG-I- and Toll-like receptor 3-mediated beta interferon induction in human hepatocytes through interference with interferon regulatory factor 3 activation and dampening of the interaction between TBK1/IKKepsilon and DDX3. *J. General Virol.* **91,** 2080–2090
74. Jiang, J., and Tang, H. (2010) Mechanism of inhibiting type I interferon induction by hepatitis B virus X protein. *Protein Cell* **1,** 1106–1117
75. Kumar, M., Jung, S. Y., Hodgson, A. J., Madden, C. R., Qin, J., and Slagle, B. L. (2011) Hepatitis B Virus Regulatory HBx Protein Binds to Adaptor Protein IPS-1 and Inhibits the Activation of Beta Interferon. *J. Virol.* **85,** 987–995
76. Hou, Z., Zhang, J., Han, Q., Su, C., Qu, J., Xu, D., Zhang, C., and Tian, Z. (2016) Hepatitis B virus inhibits intrinsic RIG-I and RIG-G immune signaling via inducing miR146a. *Sci. Rep.* **6,** 26150
77. Zhu, J., Zhang, Y., Ghosh, A., Cuevas, R. A., Forero, A., Dhar, J., Ibsen, M. S., Schmid-Burgk, J. L., Schmidt, T., Ganapathiraju, M. K., Fujita, T., Hartmann, R., Barik, S., Hornung, V., Coyne, C. B., and Sarkar, S. N. (2014) Antiviral activity of human OASL protein is mediated by enhancing signaling of the RIG-I RNA sensor. *Immunity* **40,** 936–948
78. Gack, M. U., Shin, Y. C., Joo, C. H., Urano, T., Liang, C., Sun, L., Takeuchi, O., Akira, S., Chen, Z., Inoue, S., and Jung, J. U. (2007) TRIM25 RING-finger E3 ubiquitin ligase is essential for RIG-I-mediated antiviral activity. *Nature* **446,** 916–920
79. Kino, T., Gragerov, A., Valentin, A., Tsopanomihalou, M., Ilyina-Gragerova, G., Erwin-Cohen, R., Chrousos, G. P., and Pavlakis, G. N. (2005) Vpr protein of human immunodeficiency virus type 1 binds to 14-3-3 proteins and facilitates complex formation with Cdc25C: implications for cell cycle arrest. *J. Virol.* **79,** 2780–2787
80. Aoki, H., Hayashi, J., Moriyama, M., Arakawa, Y., and Hino, O. (2000) Hepatitis C virus core protein interacts with 14-3-3 protein and activates the kinase Raf-1. *J. Virol.* **74,** 1736–1741
81. Fu, H., Subramanian, R. R., and Masters, S. C. (2000) 14-3-3 proteins: structure, function, and regulation. *Ann. Rev. Pharmacol. Toxicol.* **40,** 617–647
82. Yang, B., and Bouchard, M. J. (2012) The hepatitis B virus X protein elevates cytosolic calcium signals by modulating mitochondrial calcium uptake. *J. Virol.* **86,** 313–327
83. Bouchard, M. J., Wang, L. H., and Schneider, R. J. (2001) Calcium signaling by HBx protein in hepatitis B virus DNA replication. *Science* **294,** 2376–2378
84. Xia, W. L., Shen, Y., and Zheng, S. S. (2005) Inhibitory effect of cyclosporine A on hepatitis B virus replication in vitro and its possible mechanisms. *Hepatobiliary Pancreatic Dis. Int.* **4,** 18–22
85. Choi, Y., Gyoo Park, S., Yoo, J. H., and Jung, G. (2005) Calcium ions affect the hepatitis B virus core assembly. *Virology* **332,** 454–463
86. Coppolino, M. G., and Dedhar, S. (1998) Calreticulin. *Int. J. Biochem. Cell Biol.* **30,** 553–558
87. Raghavan, M., Wijeyesakere, S. J., Peters, L. R., and Del Cid, N. (2013) Calreticulin in the immune system: ins and outs. *Trends Immunol.* **34,** 13–21
88. Michalak, M., Corbett, E. F., Mesaeli, N., Nakamura, K., and Opas, M. (1999) Calreticulin: one protein, one gene, many functions. *Biochem. J. 344 Pt* **2,** 281–292
89. Yue, X., Wang, H., Zhao, F., Liu, S., Wu, J., Ren, W., and Zhu, Y. (2012) Hepatitis B virus-induced calreticulin protein is involved in IFN resistance. *J. Immunol.* **189,** 279–286
90. Arjonen, A., Kaukonen, R., and Ivaska, J. (2011) Filopodia and adhesion in cancer cell motility. *Cell Adhesion Migration* **5,** 421–430
91. Zhao, R., Wang, T. Z., Kong, D., Zhang, L., Meng, H. X., Jiang, Y., Wu, Y. Q., Yu, Z. X., and Jin, X. M. (2011) Hepatoma cell line HepG2.2.15 demonstrates distinct biological features compared with parental HepG2. *World J. Gastroenterol.: WJG* **17,** 1152–1159
92. Xu, Y., Qi, Y., Luo, J., Yang, J., Xie, Q., Deng, C., Su, N., Wei, W., Shi, D., Xu, F., Li, X., and Xu, P. (2017) Hepatitis B Virus X Protein Stimulates Proliferation, Wound Closure and Inhibits Apoptosis of HuH-7 Cells via CDC42. *Int. J. Mol. Sci.* **18,** 586
93. Romero-Brey, I., and Bartenschlager, R. (2016) Endoplasmic Reticulum: The Favorite Intracellular Niche for Viral Replication and Assembly. *Viruses* **8,** 160
94. Inoue, T., and Tsai, B. (2013) How Viruses Use the Endoplasmic Reticulum for Entry, Replication, and Assembly. *Cold Spring Harbor Perspectives Biol.* 5, a013250
95. Olsen, M. E., and Connor, J. H. (2017) Hypusination of eIF5A as a target for antiviral therapy. *DNA Cell Biol.* **36,** 198–201
96. Selvakumar, T. A., Bhushal, S., Kalinke, U., Wirth, D., Hauser, H., Koster, M., and Hornef, M. W. (2017) Identification of a predominantly interferon-lambda-induced transcriptional profile in murine intestinal epithelial cells. *Front. Immunol.* **8,** 1302

Manuscript proof 2

Physiological Reports

Open Access

Physiological Reports ISSN 2051-817X

ORIGINAL RESEARCH

Sequence-based searching of custom proteome and transcriptome databases

Barbara Medvar[1,2,3], Abhijit Sarkar[1,2,3], Mark Knepper[1] & Trairak Pisitkun[1,4]

1 Epithelial Systems Biology Laboratory, Systems Biology Center, National Heart, Lung, and Blood Institute, National Institutes of Health, Bethesda, Maryland
2 Vitreous State Laboratory, The Catholic University of America, Washington, District of Columbia
3 Physics Department, The Catholic University of America, Washington, District of Columbia
4 Systems Biology Center, Faculty of Medicine, Chulalongkorn University, Bangkok, Thailand

Keywords
BLAST, database, IMCD, kidney.

Correspondence
Mark A. Knepper, National Institutes of Health, Bldg. 10, Room 6N307, 10 CENTER DR, MSC-1603, Bethesda, MD 20892-1603.
Tel: +1 (301) 496 3064
Fax: +1 (301) 402 1443
E-mail: knepperm@nhlbi.nih.gov

Funding Information
None declared.

Received: 13 June 2018; Revised: 2 August 2018; Accepted: 6 August 2018

doi: 10.14814/phy2.13846

Physiol Rep, 6 (16), 2018, e13846, https://doi.org/10.14814/phy2.13846

Temporary username for databases: *clp* and temporary password: *Esbl!@#$*.

Abstract

A long-term goal in renal physiology is to understand the mechanisms involved in collecting duct function and regulation at a cellular and molecular level. The first step in modeling of these mechanisms, which can provide a guide to experimentation, is the generation of a list of model components. We have curated a list of proteins expressed in the rat renal inner medullary collecting duct (IMCD) from proteomic data from 18 different publications. The database has been posted as a public resource at https://hpcwebapps.cit.nih.gov/ESBL/Database/IMCD_Proteome_Database/. It includes 8959 different proteins. To search the IMCD Proteomic Database efficiently, we have created a Java-based program called *curated database Basic Local Alignment Search Tool* (cdbBLAST), which uses the NCBI BLAST kernel to search for specific amino acid sequences corresponding to proteins in the database. cdbBLAST reports information on the matched protein and identifies proteins in the database that have similar sequences. We have also adapted cdbBLAST to interrogate our previously published IMCD Transcriptome Database. We have made the cdbBLAST program available for use either as a web application or a downloadable .jar file at https://hpcwebapps.cit.nih.gov/ESBL/Database/cdbBLAST/. Database searching based on protein sequence removes ambiguities arising from the standard search method based on official gene symbols and allows the user efficient identification of related proteins that may fulfill the same functional roles.

Introduction

With the advent of large-scale proteomic and transcriptomic experiments for profiling gene expression, data access and integration has become rate-limiting for acquisition of biological knowledge. Access is facilitated through the creation of databases of curated datasets. For example, our laboratory alone has generated approximately 70 such databases, accessible at https://hpcwebapps.cit.nih.gov/ESBL/Database/index.html. Because of the large amount of data within these types of databases, it becomes difficult to find information about a specific protein/transcript. The question then becomes: what is the best way to find a particular protein/transcript within the databases? A general strategy to database searches is to utilize so-called "keys" or "indices" that constitute finite search target lists. In systems biology, there are a few common "keys," namely a common name for a protein/transcript, a protein/transcript's gene symbol, or the amino acid/nucleotide sequence for a protein/transcript. Problems arise when a database is searched using a common name for the protein/transcript in question; common or large proteins have multiple names and can be difficult to find if the user is not searching for the name used within the database. Searching using a gene symbol is a better option, however it is not without its own difficulties. As with searching using a common name, a well-studied protein can be linked to multiple gene symbols. A second issue that arises

from using the gene symbol as the "key" to searching databases is the inability to comprehensively search for related proteins. Unless all proteins share a similar gene symbol (e.g., Aqp1, Aqp2, etc.) it is extremely difficult to find all related proteins, for example, those with a particular domain. The best solution to the problems that arise from searching by gene symbol or a common name is to search curated databases using a protein/transcript's amino acid/nucleotide sequence. Each protein/transcript has a unique sequence, allowing the correct protein/transcript to be found regardless of the gene symbol or name used in the database. Using a sequence also allows for related proteins/transcripts to be found based on similar sequence matches.

The primary goal of this paper is to introduce a sequence-based search tool, called cdbBLAST (curated database BLAST), that uses NCBI's *blastp* kernel to uniquely find a protein/transcript within a curated database, as well as find similar proteins/transcripts, and provides information from the database on each of the proteins/transcripts in the results. Another benefit of cdbBLAST is that it allows for domain sequence searches, so it is possible to find all proteins/transcripts within a curated database that share a domain. We illustrate the use of this tool by applying it to two newly curated databases, a database of all rat inner medullary collecting duct transcripts, and a database of all rat inner medullary collecting duct proteins. The former is created by combining two published studies, one from RNA-seq and one from expression microarrays, while the latter is a created by distilling information from 18 published studies.

Methods

We curated a comprehensive list of proteins found in the rat IMCD cells from 18 studies (van Balkom et al. 2004; Hoffert et al. 2004, 2006, 2012, 2014; Barile et al. 2005; Hoorn et al. 2005; Pisitkun et al. 2006; Simons et al. 2006; Yu et al. 2006; Sachs et al. 2008; Bansal et al. 2010; Tchapyjnikov et al. 2010; Zhao et al. 2012; Bradford et al. 2014; Trepiccione et al. 2014; Pickering et al. 2016; LeMaire et al. 2017) done within our laboratory. Some of these proteomic studies include multiple experimental methods, which results in 20 "sources" describing which experimental method identified a specific protein. This database has been put together on a publicly accessible webpage (https://hpcwebapps.cit.nih.gov/ESBL/Database/IMCD_Proteome_Database/ temporary username: clp and temporary password: Esbl!@#$).

We have created a sequence-based search tool, called cdbBLAST, which allows databases to be searched for a certain protein using a protein-to-protein sequence comparison. cdbBLAST uses the NCBI *blastp* kernel to search the database for the protein in question and returns similar proteins that are found in the database as well. It also returns information from the database on each of the proteins in the results. cdbBLAST can be used as a web-based servlet or as a downloadable GUI.

When the user types (or pastes) a string of amino acids into the search box and hits submit, cdbBLAST turns that string into a .txt file, and uses it as input to the NCBI *blastp* kernel. The input needs to be a minimum of 11 amino acids in length. The blastp kernel then compares this input file to a database of sequences, and prints the results of the comparison (Fig. 1). The cdbBLAST web-based servlet then prints these results as a webpage. The cdbBLAST GUI version outputs the results directly in blastp format.

Software implementation

cdbBLAST, both the web-based servlets and the downloadable version, were written in Java (Java Development Kit 1.8 Update 121) using NetBeans IDE 8.1 as an integrated development environment. They were implemented using Apache Tomcat 8.0.15. The *blastp* kernel form NCBI that is used is called BLASTP 2.4.0+, and was downloaded from ftp://ftp.ncbi.nlm.nih.gov/blast/executables/blast+ as part of the blast 2.4.0+ folder.

cdbBLAST takes an amino acid sequence as input and compares it to a list of FASTA sequences corresponding to entries in the curated database. This list includes not only FASTA sequences and the typical FASTA metadata, but additional information from the databases that are built in to the metadata.

These FASTA sequence lists were created using the Automatic Bioinformatics Extractor (ABE) to convert the *RefSeq* protein accession numbers of the entries to FASTA amino acid sequence and metadata. The database information was then combined with the existing metadata for each protein/transcript. Next the list was copied into a Notepad file, and saved as a "filename.fasta" file. Subsequently, in the command line, the BLAST code makeblastdb.exe was run, using this new .fasta file as part of the input. This results in three new files being created: filename.fasta.phr, filename.fasta.pin, and filename.fasta.psq. These three files are required to run blastp, and thus cdbBLAST (Fig. 2). A more thorough step by step process can be found in the Appendix, downloadable from https://hpcwebapps.cit.nih.gov/ESBL/Database/cdbBLAST-Appendix/Appendix.html.

Results

We have curated a rat IMCD proteome database from 18 studies produced in our laboratory, resulting in a database of 8956 proteins. This database has been made into

COLOR

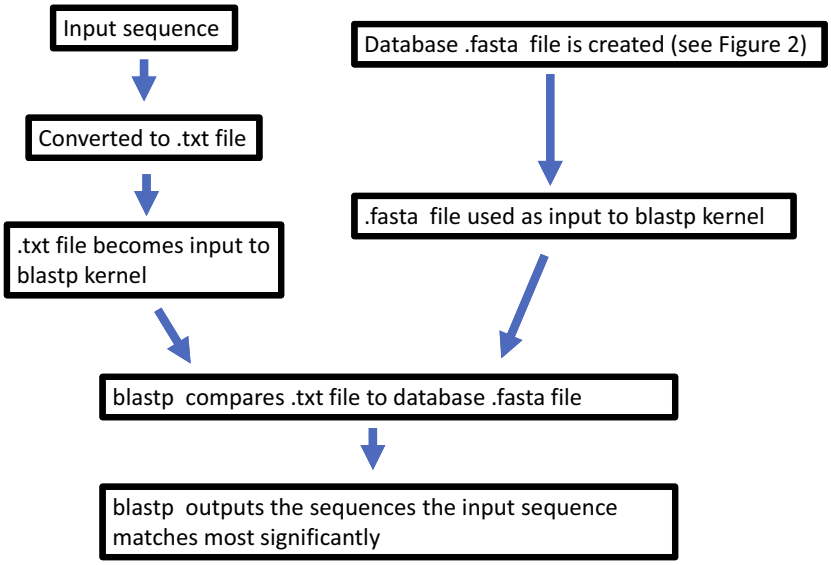

Figure 1. A flowchart explaining the algorithm of cdbBLAST. The input sequence is converted to a .txt file, which becomes the input to the BLAST kernel. This input file is compared to a .fasta database, and the sequences in the .fasta database that match most closely to the input sequence are output in the results.

COLOR

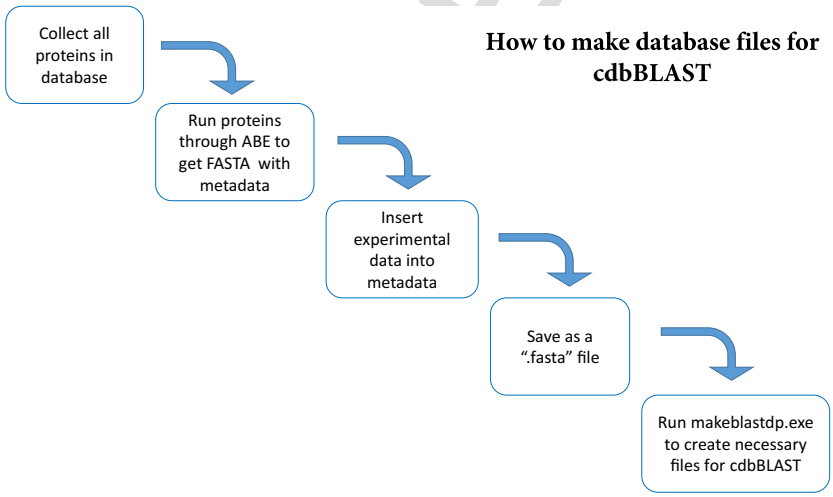

Figure 2. A flowchart explaining the process for creating a .fasta database to be used with cdbBLAST. We start with a list of all proteins* in the database. That list is then run through Automatic Bioinformatics Extractor (ABE) to get the FASTA sequence and metadata associated with each protein in the list. Next, experimental information is added to the metadata for each protein, and this new list is saved as a ".fasta" file. The .fasta file is then the input for makeblastdb.exe, which creates the three necessary files needed to run cdbBLAST. A more detailed explanation can be found in the Appendix, downloadable from https://hpcwebapps.cit.nih.gov/ESBL/Database/cdbBLAST-Appendix/Appendix.html. *This figure describes proteins being made into a database. The process for creating a database of transcripts is the same.

a publicly accessible webpage (https://hpcwebapps.cit.nih.gov/ESBL/Database/IMCD_Proteome_Database/ temporary username: clp and temporary password: Esbl!@#$) (Fig. 3). This database shows how many different experimental datasets each protein was found in, as well as its protein name, official gene symbol, accession number, and number of amino acids. The database also shows, and can be sorted by, whether the corresponding mRNA is present in the transcriptome.

To best search large databases like this rat IMCD proteome, we have created a sequence-based search tool called cdbBLAST. cdbBLAST allows the user to input a full amino acid sequence, or a partial sequence, and compare it against a list of FASTA sequences corresponding

to the proteins/transcripts in the curated database. We have created a rat IMCD proteome database and combined two existing rat IMCD transcriptome databases to be searched using cdbBLAST, which has been made publicly accessible (https://hpcwebapps.cit.nih.gov/ESBL/Database/cdbBLAST temporary username: clp and temporary

COLOR

National Heart Lung and Blood Institute

Epithelial Systems Biology Laboratory (ESBL)

IMCD Proteome Database

This database of renal inner medullary collecting duct (IMCD) proteins is based on published protein mass spectrometry data from the NHLBI Epithelial Systems Biology Laboratory. All data are from IMCD cells freshly isolated from the renal medullas of rats.

The database can be sorted by protein name, gene symbol, accession number, amino acid number, the number of sources, and if it is in the transcriptome by clicking on the respective header of the table. It is also possible to **download data as an Excel file** .

The IMCD Proteome Database was created by Barbara Medvar, Jennifer Huling, Dmitry Tchapyjnikov, Aaron N. Sachs, Brian Ruttenberg, Vinitha Jacob, Guozhong Ma, Jason D. Hoffert, Trairak Pisitkun and Mark A. Knepper. Contact us with any questions or comments.

BLAST your protein against this database

Current Database Size: 8,956 proteins.

Sources

Protein Name	Gene Symbol	Acc No.	A.A. No.	Sources*	In the Transcriptome**
enolase 1, alpha	Eno1	NP_036686.1	434	1, 2, 3, 4, 6, 7, 10, 11, 12, 13, 14,15, 16, 17, 18, 19, 20	Yes
aldehyde reductase 1	Akr1b1	NP_036630.1	316	1, 2, 3, 4, 5, 6, 9, 10, 11, 12, 15, 16, 17, 18, 19, 20	Yes
annexin A2	Anxa2	NP_063970.1	339	1, 2, 4, 5, 6, 7, 9, 10, 11, 12, 14, 15, 17, 18, 19, 20	Yes
crystallin, alpha B	Cryab	NP_037067.1	175	1, 5, 6, 7, 8, 10, 11, 12, 13, 15, 16, 17, 18, 19, 20	Yes
heat shock protein 1	Hspb1	NP_114176.3	205	1, 2, 5, 6, 8, 10, 11, 12, 13, 15, 16, 17, 18, 19, 20	Yes
keratin, type I cytoskeletal 19	Krt19	NP_955792.1	403	2, 5, 6, 8, 10, 11, 12, 13, 14, 15, 16, 17, 18, 19, 20	Yes
myosin, heavy polypeptide 9	Myh9	NP_037326.1	1961	4, 5, 6, 8, 10, 11, 12, 13, 14, 15, 16, 17, 18, 19, 20	Yes
catenin (cadherin-associated protein), alpha 1, 102kDa	Ctnna1	NP_001007146.1	908	4, 6, 8, 10, 11, 12, 13, 14, 15, 16, 17, 18, 19, 20	Yes
heterogeneous nuclear ribonucleoprotein K	Hnrnpk	NP_476482.1	463	5, 6, 8, 10, 11, 12, 13, 14, 15, 16, 17, 18, 19, 20	Yes
heat shock 105kDa/110kDa protein 1	Hsph1	NP_001011901.1	858	3, 4, 6, 10, 11, 12, 13, 14, 15, 16, 17, 18, 19, 20	Yes
keratin, type II cytoskeletal 8	Krt8	NP_955402.1	483	1, 2, 6, 7, 8, 10, 11, 12, 13, 15,	Yes

* Find the techniques used here.

** Yes means that the corresponding transcript was found in either Lee et al. PMID: 25817355 or Uawithya et al. PMID: 17956998.

NHLBI Home Search NHLBI Accessibility Information NHLBI Site Index Other Sites

Figure 3. A publicly available webpage was created to provide users with a complete list of proteins found in the rat IMCD, as identified in 18 studies. Access to this webpage can be found at https://helixweb.nih.gov/ESBL/Database/IMCD_Proteome_Database/. There is a link to a list of all sources, as well as a link to download the data to an Excel file. The data on this webpage can be sorted by the number of sources a protein is found in, amino acid number, if a protein is found in the transcriptome, or alphabetically by gene symbol, protein name, or RefSeq number.

password: Esbl!@#$) as well as downloadable as a .jar file (Fig. 4).

The proteome cdbBLAST search (Fig. 5A) allows the user to input an amino acid sequence and search the curated rat IMCD proteome database introduced in this paper. There is a link on both the main page and the results page of cdbBLAST to the proteome database. At the bottom of the search page, there is a set of criteria (e.g., expect threshold, word size, substitution matrix, and gap costs) the user can use to manipulate the results, based on NCBI's *BLAST* code (Altschul et al. 1990) (Fig. 5B). Once the user is content with the criteria and the sequence used, hitting "submit" will allow the code to run and brings up a results page. This results page shows a table at the top of the page with the proteins that match best to the search sequence. It also shows the related proteins' RefSeq number, which is a link to that protein in PubMed (National Center for Biotechnology Information, 2017), and the "score" and "e-value" as determined by NCBI's *blastp* code. The "score" is a normalized score for aligning pairs of residues between the query and the database sequences, where the "e-value" or expected value is the number of hits one can expect to see by chance. The higher the score, and the lower the e-value, the more significant the match. Below this table, each related protein is compared to the search sequence. Each comparison is labeled with the protein's RefSeq number, protein name, and what sources from the IMCD proteome that protein was found in. Between the table and the comparisons is a link labeled "Sources listed here" which allows the user to open the "Sources" page from the IMCD proteome database in another tab so they are able to see what each numbered source is without losing their cdbBLAST search results. To show an example of what the results look like, we used the partial sequence associated with the HECTc domain from Nedd4l as a sample query. Nedd4l is an E3 ubiquitin ligase most likely to ubiquitinate the water

COLOR

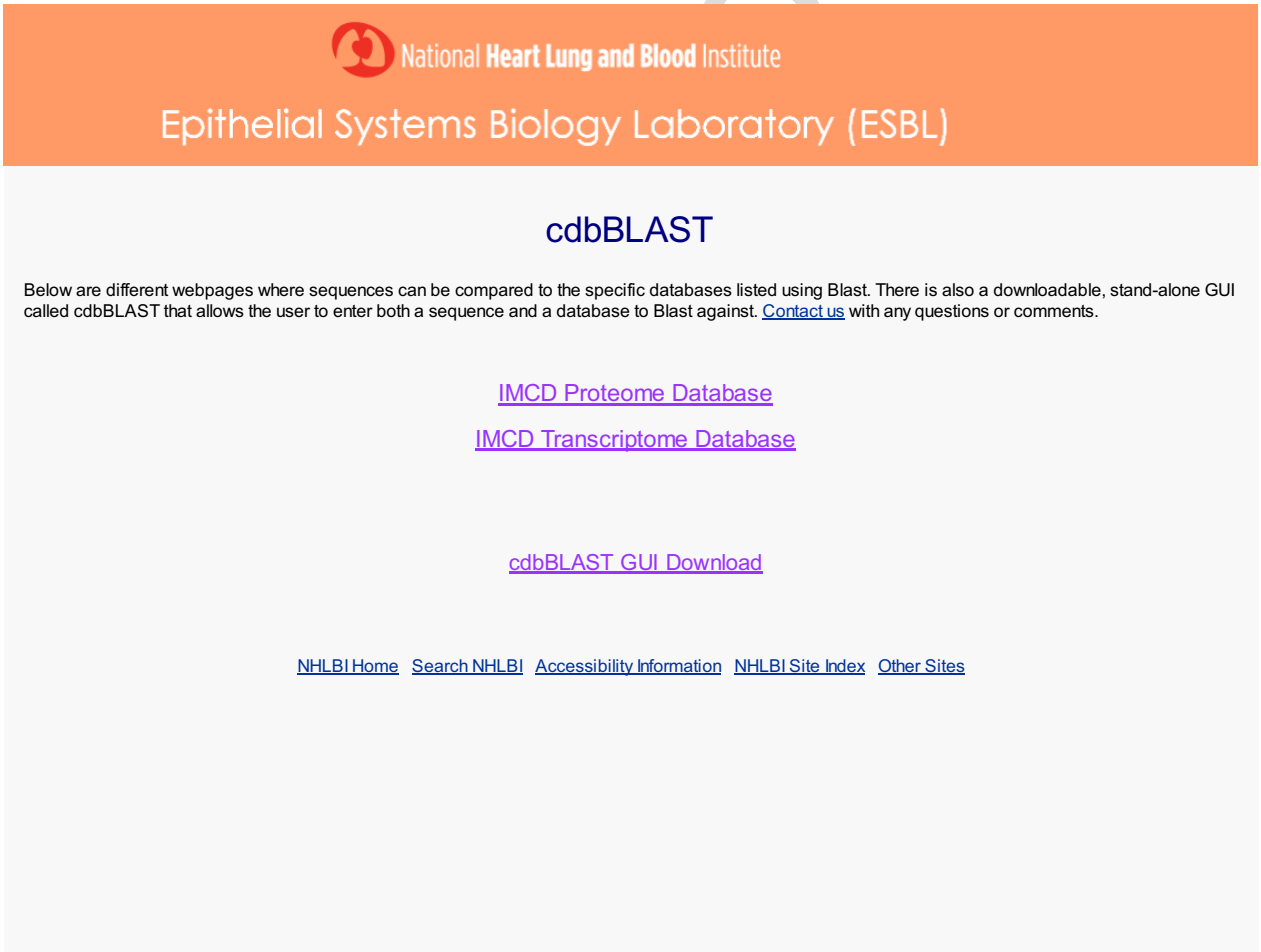

Figure 4. A screenshot of the main cdbBLAST webpage. This page has links to the IMCD Proteome and Transcriptome cdbBLAST searches, which compare an input sequence to our databases of proteins and transcripts respectively. There is also a link to the downloadable GUI version of cdbBLAST, where the user can compare a sequence of interest to their own database of sequences.

POOR QUALITY COLOR FIG

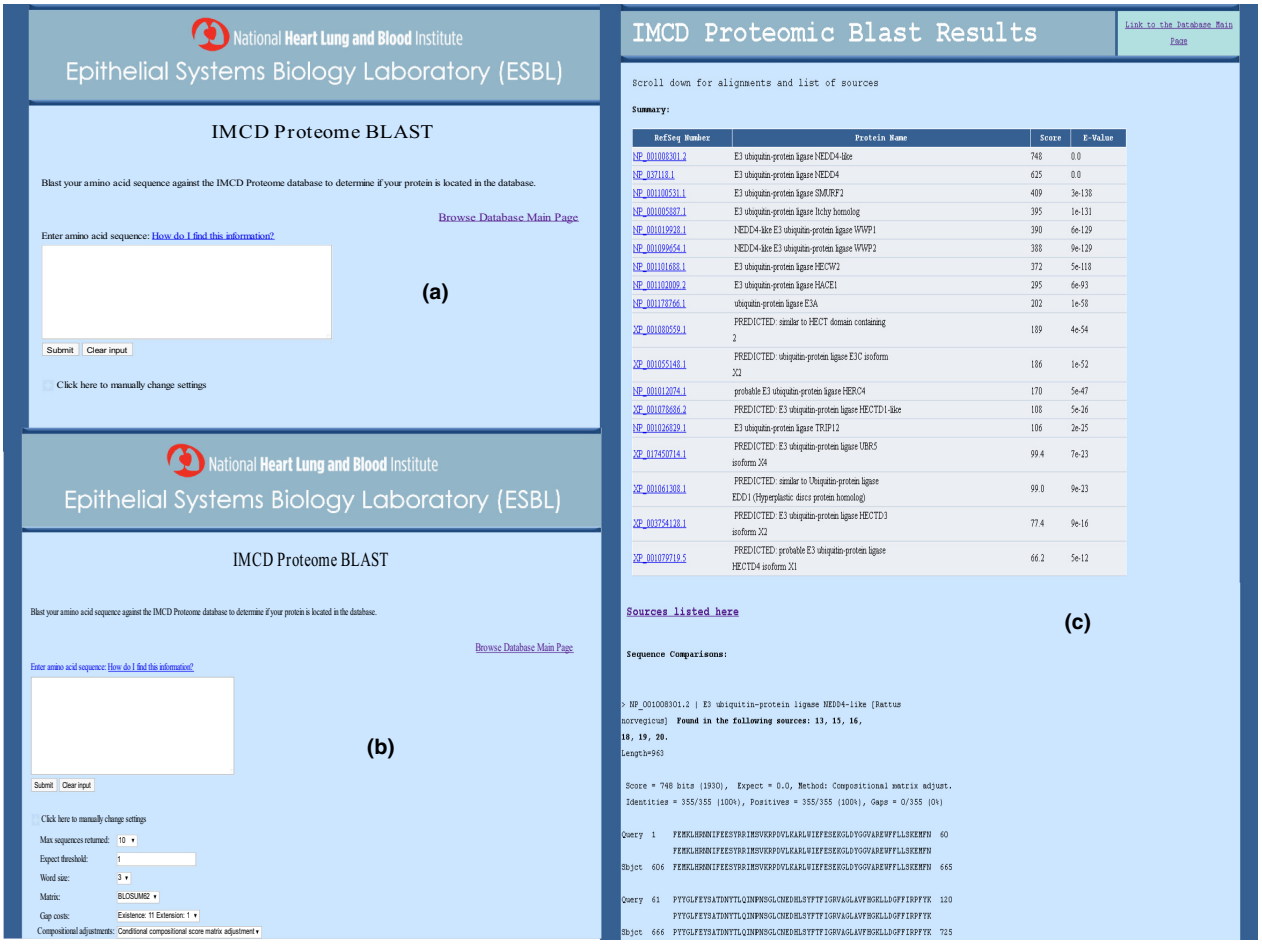

11

Figure 5. A screenshot of the rat IMCD Proteomic cdbBLAST (A) initial page where a sequence can be typed or pasted into the white box, (B) settings that can be changed to alter the results of a search, and (C)results, using Nedd4l as a sample amino acid input sequence. The results include a summary table of the proteins whose sequences best match the query (input) sequence, which includes links to their PubMed protein pages. Below this table are comparisons of these top proteins to the query sequence. Within each comparison, the sources in which that top protein is found are listed. There is a link to the original database on all three pages.

channel aquaporin-2 (Medvar et al. 2016) in IMCD cells. One use of cdbBLAST is searching a large-scale database for an amino acid sequence associated with a specific domain to find all proteins within that domain. cdbBLAST is a useful tool for this type of search because of its ability to give not only results that match exactly, but also results that are similar. As seen in Figure 5C, using the HECTc domain of Nedd4l shows results not only for Nedd4l, but also for 17 similar proteins. For Nedd4l you can also see the beginning of the sequence comparison, as well as the datasets Nedd4l was found in.

The rat IMCD transcriptome cdbBLAST search (Fig. 6A) is very similar to the proteome search. However, this database is a combination of two different transcriptomic databases: one using RNA-sequencing (Lee et al. 2015) and the other using Affymetrix techniques (Uawithya et al. 2008). The results from this cdbBLAST search are structured the same as the proteome cdbBLAST search (see above), however the comparisons are labeled with the proteins RefSeq number, protein name, and the median RPKM value and/or the normalized IMCD-Signal (depending what study that protein is found in). As an example, we searched the IMCD transcriptome using the amino acid sequence for Smad1. Smad1 is a transcription factor found in the IMCD transcriptome as seen in Figure 6C. cdbBLAST also found many very similar proteins as well, some so similar they have the same e-value as Smad1. The comparison of the query to the database shows that Smad1 was found in both transcriptomic studies used to create this database.

The downloadable version of cdbBLAST (Fig. 7) is a slightly simpler version than the web servlets. It does not allow the user to adjust the settings and there are no clickable links in the results, but the information

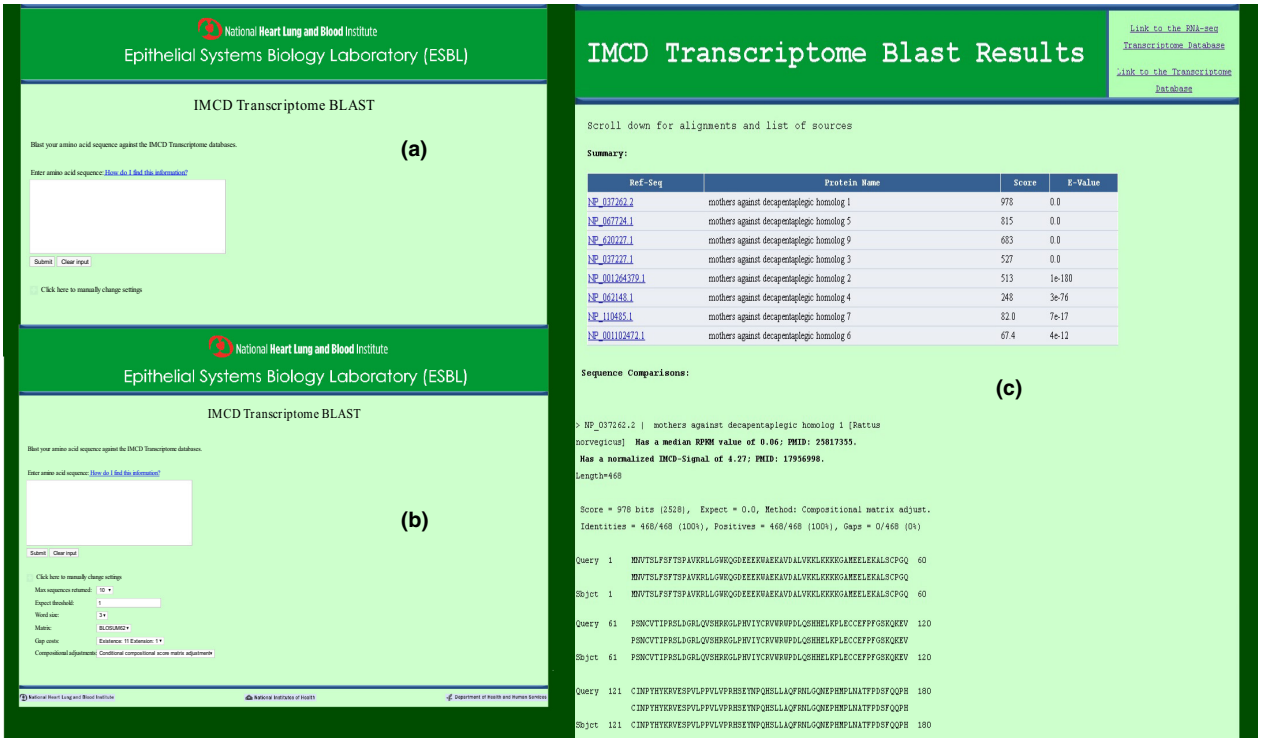

Figure 6. A screenshot of the rat IMCD Transcriptome cdbBLAST (A) initial page where a sequence can be typed or pasted into the white box, (B) settings that can be changed to alter the results of a search, and (C)results, using Smad1 as a sample amino acid input sequence. There are links to the original databases, a summary table of the transcripts whose sequences best match the query (input) sequence which includes links to their PubMed protein pages, and comparisons of these top transcripts to the query sequence. Each comparison also reports the median RPKM value and/or the normalized IMCD-Signal (depending what study that protein is found in) for that transcript.

provided is the same as the cdbBLAST web-based searches, with there being a table of similar proteins followed by sequence to sequence comparisons with database data. However, unlike the web servlets, the downloadable version of cdbBLAST can be used with any database of proteins or transcripts that has been correctly formatted. This allows users to integrate any prior data they wish into the database (and thus the output from the search), as well as allows the user to submit multiple sequences as input in a text file. A manual has been created to provide the user with a step-by-step guide to this process (see Appendix, download from https://hpcwebapps.cit.nih.gov/ESBL/Database/cdbBLAST-Appendix/Appendix.html). While this is the best use of the cdbBLAST GUI, we have also made the databases created in our laboratories available for download as well on the GUI download page.

Discussion

Our laboratory has created rat IMCD cdbBLAST searches for the proteome and transcriptome both as web-based servlets. We have also created a downloadable GUI version, with downloadable versions of our IMCD proteome and transcriptome databases available, as well as a manual explaining how the user can create a database from their own data.

cdbBLAST is a valuable tool that allows scientists to use the most unique search parameter when looking through a database: the amino acid/nucleotide sequence. With large databases created from large-scale proteomic and transcriptomic experiments becoming more common, a lot of useful data is being reported but not utilized due to the sheer volume of information available. As more is learned about the nature and function of specific proteins or transcripts, they are given new names or gene symbols. This makes older databases tedious and time consuming to search if they cannot be searched via amino acid/nucleotide sequences. There is no longer a need to do multiple searches within a database using every gene symbol from discovery to present in hopes of finding data on a specific protein/transcript.

cdbBLAST also allows the user to search for pieces of sequence, such as protein domains, allowing researchers to learn more about a group of proteins/transcripts in a single search. However, cdbBLAST requires at least 11

LOW RESOLUTION COLOR FIG

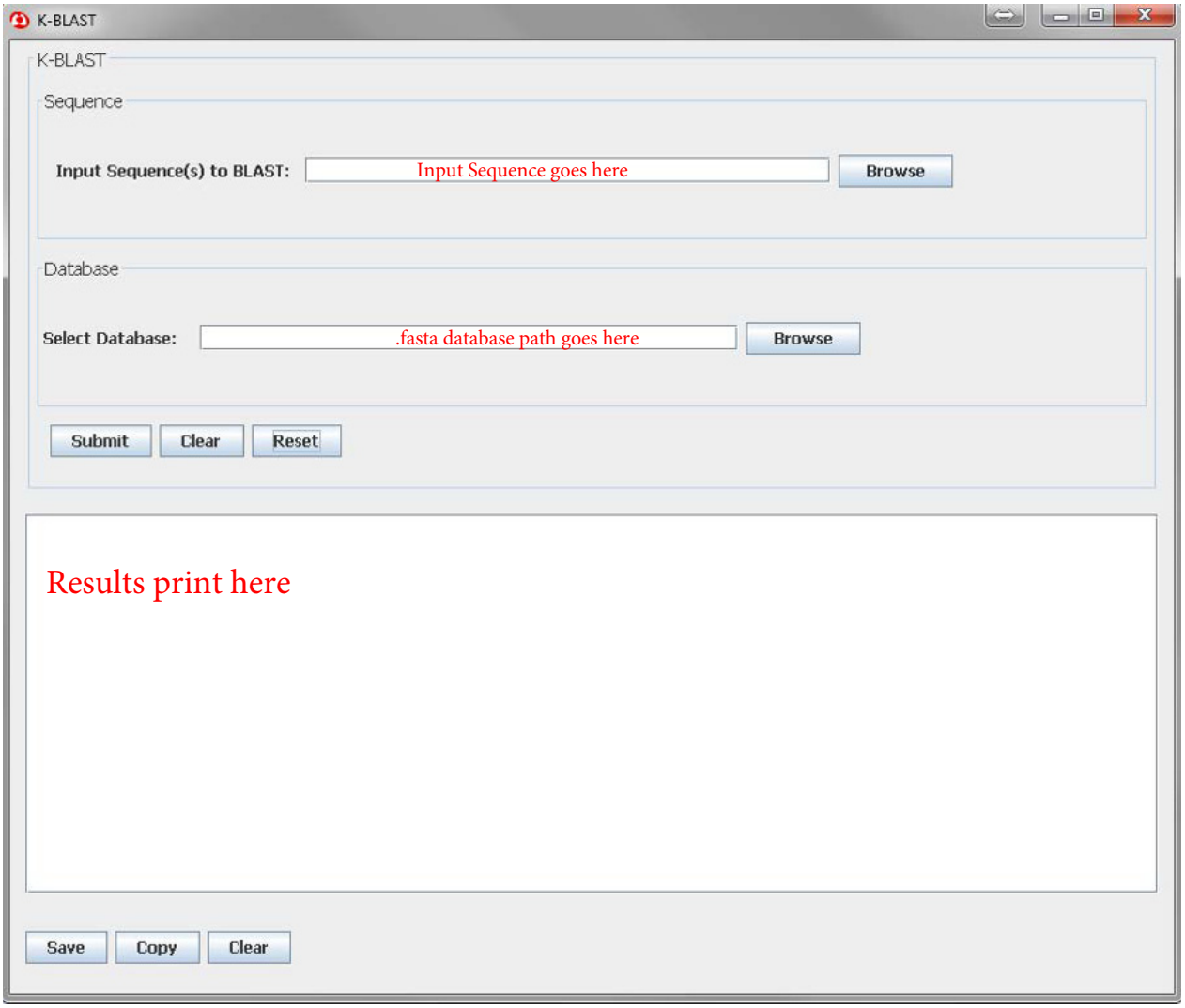

Figure 7. A screenshot of the downloadable version of cdbBLAST. Users can either type/paste in a sequence into the "Input Sequence to BLAST:" box or browse their computer for a .txt file to input. Users then browse their computer (or type in the path) for the .fasta database they either created (Fig. 2) or downloaded from our webpage before hitting "Submit". "Clear" clears only the input, while "Reset" clears the database and output sections as well. The results print similarly to the web-servlets, without any links to webpages. The results can be saved, copied, or cleared by hitting the corresponding buttons under the results box.

amino acids/nucleotides for the search to run, making it difficult search for smaller domains or motifs.

For every searched sequence using cdbBLAST, the results include proteins/transcripts that are similar to the search sequence. This makes it easier for researchers to find a related protein/transcript if the search protein/transcript is not found, or when the searched sequence is a different species than that of the database. Every protein/transcript shown in the results is accompanied by the database information associated with it, as well as a sequence comparison to the searched sequence, so the user can see how well the sequences match. For example, we have combined 18 published studies from our laboratory into one large IMCD proteome database of 8956 proteins. This database lists each proteins name, gene symbol, amino acid number, accession number, whether it is found in the transcriptome, and which of the sources (experiments from within these studies) that protein was found in. When this database is searched using cdbBLAST, each protein in the results lists the sources in which that protein was found. It is logical that the more times a protein was identified, the more likely it is to exist in the IMCD. This added information to the results of the search allows the user to see the

relevant information without having to go back to the original database.

The web-based servlets we have created using cdbBLAST focus on the rat IMCD transcriptome and proteome. Specifically, they focus on the level of expression of the transcripts in the IMCD and what proteins are found in IMCD cells, respectively. The downloadable version of cdbBLAST allows the user to create their own searchable database(s) which can include any and all information they wish, from multiple datasets. Our transcriptome and proteome cdbBLAST databases are also available to be downloaded and used with this version. While amino acid/nucleotide sequences remain consistent through time, more information is learned about proteins and transcripts constantly. With the downloadable version of cdbBLAST, new information can be added to an existing searchable database with ease (see Appendix, download from https://hpcwebapps.cit.nih.gov/ESBL/Database/cdbBLAST-Appendix/Appendix.html).

Conflict of Interest

None declared.

References

Altschul, S. F., W. Gish, W. Miller, E. W. Myers, and D. J. Lipman. 1990. Basic local alignment search tool. J. Mol. Biol. 215:403–410.

van Balkom, B. W., J. D. Hoffert, C. L. Chou, and M. A. Knepper. 2004. Proteomic analysis of long-term vasopressin action in the inner medullary collecting duct of the Brattleboro rat. Am. J. Physiol. Renal Physiol. 286:F216–F224.

Bansal, A. D., J. D. Hoffert, T. Pisitkun, S. Hwang, C. L. Chou, E. S. Boja, et al. 2010. Phosphoproteomic profiling reveals vasopressin-regulated phosphorylation sites in collecting duct. J. Am. Soc. Nephrol. 21:303–315.

Barile, M., T. Pisitkun, M. J. Yu, C. L. Chou, M. J. Verbalis, R. F. Shen, et al. 2005. Large scale protein identification in intracellular aquaporin-2 vesicles from renal inner medullary collecting duct. Mol. Cell Proteomics 4:1095–1106.

Bradford, D., V. Raghuram, J. L. Wilson, C. L. Chou, J. D. Hoffert, M. A. Knepper, et al. 2014. Use of LC-MS/MS and Bayes' theorem to identify protein kinases that phosphorylate aquaporin-2 at Ser256. Am. J. Physiol. Cell Physiol. 307:C123–C139.

Hoffert, J. D., B. W. van Balkom, C. L. Chou, and M. A. Knepper. 2004. Application of difference gel electrophoresis to the identification of inner medullary collecting duct proteins. Am. J. Physiol. Renal Physiol. 286:F170–F179.

Hoffert, J. D., T. Pisitkun, G. Wang, R. F. Shen, and M. A. Knepper. 2006. Quantitative phosphoproteomics of vasopressin-sensitive renal cells: regulation of aquaporin-2 phosphorylation at two sites. Proc. Natl Acad. Sci. USA 103:7159–7164.

Hoffert, J. D., T. Pisitkun, F. Saeed, J. H. Song, C. L. Chou, and M. A. Knepper. 2012. Dynamics of the G protein-coupled vasopressin V2 receptor signaling network revealed by quantitative phosphoproteomics. Mol. Cell Proteomics 11:M111 014613.

Hoffert, J. D., T. Pisitkun, F. Saeed, J. L. Wilson, and M. A. Knepper. 2014. Global analysis of the effects of the V2 receptor antagonist satavaptan on protein phosphorylation in collecting duct. Am. J. Physiol. Renal Physiol. 306:410–421.

Hoorn, E. J., J. D. Hoffert, and M. A. Knepper. 2005. Combined proteomics and pathways analysis of collecting duct reveals a protein regulatory network activated in vasopressin escape. J. Am. Soc. Nephrol. 16:2852–2863.

Lee, J. W., C. L. Chou, and M. A. Knepper. 2015. Deep sequencing in microdissected renal tubules identifies nephron segment-specific transcriptomes. J. Am. Soc. Nephrol. 26:2669–2677.

LeMaire, S. M., V. Raghuram, C. R. Grady, C. M. Pickering, C. L. Chou, E. N. Umejiego, et al. 2017. Serine/threonine phosphatases and aquaporin-2 regulation in renal collecting duct. Am. J. Physiol. Renal Physiol. 312:F84–F95.

Medvar, B., V. Raghuram, T. Pisitkun, A. Sarkar, and M. A. Knepper. 2016. Comprehensive database of human E3 ubiquitin ligases: application to aquaporin-2 regulation. Physiol. Genomics 48:502–512.

National Center for Biotechnology Information (NCBI) [Internet]. 2017. Bethesda (MD): National Library of Medicine (US) NCfBI. https://www.ncbi.nlm.nih.gov/. [October 1, 2017].

Pickering, C. M., C. Grady, B. Medvar, M. Emamian, P. C. Sandoval, Y. Zhao, et al. 2016. Proteomic profiling of nuclear fractions from native renal inner medullary collecting duct cells. Physiol. Genomics 48:154–166.

Pisitkun, T., J. Bieniek, D. Tchapyjnikov, G. Wang, W. W. Wu, R. F. Shen, et al. 2006. High-throughput identification of IMCD proteins using LC-MS/MS. Physiol. Genomics 25:263–276.

Sachs, A. N., T. Pisitkun, J. D. Hoffert, M. J. Yu, and M. A. Knepper. 2008. LC-MS/MS analysis of differential centrifugation fractions from native inner medullary collecting duct of rat. Am. J. Physiol. Renal Physiol. 295: F1799–F1806.

Simons, B. L., G. Wang, R. F. Shen, and M. A. Knepper. 2006. In vacuo isotope coded alkylation technique (IVICAT); an N-terminal stable isotopic label for quantitative liquid chromatography/mass spectrometry proteomics. Rapid Commun. Mass Spectrom. 20:2463–2477.

Tchapyjnikov, D., Y. Li, T. Pisitkun, J. D. Hoffert, M. J. Yu, and M. A. Knepper. 2010. Proteomic profiling of nuclei

from native renal inner medullary collecting duct cells using LC-MS/MS. Physiol. Genomics 40:167–183.

Trepiccione, F., T. Pisitkun, J. D. Hoffert, S. B. Poulsen, G. Capasso, S. Nielsen, et al. 2014. Early targets of lithium in rat kidney inner medullary collecting duct include p38 and ERK1/2. Kidney Int. 86:757–767.

Uawithya, P., T. Pisitkun, B. E. Ruttenberg, and M. A. Knepper. 2008. Transcriptional profiling of native inner medullary collecting duct cells from rat kidney. Physiol. Genomics 32:229–253.

Yu, M. J., T. Pisitkun, G. Wang, R. F. Shen, and M. A. Knepper. 2006. LC-MS/MS analysis of apical and basolateral plasma membranes of rat renal collecting duct cells. Mol. Cell Proteomics 5:2131–2145.

Zhao, B., M. A. Knepper, C. L. Chou, and T. Pisitkun. 2012. Large-scale phosphotyrosine proteomic profiling of rat renal collecting duct epithelium reveals predominance of proteins involved in cell polarity determination. Am. J. Physiol. Cell Physiol. 302:C27–C45.